Microscale topographical cues regulate mesenchymal stem cell behaviors

A Dissertation

Submitted in Partial Fulfilment of the

Requirements for the Degree of Doctor rerum naturalium (Dr. rer. nat.)

to the Department of Biology, Chemistry and Pharmacy

of Freie Universität Berlin

by

Jie Zou

Berlin, 2019

Supervisor: Prof. Dr. Andreas Lendlein

(Universität Potsdam and Freie Universität Berlin)

2nd examiner: Prof. Dr. Nora Kulak

(Freie Universität Berlin)

Date of defense: 05.09.2019

Contents

Acknowledgement

This work was carried out in the Institute for Biomaterials Research of the Helmholtz Center Geesthacht. I greatly appreciate to all people who have helped me during my doctoral study.

Firstly, I would like to express my heartfelt gratitude to my supervisors Prof. Andreas Lendlein and Prof. Nan Ma for giving me the opportunity to conduct all the research in this thesis. Thanks for their fruitful scientific guidance, suggestions and discussions throughout my research. Thanks for spending their precious time reviewing my manuscripts and giving lots of valuable comments and suggestions. Their professional knowledge opened my mind and enhanced my understanding of the study.

I am in gratitude to Dr. Weiwei Wang who has given me valuable suggestion in the designing of experiments and helped me a lot in scientific writing. I greatly appreciate his valuable suggestion and the patience for my questions and problems.

I would also like to thank Dr. Xun Xu and Dr. Zhengdong Li for their valuable suggestion of experiments and the guiding of characterization methods and technologies.

I am also thankful to Dr. Karl Kratz for the supplying of PC and PS insterts that are the main experimental materials in my study, to Dr. Axel T. Neffe for providing of ArcGel materials, to Ms.Manuela Keller for technical support of materials surfaces roughness characterization.

I am very grateful to all of the group members for their kind help, particularly to Dr. Toralf Roch, Xianlei Sun, Zijun Deng, Thanga Bhuvanesh Vijaya Bhaskar, Yan Nie, Ms Anja Müller-Heyn and Wintai Tung. The group have been a source of friendships as well as good advice and multidisciplinary knowledge and culture transfer.

I would like to extend my sincerest thanks and appreciation to our PhD coordinators Dr. Michael Schröter and Dr. Anne-Christin Schöne for coordinating/ organizing MCM, seminar and thesis submission procedures.

I would like to extend my thanks to my friends Shuo Zhou, Dr. Quanchao Zhang, Dr. Xinzhou Peng, Wan Yan, Yi Jiang, Yue Liu, Dr. Zewang You and Dr. Li Wang for their kind helps of life.

I wish to acknowledge the financial support provided by Helmholtz Graduate School for Macromolecular Bioscience for my study, travel and living in Berlin for last 5 years.

I would like to owe my deepest gratefulness to my family for their continuous support and sincere love, encouraging me to overcome so many challenges. I am indebted to my father, my aunt and my sisters for their love and understanding, which makes it possible for me to complete the doctoral work.

At last, I would like to dedicate this thesis to my wife Ms. Jing Li. She and our daughter have accompanied me through all the joys and sorrows in the past, which would be the best memories of our lives.

Foreword

This thesis is a cumulative work of the following manuscripts:

1. Jie Zou et al. Evaluation of human mesenchymal stem cell senescence, differentiation and secretion behavior cultured on polycarbonate cell culture inserts. Clinical Hemorheology and Microcirculation. 2018; 70: 573-583. https://doi.org/10.3233/CH-189322
2. Jie Zou et al. Substrate surface topography promotes human bone marrow mesenchymal stem cell osteogenic differentiation via histone modification of osteogenic genes. (Manuscript for Chapter 3 was submitted to Biomaterials).
3. Jie Zou et al. Adipogenic differentiation of human adipose derived mesenchymal stem cells in 3D architectured gelatin based hydrogels (ArcGel). Clinical Hemorheology and Microcirculation. 2017; 67: 297–307. https://doi.org/10.3233/ CH-179210

Summary

Objective: Stem cell behaviors and lineage commitments are driven by the mechanical properties of substrate. The designing of substrate topographic surface to regulate stem cell behaviors is an attractive method to enhance their therapeutic potential. The aim of this study was to evaluate the influence of substrate topographic surface on the human bone marrow mesenchymal stem cell (hBMSC) differentiation and to investigate the underlying mechanism.

Methods: Synthetic polymers were fabricated into inserts that fit the standard 24-well tissue culture plate via injection molding. Three molds with different roughness surface were utilized to manufacture the inserts with different topographic surfaces. Polycarbonate (PC) inserts were selected for hBMSCs cultivation. The cell compatibility of PC was evaluated by comparing the behaviors of hBMSCs on PC, polystyrene (PS) and TCP surface. Then, hBMSCs were cultured on PC inserts with three kinds of topographic surfaces, and the osteogenic and adipogenic differentiation levels were tested. For the study of the underlying mechanism, the contractility of cells that cultured on different topographic surfaces was evaluated. After that, the influence of cell contractility on nuclear deformation, mechanosensory factor nuclear translocation and the composition of nuclear lamina as well as the global histone modification level were investigated. Furthermore, ChIP-PCR method was used to analyze the enrichment of modified histone located on specific gene promoters. For the evaluation of stem cells behaviors on 3D topographic scaffold, gelatin was used to fabricate 3D architectured gelatin based hydrogel, and the behaviors of human adipose derived mesenchymal stem cells on the gelatin based hydrogel were evaluated.

Results: PC presented a high cell compatibility for the cultivation of hBMSCs. Appropriate surface topographical cues promoted cell contractility. The surface topographical cues mediated cell contraction force transmitted to nucleus via linker of nucleoskeleton and cytoskeleton (LINC) complex proteins, which resulted in the cell nuclear deformation, enhanced the mechanosensor protein YAP nuclear translocation and elevated lamin A/C expression. Furthermore, the mechanical force propagated to the chromatin and led to changing of histone modification level as well as regulated the enrichment of H3K27me3 and H3K9ac located on the osteogenic differentiation related gene promoters, subsequently, promoted hBMSC osteogenic differentiation. The 3D architectured gelatin based hydrogel presented high cell compatibility for hADSC cultivation and differentiation.

Conclusion: Substrate physical properties play an important role in regulating stem cell behaviors. Appropriate surface topographical cues affect cell contractility. The surface topographical cues mediated cell contraction force results in nuclear deformation and influences chromatin status. Furthermore, the contraction force regulates the enrichment of modified histone located on the specific gene promoters, and then modulates stem cell behaviors and fate.

Zusammenfassung

Ziel: Das Verhalten der Stammzellen und ihrer Herkunftsverpflichtungen werden von den mechanischen Eigenschaften des Substrates bestimmt. Die Gestaltung der topographischen Oberfläche des Substrats ist eine attraktive Methode, um ihr therapeutisches Potenzial zu erhöhen. Das Ziel dieser Studie war, den Einfluss der topographischen Oberfläche des Substrats auf die Differenzierung der menschliche Knochen-Mesenchym-Stammzelle (hBMSC) zu evaluieren und die zugrundeliegenden Mechanismen zu untersuchen.

Methoden: Synthetische Polymere wurden als Einsätze präpariert, die durch Spritzgießen mit der Standard-Gewebekulturplatte mit 24 Vertiefungen zusammenpassen. Drei verschiedene topographische Marker wurden verwendet, um die Einsätze mit unterschiedlichen topographischen Oberflächen herzustellen. Für die Kultivierung der hBMSC wurden Polycarbonat (PC)- Einsätze ausgewählt. Die Zellkompatibilität von Polycarbonat wurde evaluiert, indem das Verhalten der hBMSC auf PC-, Polystyren- (PS-) und TCP-Oberflächen verglichen wurde. Daraufhin wurden hBMSC auf PC- Einsätze mit drei verschiedenen topographischen Oberflächen kultiviert und die osteogenen und adipogenen Differenzierungsstufen wurden getestet. Für das Studium der zugrundeliegenden Mechanismen wurde die Kontraktionsfähigkeit von Zellen evaluiert, die auf verschiedenen Oberflächen kultiviert wurden. Danach wurde der Einfluss der Zellkontraktionsfähigkeit auf Zellkern Deformation, Mechanosensor-Faktor Kerntranslokation und den Aufbau von nukleare Lamina untersucht, sowie auch auf das Niveau der globalen Histon-Modifikation. Darüber hinaus wurde die ChIP-PCR-Methode genutzt, um die Anreicherung von modifiziertem Histon auf spezifische Genpromotoren zu analysieren. Für die Evaluation des Stammzellenverhaltens auf Topographisches 3D Schafott wurde Gelatine zu einem gelatinebasierten Hydrogel mit 3D-Architektur verarbeitet, und das Verhalten von aus menschlichem Fett stammenden mesenchymalen Stammzellen auf dem auf Gelatine basierenden Hydrogel wurde bewertet.

Ergebnisse: PC zeigte eine hohe Zellkompatibilität für die Kultivierung von hBMSC. Angemessene Oberflächentopographische Hinweise förderten die Zellkontraktionsfähigkeit. Die Oberflächentopographische Hinweise übermittelten die Zellkontraktionskraft, die über Linker von Nukleoskelett und Zytoskelett (LINC) komplexe Proteine auf den Kern übertragen wurde, was zur Zellkern Verformung, der Verbesserung der Kern Translokation des mechanosensorischen Proteins YAP sowie erhöhter lamin A / C Ausdruck führte.

Darüber hinaus führte die mechanische Kraft, die sich zum Chromatin ausbreitete und zu einer Änderung des Histonmodifikationsgrades führte, sowie zur Regulierung der Anreicherung von H3K27me3 und H3K9ac, die sich auf den osteogenetischen Differenzierungs-Genpromotoren befanden, in der Folge zur Förderung der osteogenetischen hBMSC-Differenzierung. Das auf 3D-Gelatine basierende Hydrogel zeigte eine hohe Zellkompatibilität für die Kultivierung und Differenzierung von hADSC.

Fazit: Die physikalischen Eigenschaften des Substrats spielen bei der Regulierung des Stammzellenverhaltens eine wichtige Rolle. Geeignete Oberflächen Topographische Hinweise beeinflussen die Kontraktionsfähigkeit der Zelle. Die durch den Oberflächen Topographische Hinweise übertragene Zellkontraktionskraft resultiert in der Deformation des Zellkerns und beeinflusst den Zustand des Chromatins. Darüber hinaus reguliert die Kontraktionskraft die Anreicherung modifizierter Histon auf den spezifischen Genpromotor und ändert damit Stammzellverhalten und Schicksal.

Chapter I

Introduction

1. Introduction

1.1 Mesenchymal stem cells

Mesenchymal stem cells (MSCs) are multipotent, non-hematopoietic stromal cells that exist in adult tissues of different sources, including bone marrow, adipose tissue, peripheral blood amniotic membrane, dental tissues, endometrium, limb bud, menstrual blood, placenta and fetal membrane, salivary gland, skin and foreskin, sub-amniotic umbilical cord lining membrane and synovial fluid[1]. MSCs are capable of differentiating into various mesenchymal lineages in vitro, including bone, muscle, cartilage and fat, as well as forming cells to other germ layers, such as keratinocytes and neuron-like cells [2, 3]. In addition to the multilineage differentiation potential, MSCs have high self-renewal potential. Long cell culture experiments had found that MSCs could show up to 50 population doublings (PDs) in 10 weeks *in vitro*[4], but the long-term cultivation of MSCs resulted in the decline of their multipotency [5]. Immunomodulatory capability is another important function of MSCs. Transplantation of MSCs would not result in substantial alloreactivity, which reduces the lysis of MSCs by natural killer (NK) cells in the body [6] and MSCs could regulate NK cells and cytotoxic T cells functions by different pathways [7, 8]. Due to the high self-renewal capacity, multilineage differentiation potential, immunoregulatory effects, easily accessibility, as well as fewer ethical issues compare with embryonic stem cell, MSCs are considered a promising cell source for cell therapy. Currently, MSCs have been used to treat some diseases such as bone and cartilage diseases, cardiovascular diseases, autoimmune diseases, chronic and acute graft versus host disease, liver diseases, cancer, crohn disease and multiple sclerosis [9, 10].

1.2 Biomaterials for stem cells

Biomaterial by definition is a substance, synthetic or natural, that can be used as a system or part of a system that treats, augments, or replaces any tissue, organ, or function of the body [11]. Ideally, biomaterials should perform similar structural, physical and biochemical functions to the natural extracellular matrix (ECM), which provides suitable and effective physical and chemical signals for the supporting of stem cell proliferation, migration, secretion and differentiation. Biomaterials need to meet some requirements such as biocompatibility, biofunctionality, biodegradation, non-toxicity and suitable mechanical properties [11].

Biomaterials can be divided into natural biomaterials (such as agarose, collagen, alginate, chitosan, hyaluronate, and fibrin) and synthetic biomaterials (such as Poly(lactic acid) (PLA), poly(ethylene) (PE), polyurethanes (PUR), Poly(ε-caprolactone) (PCL), poly(glycolide) (PGA)

and hydroxyapatite (HA) as well as tri-calcium phosphate (TCP)) [12-14]. These biomaterials are engineered to cause desirable cellular interaction materials, which are named scaffolds. Stem cells are often seeded on the scaffolds for the supporting the defected tissue reparation or new tissue formation. To provide better microenvironments for the stem cell attachment, growth and differentiation, the scaffolds are fabricated into porous network structures that mimic the extracellular matrix of the native tissue. The porous structure of scaffolds could provide space for cell adhesion, migration and proliferation, and facilitating the transport of oxygen and nutrients as well as the elimination of cellular metabolic.

1.3 Substrate surface chemical properties control stem cell behaviors and fate

MSCs are typical adherent cells, which are able to grow and differentiate only when the cells adhere to substrates. Since MSCs do not directly respond to the substrate surface instead of interacting with the protein adsorbed onto the surface [15], the protein composition, orientation as well as conformation influence cell-surface interactions and regulate many signaling pathways, which control MSC proliferation, migration, secretion and differentiation. The protein adsorption on the surface was regulated by surface physical and chemical properties such as wettability, charge and chemical functional groups. It is well known that the surface wettability is a key factor in regulating proteins (peptides) absorption and modulating cell behaviors [16, 17]. On hydrophobic surface, more hydrophobic parts of protein will stick to the surface, which would decrease the interaction of these parts with the aqueous phase, and the protein would denature due to the rearrangements of protein structure [18]. In a recent study it was found that the hydrophobicity of surface regulated the protein deformation and formation of nano-topography on the surface, which further regulated MSCs differentiation [19]. Proteins do not stick to completely hydrophobic surface, so cells cannot attach to the surface. A previous study found that the best wettability of a surface for cell adhesion was water contact angle in the range between 57° to 65°; however, once the surface contact angle was higher than 97° or lower than 48°, cell adhesion would decrease [20]. In addition to the surface wettability, the surface charge plays another key role in regulating protein adsorption. The surface charge influences protein adsorption thermodynamics, kinetic, conformation as well as desorption kinetics [21], which further influence stem cell behaviors. The different chemical groups' functionalities not only influence surface wettability and charge property but also directly regulate stem cell behaviors. Amino ($-NH_2$) surface could improve stem cell adhesion, proliferation and enhanced the stem cell osteogenic differentiation potential, and the surfaces

with modified by hydroxyl (−OH), carboxyl (−COOH), or methyl ($-CH_3$) preferred to maintain the mesenchymal stem cell-like phenotype [22].

1.4 Substrate surface physical cues affect stem cell behaviors and fate

In addition to the surface chemical properties, the physical microenvironment cues presented by substrates are important factors to regulate stem cell behavior and functions. The physical microenvironment cues include substrate stiffness, mechanical strain of substrate as well as topography of the substrate surface. The stiffness of substrate, which matched the stiffness of native tissue, could guide stem cell differentiation down corresponding tissue lineages. For example, the soft substrate (0.1-1.0 KPa) mimicking the brain tissue induced MSC neurogenic differentiation, stiffer substrate (8-17 KPa) similar to muscle stimulate MSC myogenesis and the rigid substrate (25-40 KPa) that similar to the bone stiffness enhance MSCs osteogenic differentiation[23]. The substrate surface topography plays an important role in regulating various stem cell behaviors (chapter I, Table 1) as well. Long-term (8 weeks) cultivation of MSCs cultured on nanoscale substrate could maintain MSC multipotency [24]. Micro grooves surface and aligned fibers scaffold can promote the stem cell adipogenic, myogenic and neuronal differentiation [25, 26], and MSCs on the square micro pattern surface had higher osteogenic differentiation level compared with MSCs on round micro pattern surface[27]. The roughness of surface also could regulate stem cell behaviors like cell adhesion, migration, proliferation, secretion and differentiation [28-31]. Surface roughness provides osteoblasts and mesenchymal stem cells (MSCs) with structural cues to promote tissue regeneration and new bone formation [32, 33]. However, on different substrate the range of roughness that regulated stem cell osteogenic differentiation was different. On the poly(ε-caprolactone) surface with gradient roughness, the result indicated surface roughness with an average roughness (Ra) of 2.1-3.1 μm and a mean distance between peaks (RSm) of 48.1-71.1 μm accentuated the osteogenic differentiation of hBMSCs [34], on the hydroxyapatite substrate, the rough surface with Ra closed to 1 μm enhances MSCs osteogenic differentiation [35]. The discrepancy may be caused by the different substrates used in these experiments.

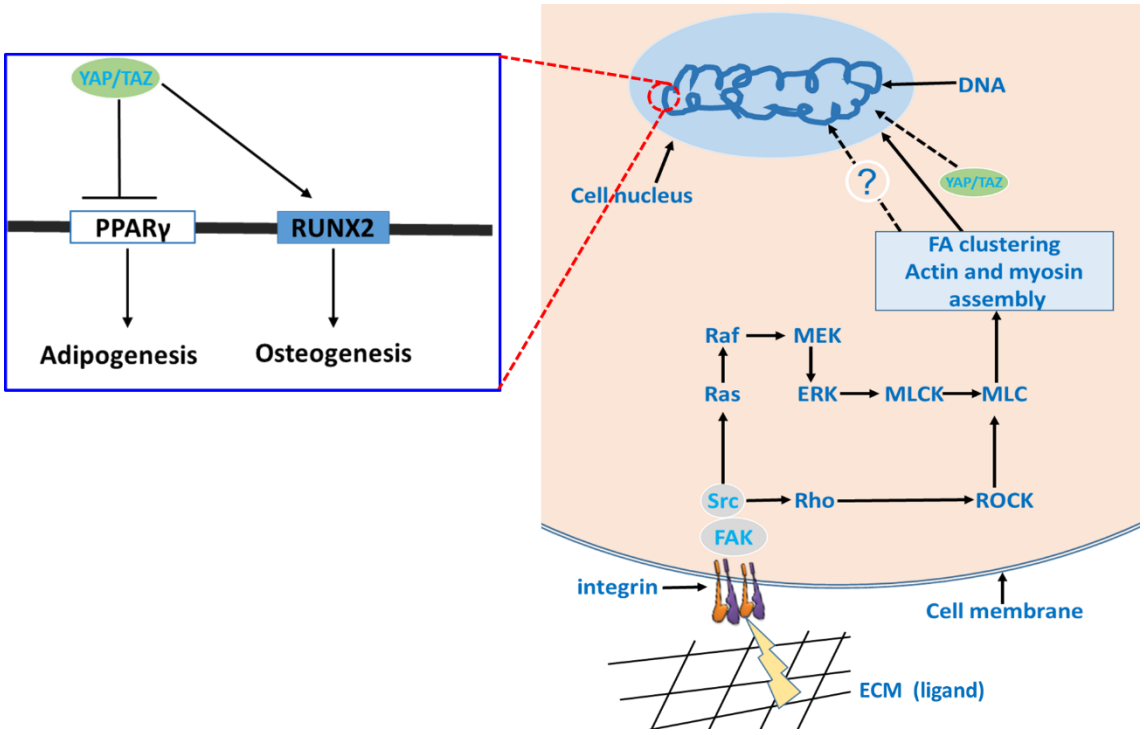

Fig.1 Schematic of substrate properties regulating cell contractility, and then influence stem cell fate. FAK, focal adhesion kinase; Src, Rous sarcoma oncogene cellular homolog; Ras, Ras small GTPases; Raf, Raf serine/threonine-protein kinase; MAPK, mitogen-activated protein kinases; ERK, extracellular signal-regulated kinases; MEK, MAPK/ERK kinase; MLCK, myosin light-chain kinase; MLC, myosin light chain; Rho, Rho guanine nucleotide exchange factors; ROCK, Rho-associated kinase; YAP, Yes-associated protein; TAZ, transcriptional coactivator with PDZ-binding motif; Runx2, Runt-related transcription factor 2; PPARγ, peroxisome proliferator-activated receptor γ.

Table 1: Example of studies, topography influenced the stem cell behaviors and fate

Substrates	Cell source	Topographical feature	Highlights	Ref.
Si	rANSCs	Linear micro-pattern (LMP), circular micro-pattern (CMP) and dot micro-pattern (DMP)	LMP and CMP both significantly enhance ANSC differentiation to neurons	[36]
PDMS	hBMSCs	Micro-pattern (rectangles, Flower and Star Shapes)	Geometric features that increased actomyosin contractility promote osteogenesis	[27]
PLLA	rMSCs	Randomly and oriented PLLA fiber scaffold	Aligned substrate enhanced tenogenic differentiation, randomly-oriented fiber scaffolds enhanced osteogenic differentiation	[37]
PMMA	hBMSCs	Nanoscale ordered disorder pits	Nanoscale disorder pits stimulate MSCs osteogenic differentiation	[38]
PTMC	hBMSCs	Convex and concave spherical structures with diameters ranging from 250 μm to 750 μm	Convex surfaces (diameters 250 μm) promote osteogenic differentiation.	[39]
Alumina ceramics	hMSCs	Grooves (Ridge: 0-180 μm and Groove: 0-180 μm)	Enhanced the adhesion and osteogenesis.	[40]
HA	hBMSCs	Roughness (Ra form 0.2 μm to 1.65 μm)	MSCs on rough surface (Ra form 0.77 μm to 1.09 μm) showed strongest osteogenic differentiation.	[35]
PCL	hBMSCs	Roughness (Ra: 0.5–4.7 μm, and RSm 214 μm - 33 μm)	Rough surface with Ra ~ 0.93 μm/RSm ~ 135 μm enhanced hBMSCs osteogenic differentiation.	[41]
PLLA	rESCs	Electrospun PLLA scaffolds	Enhanced cell proliferation rate and promoted the production of nerve growth factor (NGF) and endothelial growth factor (VEGF)	[42]
PS	hADSCs	Square-shaped or round-shaped microwells	Square-shaped microwells promotes the proliferation and osteogenic differentiation compared with the round-shaped microwells.	[43]

rANSCs: Rat adult neural stem cells; hBMSCs: human bone marrow mesenchymal stem cells;rESCs: Rat Embryonic Stem Cells; hADSCs: human adipose-derived mesenchymal stem cells

PDMS: polydimethylsiloxane; PLLA: poly (l-lactic acid); PMMA: Polymethyl methacrylate; PTMC: poly (trimethylene carbonate); HA: Hydroxyapatite; PCL: polycaprolactone; PS: polystyrene

1.5 The mechanism of topographic surface influence stem cell behaviors

Accumulating evidences from the interaction studies of surface properties and stem cell behaviors showed that substrate stiffness and topography had similar manners of influencing stem cell focal adhesion assembly and organization via mediation of binding and clustering of integrins [44]. The soft substrate, compared to stiff substrate, can enhance the integrin β1 activation and internalization [45], which further influences the focal adhesion assembly and organization. Nanoscale substrate surface regulates focal adhesion assembly and organization via modulating the spatial of protein adsorption on the surface [46]. Also, stem cells on the microscale topographic surfaces can sense the radii of local curvature, which activates the cell membrane integrin, further regulating focal adhesion formation and organization [31]. As a vital cell membrane receptors, integrin, when activated further results in downstream focal adhesion kinase (FAK)/extracellular regulated protein kinases (ERK) and Rho/ Rho-associated protein kinase (ROCK) pathways activation and leads to cytoskeletal actin (F-actin) polymerization and myosin light chain (MLC) activation [47]. The F-actin polymerization and MLC activation are regulated by the expression of the small GTPase RhoA and its downstream effectors Rho-associated protein kinase (ROCK) [48]. In addition, Khatiwala [49] had demonstrated the RhoA-ROCK pathway affects the MAPK pathway(Ras-Raf-MEK-ERK), the level MEK expression, and the ERK-MAPK pathway could activate the phosphorylation of RNUX2 which is a gene of bone related transcription factor and essential for the stem cell osteogenic differentiation[50].

Cell cytoskeleton networks connect to the nucleus by linker of nucleoskeleton and cytoskeleton (LINC) complex proteins that are constituted by nesprins, SUN and lamin proteins, thereby the nucleus can feel the cell contraction force that is mediated by the substrate physical properties [51]. The mechanical force applied on the cell nucleus that resulted in the cell nuclear deformation, specifically, altered the nuclei aspect ratio [52]. The effect of increase of cell cytoskeleton tension not only influences the shape of the nuclei but also leads the structural reorganization and condensation of the nucleus. Werner and colleagues indicated the local curvature of surface topography mediated cell contraction force increasing, which led to the nuclear deformation and increasing of the lamin-A expression to resist the contraction force [53]. In addition, the increased contraction force can enhance the nuclear transcription factor YAP/ TAZ nuclear translocation [49, 50]. The schematic of substrate properties regulate cell contractility and YAP nuclear translocation was showed in Fig. 1 (chapter I).

The inner nuclear membrane encases the genome. The mechanical force applied on nucleus could propagate into nucleus and in consequence influence chromatin organization and accessibility of gene transcription. Mechanical force as a potent regulator could guide stem cell behaviors via regulating epigenetic status. The external mechanical force applied on stem cell led to the enhancement of H3K27me3 expression and then affected the stem cell lineage [54]. In addition, the internal force that was generated by the actomyosin also regulated the methylation and acetylation of H3, and further influenced gene reprogramming, thereby regulating the cell fate and function [55]. The epigenetic status and lineage commitments of stem cells can be regulated by the substrate topography mediated mechanical force. However, how the substrate surface physical cues regulate stem cell epigenetic status, and how the changed epigenetic status control the specific genes expression and subsequently regulate stem cell lineage commitments are still unknown.

2. Motivation

Stem cell behaviors and lineage commitments are driven by the surface topographical cues of substrate. It is necessary to explore the underlying mechanism how material surface topography affects stem cell fate. A better understanding of the mechanism would give us new insight into designing and developing biomedical devices. The aim of this thesis is to study the mechanism of surface topographical cues influencing hBMSCs differentiation.

The specific aims were:

1) To find a suitable material for the hBMSC cultivation in vitro, and evaluate the influence of material surface properties on cell behaviors.

2) To investigate the influence of substrate surface topographical cues on hBMSC differentiation and further explore the mechanism.

3) To evaluate the influence of the 3D scaffold physical properties and microstructure on MSCs behaviors.

3. Hypothesis

1) PC is a suitable substrate for the cultivation of hBMSCs without further modification.

2) The substrate surface topographical cues influence hBMSC differentiation via a mechanism of regulating cell contraction force modulating histone modification. The hBMSCs on the

topographic surfaces could sense the surface topographical cues and transfer the physical signal to biological signals, which further led to the increasing cell contraction force. The increased cell contraction force resulted in nuclear deformation and changing of histone modification level, consequently, modulating the stem cells differentiation lineages.

3) The 3D architecture gelatin based hydrogel (ArcGel) has high cell compatibility for hADSC adhesion, proliferation and differentiation, and a great potential for the usage of adipose tissue regeneration.

4. Strategy

1) To evaluate the influence of substrate surface chemical properties on hBMSC behaviors, polycarbonate (PC) and polystyrene (PS) were selected as materials for evaluation of cell behaviors. Polycarbonate (PC) and polystyrene (PS) were fabricated to the standard 24-well tissue culture fitting inserts via injection molding. The PC inserts were applied for hBMSCs cultivation, and the PS inserts without surface modification and PS based tissue culture plate (TCP) were used as the negative and positive reference materials, respectively. The behaviors of cell adhesion and cell morphology on different substrates were evaluated by immunofluorescence staining. The senescence levels and of hBMSCs on different surfaces were measured by senescence assay kit. The paracrine factors secreted by hBMSCs on different materials were quantified using a Bio-Plex® 200 system. Finally, the differentiation potential of hBMSCs on PC, PS and TCP were characterized by staining.

2) To verify the hypothesis of how substrate topographic surface influences hBMSCs differentiation, PC inserts with three kinds of topography surfaces were fabricated. A smooth surface (sPC) was used here as a control. A surface (mPC) with the value of profile roughness parameter (average peak spacing: RSm) comparable to hBMSC dimension (~ 100 μm in adhesion), while a surface (hPC) with 2.5D topography, and the value of RSm was similar to the pore size of spongy bone. hBMSCs were cultured on the PC inserts with different topographic surfaces. The biological effects of topographical cues on the hBMSC differentiation were evaluated by measuring the expression levels of osteogenic and adipogenic differentiation marker proteins. To explore the underlying mechanism of topographical cues regulating stem cell differentiation, the cell contractility of MSCs on different topographic surfaces was tested by cell contraction assay kit. Furthermore, the influence of cell contractility on cell nuclear deformation and histone modification were evaluated through the analysis of immunostaining images, western blot, flow cytometry and ChIP-PCR.

3) To investigate the influence of 3D scaffold physical properties and microstructure on MSCs behaviors, 3D architecture gelatin based hydrogel (ArcGel) was prepared and hADSCs were seeded on the ArcGel. The hADSCs proliferation were tested by CCK-8 Kit, and the migration of cells were characterized through immunostaining and laser confocal microscopy at different time points. The apoptosis level of hADSCs on the ArcGel was measured by Caspase-Glo @ Kit. Finally, to evaluate the potential of ArcGel for the usage of adipose tissue regeneration, the potential for ArcGel maintaining the adipogenesis of hADSCs were evaluated by ELISA kit.

References

1. Ullah, I., R.B. Subbarao, and G.J. Rho, *Human mesenchymal stem cells - current trends and future prospective.* Bioscience Reports, 2015. **35** (2): p. e00191-00209
2. Zhu, J.L., et al., *Effects of neuritin on the differentiation of bone marrow-derived mesenchymal stem cells into neuron-like cells.* Molecular Medicine Reports, 2017. **16**(3): p. 3201-3207.
3. Sasaki, M., et al., *Mesenchymal stem cells are recruited into wounded skin and contribute to wound repair by transdifferentiation into multiple skin cell type.* Journal of Immunology, 2008. **180**(4): p. 2581-2587.
4. Colter, D.C., et al., *Rapid expansion of recycling stem cells in cultures of plastic-adherent cells from human bone marrow.* Proceedings of the National Academy of Sciences of the United States of America, 2000. **97**(7): p. 3213-3218.
5. Chen, G.C., et al., *Monitoring the biology stability of human umbilical cord-derived mesenchymal stem cells during long-term culture in serum-free medium.* Cell and Tissue Banking, 2014. **15**(4): p. 513-521.
6. Rasmusson, I., et al., *Mesenchymal stem cells inhibit the formation of cytotoxic T lymphocytes, but not activated cytotoxic T lymphocytes or natural killer cells.* Transplantation, 2003. **76**(8): p. 1208-1213.
7. Selmani, Z., et al., *Human leukocyte antigen-G5 secretion by human mesenchymal stem cells is required to suppress T lymphocyte and natural killer function and to induce CD4(+)CD25(high)FOXP3(+) regulatory T cells.* Stem Cells, 2008. **26**(1): p. 212-222.
8. Zhao, Z.G., et al., *Immunosuppressive properties of mesenchymal stem cells derived from bone marrow of patients with chronic myeloid leukemia.* Immunological Investigations, 2008. **37**(7): p. 726-739.
9. Kim, N. and S.G. Cho, *Clinical applications of mesenchymal stem cells.* Korean Journal of Internal Medicine, 2013. **28**(4): p. 387-402.
10. Kim, N. and S.G. Cho, *New Strategies for Overcoming Limitations of Mesenchymal Stem Cell-Based Immune Modulation.* International Journal of Stem Cells, 2015. **8**(1): p. 54-68.
11. Williams, D.F., The Williams dictionary of biomaterials. 1999, Liverpool: Liverpool University Press. xvii, 343
12. Reis, R.L. and D. Cohn, Polymer based systems on tissue engineering, replacement, and regeneration. NATO science series Series II, Mathematics, physics, and chemistry. 2002, Boston, Mass.: Kluwer Academic Publishers. xii, 422
13. O'Brien, F.J., Biomaterials & scaffolds for tissue engineering. Materials Today, 2011. 14(3): p. 88-95.
14. Strohbach, A. and R. Busch, Polymers for Cardiovascular Stent Coatings. International Journal of Polymer Science, 2015. 2015:1-11.
15. Tamada, Y. and Y. Ikada, *Effect of Preadsorbed Proteins on Cell-Adhesion to Polymer Surfaces.* Journal of Colloid and Interface Science, 1993. **155**(2): p. 334-339.
16. Wang, J., et al., *Effect of Topological Structures on the Self-Assembly Behavior of Supramolecular Amphiphiles.* Langmuir, 2015. **31**(51): p. 13834-13841.
17. Bu, Y.Z., et al., *Synthesis and Properties of Hemostatic and Bacteria-Responsive in Situ Hydrogels for Emergency Treatment in Critical Situations.* Acs Applied Materials & Interfaces, 2016. **8**(20): p. 12674-12683.
18. Zhai, J.L., et al., *Protein folding at emulsion oil/water interfaces.* Current Opinion in Colloid & Interface Science, 2013. **18**(4): p. 257-271.

19. Razafiarison, T., et al., *Biomaterial surface energy-driven ligand assembly strongly regulates stem cell mechanosensitivity and fate on very soft substrates.* Proceedings of the National Academy of Sciences of the United States of America, 2018. **115**(18): p. 4631-4636.
20. Schaap-Oziemlak, A.M., et al., *Biomaterial-stem cell interactions and their impact on stem cell response.* Rsc Advances, 2014. **4**(95): p. 53307-53320.
21. Hartvig, R.A., et al., *Protein Adsorption at Charged Surfaces: The Role of Electrostatic Interactions and Interfacial Charge Regulation.* Langmuir, 2011. **27**(6): p. 2634-2643.
22. Yu, T.T., et al., *Influence of Surface Chemistry on Adhesion and Osteo/Odontogenic Differentiation of Dental Pulp Stem Cells.* Acs Biomaterials Science & Engineering, 2017. **3**(6): p. 1119-1128.
23. Engler, A.J., et al., *Matrix elasticity directs stem cell lineage specification.* Cell, 2006. **126**(4): p. 677-89.
24. McMurray, R.J., et al., *Nanoscale surfaces for the long-term maintenance of mesenchymal stem cell phenotype and multipotency.* Nature Materials, 2011. **10**(8): p. 637-644.
25. Wang, P.Y., et al., *Modulation of osteogenic, adipogenic and myogenic differentiation of mesenchymal stem cells by submicron grooved topography.* Journal of Materials Science-Materials in Medicine, 2012. **23**(12): p. 3015-3028.
26. Yim, E.K.F., S.W. Pang, and K.W. Leong, *Synthetic nanostructures inducing differentiation of human mesenchymal stem cells into neuronal lineage.* Experimental Cell Research, 2007. **313**(9): p. 1820-1829.
27. Kilian, K.A., et al., *Geometric cues for directing the differentiation of mesenchymal stem cells.* Proceedings of the National Academy of Sciences of the United States of America, 2010. **107**(11): p. 4872-4877.
28. Andrukhov, O., et al., *Proliferation, behavior, and differentiation of osteoblasts on surfaces of different microroughness.* Dental Materials, 2016. **32**(11): p. 1374-1384.
29. Biazar, E., et al., *The relationship between cellular adhesion and surface roughness in polystyrene modified by microwave plasma radiation.* International Journal of Nanomedicine, 2011. **6**: p. 631-639.
30. Wu, F., et al., *Protein-crystal interface mediates cell adhesion and proangiogenic secretion.* Biomaterials, 2017. **116**: p. 174-185.
31. Li, Z.D., et al., *Integrin beta 1 activation by micro-scale curvature promotes pro-angiogenic secretion of human mesenchymal stem cells.* Journal of Materials Chemistry B, 2017. **5**(35): p. 7415-7425.
32. Bachle, M. and R.J. Kohal, *A systematic review of the influence of different titanium surfaces on proliferation, differentiation and protein synthesis of osteoblast-like MG63 cells.* Clinical Oral Implants Research, 2004. **15**(6): p. 683-692.
33. Boyan, B.D., et al., *Osteoblasts generate an osteogenic microenvironment when grown on surfaces with rough microtopographies.* Eur Cell Mater, 2003. **6**: p. 22-7.
34. Faia-Torres, A.B., et al., *Differential regulation of osteogenic differentiation of stem cells on surface roughness gradients.* Biomaterials, 2014. **35**(33): p. 9023-9032.
35. Yang, W., et al., *Surface topography of hydroxyapatite promotes osteogenic differentiation of human bone marrow mesenchymal stem cells.* Mater Sci Eng C Mater Biol Appl, 2016. **60**: p. 45-53.
36. Qi, L., et al., *The Effects of Topographical Patterns and Sizes on Neural Stem Cell Behavior.* Plos One, 2013. **8**(3).

37. Yin, Z., et al., *Electrospun scaffolds for multiple tissues regeneration in vivo through topography dependent induction of lineage specific differentiation.* Biomaterials, 2015. **44**: p. 173-185.
38. Dalby, M.J., et al., *The control of human mesenchymal cell differentiation using nanoscale symmetry and disorder.* Nature Materials, 2007. **6**(12): p. 997-1003.
39. Werner, M., et al., *Surface Curvature Differentially Regulates Stem Cell Migration and Differentiation via Altered Attachment Morphology and Nuclear Deformation.* Advanced Science, 2017. **4**(2).
40. Kim, S.Y., et al., *Effect of topographical control by a micro-molding process on the activity of human Mesenchymal Stem Cells on alumina ceramics.* Biomater Res, 2015. **19**: p. 23.
41. Faia-Torres, A.B., et al., *Osteogenic differentiation of human mesenchymal stem cells in the absence of osteogenic supplements: A surface-roughness gradient study.* Acta Biomater, 2015. **28**: p. 64-75.
42. Alessandri, M., et al., *Influence of biological matrix and artificial electrospun scaffolds on proliferation, differentiation and trophic factor synthesis of rat embryonic stem cells.* Matrix Biol, 2014. **33**: p. 68-76.
43. Xu, X., et al., *Controlling Major Cellular Processes of Human Mesenchymal Stem Cells using Microwell Structures.* Advanced Healthcare Materials, 2014. **3**(12): p. 1991-2003.
44. Yang, Y., et al., *Biophysical Regulation of Cell Behavior-Cross Talk between Substrate Stiffness and Nanotopography.* Engineering, 2017. **3**(1): p. 36-54.
45. Du, J., et al., *Integrin activation and internalization on soft ECM as a mechanism of induction of stem cell differentiation by ECM elasticity.* Proceedings of the National Academy of Sciences of the United States of America, 2011. **108**(23): p. 9466-9471.
46. Wu, K.C., et al., *Nanotechnology in the regulation of stem cell behavior.* Science and Technology of Advanced Materials, 2013. **14**(5).
47. Provenzano, P.P. and P.J. Keely, *Mechanical signaling through the cytoskeleton regulates cell proliferation by coordinated focal adhesion and Rho GTPase signaling.* Journal of Cell Science, 2011. **124**(8): p. 1195-1205.
48. Bhadriraju, K., et al., *Activation of ROCK by RhoA is regulated by cell adhesion, shape, and cytoskeletal tension.* Experimental Cell Research, 2007. **313**(16): p. 3616-3623.
49. Khatiwala, C.B., et al., *ECM Compliance Regulates Osteogenesis by Influencing MAPK Signaling Downstream of RhoA and ROCK.* Journal of Bone and Mineral Research, 2009. **24**(5): p. 886-898.
50. Franceschi, R.T., et al., *Multiple signaling pathways converge on the Cbfa1/Runx2 transcription factor to regulate osteoblast differentiation.* Connective Tissue Research, 2003. **44**: p. 109-116.
51. Starr, D.A. and H.N. Fridolfsson, *Interactions Between Nuclei and the Cytoskeleton Are Mediated by SUN-KASH Nuclear-Envelope Bridges.* Annual Review of Cell and Developmental Biology, Vol 26, 2010. **26**: p. 421-444.
52. Heo, S.J., et al., *Differentiation alters stem cell nuclear architecture, mechanics, and mechano-sensitivity.* Elife, 2016. **5**: p. e18207-18228
53. Werner, M., et al., *Surface Curvature Differentially Regulates Stem Cell Migration and Differentiation via Altered Attachment Morphology and Nuclear Deformation.* Adv Sci (Weinh), 2017. **4**(2): p. 1600347.

54. Le, H.Q., et al., *Mechanical regulation of transcription controls Polycomb-mediated gene silencing during lineage commitment*. Nature Cell Biology, 2016. 18(8): p. 864-875
55. Downing, T.L., et al., *Biophysical regulation of epigenetic state and cell reprogramming.* Nature Materials, 2013. **12**(12): p. 1154-1162.

Chapter II

Evaluation of human mesenchymal stem cell senescence, differentiation and secretion behavior cultured on polycarbonate cell culture inserts

Clinical Hemorheology and Microcirculation 2018; 70: 573-583.

https://doi.org/10.3233/CH-189322

Evaluation of human mesenchymal stem cell senescence, differentiation and secretion behavior cultured on polycarbonate cell culture inserts

Jie Zou [1, 2 #], Weiwei Wang [1 #], Karl Kratz [1, 3], Xun Xu [1, 2], Yan Nie [1], Nan Ma [1, 2, 3 *] and Andreas Lendlein [1, 2, 3 *]

[1] Institute of Biomaterial Science and Berlin-Brandenburg Center for Regenerative Therapies, Helmholtz-Zentrum Geesthacht, Kantstraße 55, 14513 Teltow, Germany
[2] Institute of Chemistry and Biochemistry, Freie Universität Berlin, Takustraße 3, 14195 Berlin, Germany
[3] Helmholtz Virtual Institute - Multifunctional Materials in Medicine, Berlin and Teltow, Kantstraße 55, 14513 Teltow, Germany

[#]These authors contributed equally to this work.

Corresponding Authors: nan.ma@hzg.de; andreas.lendlein@hzg.de

Abstract

Polycarbonate (PC) substrate is well suited for culturing human mesenchymal stem cells (MSCs) with high proliferation rate, low cell apoptosis rate and negligible cytotoxic effects. However, little is known about the influence of PC on MSC activity including senescence, differentiation and secretion. In this study, the PC cell culture insert was applied for human MSC culture and was compared with polystyrene (PS) and standard tissue culture plate (TCP). The results showed that MSCs were able to adhere on PC surface, exhibiting a spindle-shaped morphology. The size and distribution of focal adhesions of MSCs were similar on PC and TCP. The senescence level of MSCs on PC was comparable to that on TCP, but was significantly lower than that on PS. MSCs on PC were capable of self-renewal and differentiation into multiple cell lineages, including osteogenic and adipogenic lineages. MSCs cultured on PC secreted a higher level inflammatory cytokines and pro-angiogenic factors including FGF2 and VEGF. Conclusively, PC represents a promising cell culture material for human MSCs.

Key words: polycarbonate, human mesenchymal stem cells, differentiation, cytokine secretion, senescence

1. Introduction

Mesenchymal stem cells (MSCs) attracted interest because of their promising therapeutic potential in regenerative medicine due to their self-renewal, multi-lineages differentiation potential and the secretion of a variety of functional cytokines [1, 2]. MSCs can be obtained from different tissues, such as bone marrow, adipose tissue and umbilical cord tissue [3, 4]. However, the quantity of MSCs that separated from those tissues can not satisfy the needs of clinic cell therapy (10–400 million MSCs per treatment) [5]. Therefore, the isolated MSCs need to be expanded *in vitro* before implantation. It has been shown that MSCs are very sensitive to the substrate properties such as the extracellular matrix (ECM) stiffness [6], surface topography [7] and chemical property of the culture surface [8]. The functions and behavior of MSCs can be influenced during the period of cell expansion *in vitro* [9].

Polycarbonate (PC) has technological significance in life science applications, such as intravenous connection components or cell culture devices [10, 11]. Favorable properties of PC include the high light transmittance, impact toughness, dimensional stability, creep resistance and thermoplastic process ability [12]. In addition, PC can be sterilized by a variety of methods including ethylene oxide (EtO), irradiation and steam autoclaving. As cell culture devices, PC exhibited excellent cell compatibility, favoring cell adhesion and proliferation [13]. However, there are few reports about the influence of PC on the most important behaviors of MSCs such as senescence, differentiation and secretion.

The aim of this study was to evaluate the cellular response of human bone marrow mesenchymal stem cells (hBMSCs) to PC. The PC inserts were applied for hBMSC cultivation without further modification. In parallel, the commercial polystyrene-based tissue culture plate (TCP) with surface modification for adherent cells and the polystyrene (PS) inserts without surface modification were used as the positive and negative reference materials, respectively. The cell adhesion, morphology, senescence, cytokine secretion, and differentiation of hBMSCs on PC, PS and TCP were compared.

2. Materials and methods

2.1 Materials for cell culture

The polycarbonate (PC, trade name Makrolon® 2805, Bayer, Germany) and polystyrene (PS, Type 158K, BASF, Germany) cell culture inserts were fabricated via injection molding [14]. The surfaces of PS and PC inserts showed the similarity in both mechanical properties and surface profile, as reported previously [13]. The Young's modulus of PC and PS was 13 ± 2

and 16 ± 4 GPa respectively, as measured with AFM indentation. Profilometry analysis at an area of 7 × 7 mm^2 indicated that the bottom roughness of the inserts is at a similar level (root mean square roughness (Rq) = 0.12 ± 0.04 µm for PS and 0.34 ± 0.13 µm for PC). In addition, the PS and PC presented comparable surface wettability (water advancing contact angle 85 ± 8° for PC and 99 ± 5° for PS), as determined via water contact angle measurement using the captive bubble method [13]. Prior to cell culture, the PC and PS inserts were sterilized via gas sterilization (gas phase: 10% (v/v) ethylene oxide, 54 °C, 65% relative humidity, 1.7 bar, 3 hours of gas exposure time and 21 hours of aeration phase). In addition, the tissue culture plate (TCP, Coring, New York, USA) was used in this study as a positive control material.

2.2 Human bone marrow mesenchymal stem cells (hBMSCs)

The hBMSCs were purchased from Merck Millipore (SCC034, Merk Millipore, Darmstadt, Germany). The cells were maintained in MesenPRO RS™ growth medium (ThermoFisher Scientific, Waltham, USA), in a humidified atmosphere containing 5% (v/v) CO_2. The medium was changed in every 3 days. For hBMSC phenotype characterization, the cells were harvested and stained with a Human MSC Analysis Kit (StemflowTM, BD Biosciences, Heidelberg, Germany) according to the manufacturer's instruction. A flow cytometer (MACSQuant®, Miltenyi Biotec, Bergisch Gladbach, Germany) was used to analyze the cells and the data was processed using Flowjo software (Tree Star Inc., Ashland OR, USA).

2.3 Immunostaining

Cells were fixed with 4% (w/v) paraformaldehyde (Sigma–Aldrich, St. Louis, MO USA) and permeabilized with 0.1% (v/v) Triton X-100 (Sigma–Aldrich, St. Louis, MO, USA), then blocked with 3% (w/v) BSA buffer. Vinculin was stained with mouse anti-human vinculin monoclonal antibody (Merck Millipore, Darmstadt, Germany) and Alexa Fluor® 488 labeled IgG antibody (Life Technologies, Darmstadt, Germany). F-actin was stained with ActinRed™ 555 (Life Technologies, Darmstadt, Germany). After washing, the cells were visualized with a confocal laser scanning microscope (LSM 780 META, Carl Zeiss, Jena Germany).

2.4 Senescence assay

The senescence-associated β-galactosidase activity of hBMSCs cultured on different materials was quantified using a cellular senescence assay kit (Cell Biolabs, Inc., San Diego, CA, USA) according to the manual introduction at different time points (day 1, 8, 15 and 22). The concentration of the total protein in the cell extraction was determined using a BCA protein

assay kit (Thermo Fisher Scientific, Bonn, Germany). The cellular senescence level was expressed as the fluorescent intensity normalized with the amount of total protein.

2.5 Secretion assay

The cytokines in the conditioned medium and the cell number were quantified at day 4, 7, 10, 13, 16 and 19. The cytokines in the conditioned medium were quantified using a Bio-Plex® 200 system (BioRad, Munich, Germany) according to the manufacturer's instructions. The cell numbers at different time points were determined using a Cell Counting Kit-8 (CCK-8, Dojindo Molecular Technologies, Munich, Germany) as described before [13]. To evaluate the activity of cell secretion, the cytokine amount was normalized with the cell number.

2.6 Differentiation assay

For the differentiation study, the hBMSCs were cultured in osteogenic (StemPro Osteogenesis differentiation kit) and adipogenic (StemPro Adipogenesis differentiation kit) induction media, respectively. The induction media were changed in every 3 days. To evaluate the adipogenic differentiation, the cells were cultured in adipogenic induction medium for 14 days. Then the cells were fixed with 4% (w/v) paraformaldehyde and permeabilized with 0.1% (v/v)Triton X-100 solution. After blocking with 3% (w/v) BSA, staining was performed using rabbit anti-human FABP-4 monoclonal antibody (Merck Millipore, Darmstadt, Germany) and Alexa Fluor® 488 labeled IgG antibodies (Life Technologies, Darmstadt, Germany). Cell nuclei were stained with SYTOX Green Nucleic Acid Stain (Life Technologies, Darmstadt, Germany). The stained samples were scanned with a confocal laser scanning microscope (LSM 780, Carl Zeiss, Jena, Germany). Osteogenic differentiation was evaluated after culturing the cells in osteogenic induction medium for 21 days. The cells were fixed with 4% (w/v) paraformaldehyde, and Alizarin red S (Sigma–Aldrich, St. Louis, MO, USA) staining was performed to detect the mineral deposition.

2.7 Statistics

The number of replication for quantitative experiments was three as indicated in figure legend, and the data were expressed as mean ± standard deviation (SD). Statistical analysis was performed using two-tailed independent samples t-test, and a significant level (Sig.) < 0.05 was considered to be statistically significant.

3. Results

3.1 hBMSC phenotype

To analyze the phenotype of the cells, the cell morphology and surface markers were characterized. The cells presented the typical MSC's spindle-shaped morphology (Fig. 1A). Furthermore, the cell surface markers were analyzed with flow cytometry. The results indicated that the typical MSC markers (CD44, CD73, CD90 and CD105) were well preserved in the cells and the non-MSC markers (CD45, CD34, CD11b, CD19 and HLA-DR) were not detected (Fig. 1 B- F).

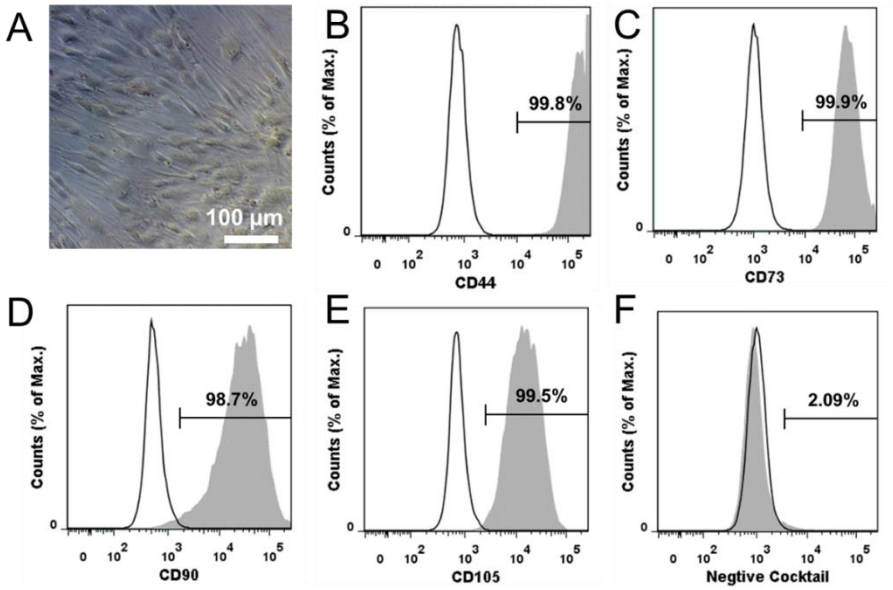

Fig. 1 Characterization of hBMSCs. A: The image of hBMSCs growing on TCP. B, C, D, and E: characterization of MSC phenotypic markers (CD44, CD90, CD105 and CD73). F: characterization of non-MSC markers (CD45, CD34, CD11b, CD19 and HLA-DR).

3.2 Immunostaining of focal adhesion complex

To study the cell-material interaction, the formation of focal adhesions (FAs) was examined by immunofluorescent staining of vinculin and F-actin (Fig. 2). As hBMSCs were difficult to attach and spread on PS surface, the FA formation of cells on PC and TCP surfaces were characterized. After 4 days of cultivation in growth medium, the cells spread out on the PC and TCP. The F-actin cytoskeleton organization and FA complex formation were similar in cells growing on PC and TCP.

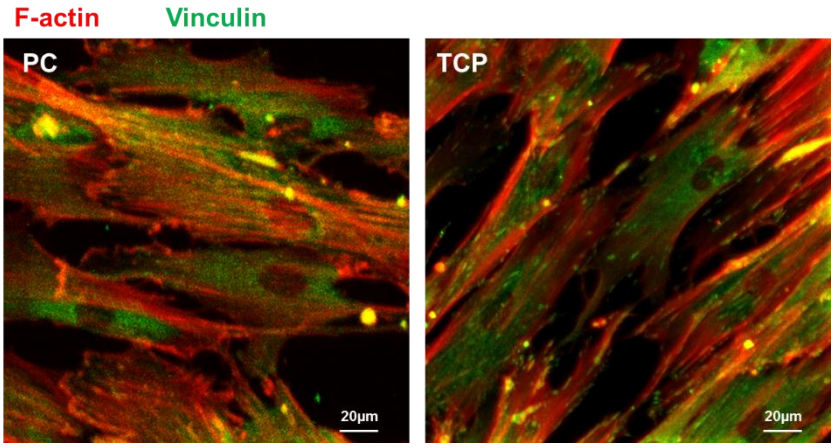

Fig. 2 Representative laser scanning microscopic images of hBMSCs cultured on PC and TCP for 4 days. F-actin (red) and vinculin (green) were fluorescently stained. (bar = 20 μm)

3.3 Senescence of hBMSCs

The influence of culture materials on hBMSC senescence level was evaluated by measuring the activity of senescence-associated β-galactosidase (SA-β-gal). The results indicated that in the early stage (day 1) the senescence level of hBMSCs on TCP surface was significantly higher than that on PS. With the elongation of cultivation, the senescence level increased on all of the tested surfaces. The senescence level of cells on PS was higher than that on PC and TCP at day 8 and day 22. There was no significant difference of the senescence level between the cells cultured on PC and TCP (Fig. 3).

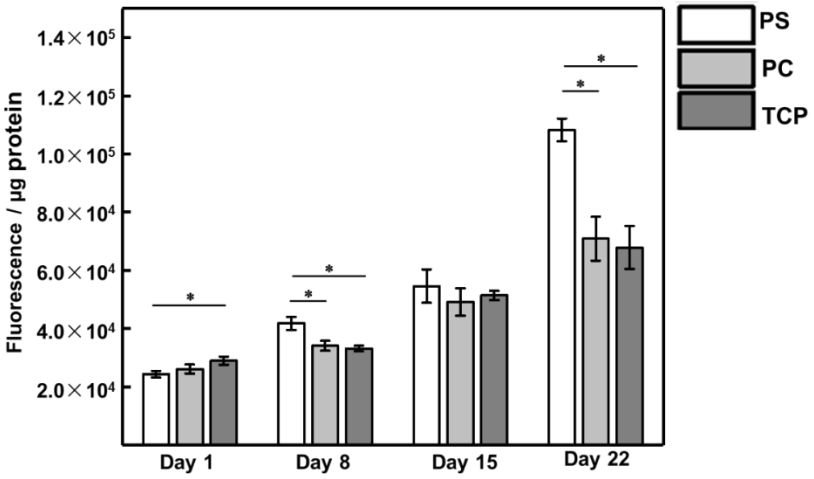

Fig. 3 The senescence level of hBMSCs cultured on different materials at the indicated time points. (n = 3; *Sig < 0.05)

3.4 Cytokine secretion

To analyze the paracrine factors secreted by hBMSCs on different materials, the conditioned media of hBMSC cultures were collected and the factors were quantified (Fig. 4). The paracrine factors secretion level of cells on PS is higher than that on TCP and PC. In the early stage (day 4) the cells on PC showed a higher secretion level than the cells on TCP except for the MCAF secretion. Compared to TCP, the cells on PC secreted the higher level of inflammatory cytokines such as IL-6, IL-17, IFN-γ and TNF-α as well as pro-angiogenic factors including FGF2 and VEGF.

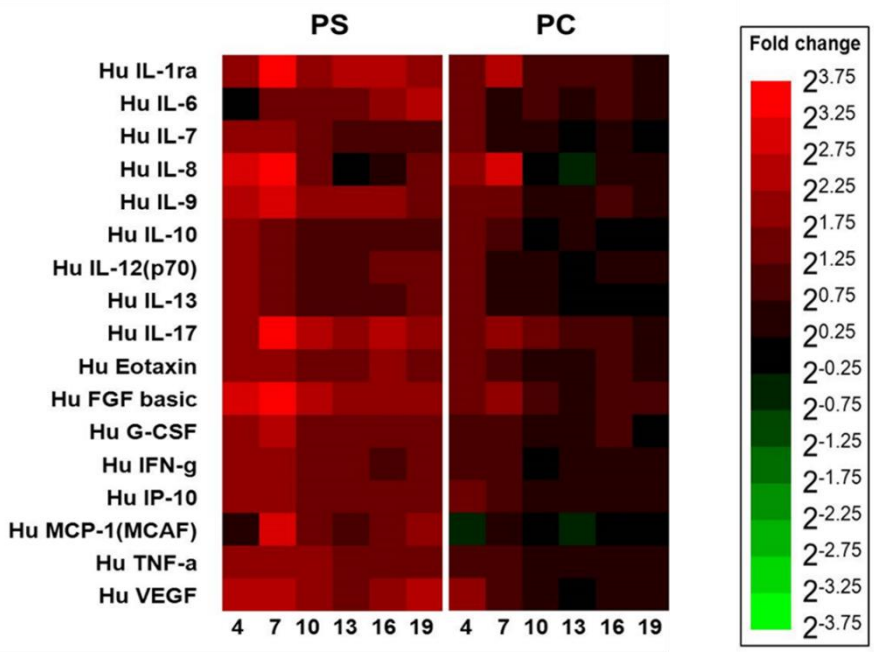

Fig. 4 The heatmap showed the fold change (compared to TCP) of protein secretion over time by hBMSCs seeded on different materials.

3.4 Differentiation of hBMSCs

The osteogenic and adipogenic differentiation of hBMSCs on different materials were examined by Alizarin Red S (ARS) staining and FABP-4 immunostaining, respectively. The results indicated that hBMSCs did not differentiate in the non-induced medium on all of the tested surfaces (Fig. 5). When cultured in osteogenic induction medium, the cells could differentiate into osteoblasts (Fig. 5A). In addition, the immunofluorescence staining of FABP-4 indicated that the hBMSCs could be induced for adipogenic differentiation when adipogenic induction medium was applied (Fig. 5B).

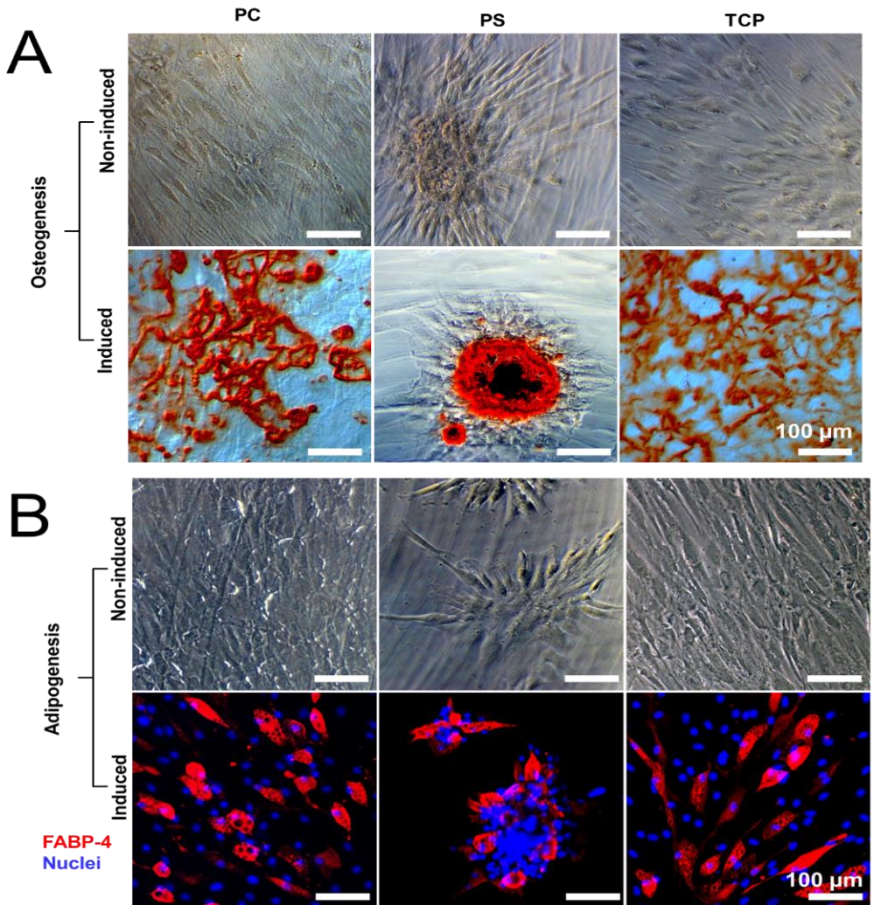

Fig. 5 Differentiation of hBMSCs. A: The representative images of alizarin red S (ARS) staining for characterization of hBMSC osteogenic differentiation on different materials (bar = 100 μm). B: The representative laser scanning microscopic images of FABP-4 immunostaining for characterization of hBMSC adipogenic differentiation (red: FABP-4; blue: nuclei; bar = 100 μm).

4. Discussion

The cell behavior can be regulated by substrate properties such as the surface free energy, the surface polarity [15], the presence of functional groups [16], the stiffness of substrate [17], and the surface topography [18]. The cells actively sense and react to the substrates through the activation of cell surface integrin and then the focal adhesion (FA) complex formation [19-21]. The cell surface integrin activation can further activate the focal adhesion kinase (FAK) which is indispensable for the focal adhesion complex formation [22]. The FA complex consist of many signaling molecules, including the vinculin, talin, paxillin, Src and Cas [23-25]. These signaling molecules can be regulated by chemical and physical properties of the substrates, and play a key role for remolding the size, shape and distribution of FAs [26]. The FAs can be found at the peripheral and central areas of the cells. They are linked with the terminal of F-

actin to regulate cells via transfer the signaling from the outside to inside [27]. Here, the formation and distribution of FAs were characterized by staining F-actin and vinculin. The images showed that the distribution and size of FAs on PC were comparable to that on TCP, indicating the excellent cell compatibility of PC for hBMSC adhesion. This observation was in line with our previous results [13].

MSCs are multipotent cells, which are capable of extensively replicating and maintaining their multi-potential during culture. However, the long-term cell cultivation *in vitro* may lead to cellular aging, alteration of genetic and epigenetic features as well as spontaneous cell transformation [28]. The primary cells do not grow infinitely, but undergo only a limited number of cell division, in a process called cellular senescence [29]. The MSCs cease growth *in vitro* at about 40 to 50 cell doublings [30]. The stem cell senescence could result in impaired regenerative capacity and reduced tissue function, which might consequently lead to organismal aging i*n vivo* [31-34].

The senescent cells undergo irreversible growth arrest but the metabolism is active. They normally present a large and flat morphology, and display the characteristic changes in gene expression. Senescent cells typically exhibit an increase of senescence-associated β-galactosidase (SA-β-gal) activity [35, 36]. In this study, the result showed that with the elongation of cultivation the senescence level of hBMSCs increased on all of the tested materials, which could be explained by the regulation from the genetic factors. The senescence level of hBMSCs on PS was significantly higher than that on PC and TCP, which might be caused by the poor cell adhesion and spreading of cells on PS [13].

In addition to growth arresting, morphology change and accumulation of lipofuscin in cell plasma, senescence in stem cells could cause the damage of DNA and the alteration of functions [35]. In senescent MSCs, the potential of differentiation decreased with the disruption of the balance between osteogenic and adipogenic differentiation [37-39]. Moreover, long-term cultivation of MSCs could result in the complete loss of osteogenic potential and the decrease of adipogenic potential [40]. In this study, similar to hBMSCs on TCP, cells cultured on PC could be induced to differentiate towards osteogenic and adipogenic lineages by induction medium, and keep undifferentiated status in growth medium. These results demonstrated that the hBMSCs were capable of maintaining their self-renewing and differentiation potential on PC.

MSCs can secrete a broad range of paracrine factors [1, 2, 41, 42]. These factors could exert the anti-inflammatory, anti-apoptotic, anti-fibrotic and pro-angiogenic functions [43]. The secretion of MSCs could be modulated by various cues from the microenvironment, such as the extracellular matrix (ECM) stiffness [6], surface topography[7] and the chemical property of substrate surface [8]. In our study, the hBMSCs on PS showed higher secretion activity compared to that on PC and TCP, which might be due to the poor cell adhesion and low cell number on PS. Notably, the higher secretion activity of inflammatory cytokines and pro-angiogenic factors including FGF2 and VEGF was observed in cells on PC, as compared to those on TCP. Since VEGF is one of the most important grow factors for promoting angiogenesis [44], this observation suggested that the pro-angiogenic capacity of MSCs might be improved by cultivation on PC.

In summary, our results demonstrated the high cell biocompatibility of PC for stem cell cultivation. The hBMSCs could attach on PC, forming FAs and cytoskeleton similar to those on TCP. Their self-renewal and differentiation potential could be maintained. Compared to TCP, hBMSCs on PC presented a comparable level of senescence and a higher secretion activity.

5. Conclusion

In this study, the hBMSC senescence level, secretion behavior and differentiation potential on PC were evaluated comparing cell culture on TCP and PS. The PC showed high cell compatibility for hBMSC adhesion and spreading. Cells on PC presented the similar focal adhesion and cytoskeletal structure, as compared to TCP. The cellular senescence of hBMSCs on PC was at a comparable level to that on TCP. Cells on PC showed a higher secretion activity than on TCP, with the upregulated inflammatory cytokines and pro-angiogenic factors. The hBMSCs could maintain their stemness in growth medium on PC, and could undergo osteogenic and adipogenic differentiation. Conclusively, PC represents a promising culture material for stem cells.

Acknowledgements

The authors acknowledge Robert Jeziorski and Mario Rettschlag for preparation of sterilized PS and PC inserts. This work was financially supported by the Helmholtz Association (Helmholtz-Portfolio Topic “Technology and Medicine”, Helmholtz Virtual Institute “Multifunctional Biomaterials for Medicine” (VH-VI-423), Helmholtz Graduate School of Macromolecular Bioscience (MacroBio), and programme-oriented funding).

Reference

1. Hsiao, S.T.F., et al., *Comparative Analysis of Paracrine Factor Expression in Human Adult Mesenchymal Stem Cells Derived from Bone Marrow, Adipose, and Dermal Tissue.* Stem Cells and Development, 2012. **21**(12): p. 2189-2203.
2. de Girolamo, L., et al., *Mesenchymal Stem/Stromal Cells: A New "Cells as Drugs" Paradigm. Efficacy and Critical Aspects in Cell Therapy.* Current Pharmaceutical Design, 2013. **19**(13): p. 2459-2473.
3. Passeri, S., et al., *Isolation and expansion of equine umbilical cord-derived matrix cells (EUCMCs).* Cell Biology International, 2009. **33**(1): p. 100-105.
4. Toupadakis, C.A., et al., *Comparison of the osteogenic potential of equine mesenchymal stem cells from bone marrow, adipose tissue, umbilical cord blood, and umbilical cord tissue.* American Journal of Veterinary Research, 2010. **71**(10): p. 1237-1245.
5. Estrada, J.C., et al., *Human mesenchymal stem cell-replicative senescence and oxidative stress are closely linked to aneuploidy.* Cell Death & Disease, 2013. **4**: p. 691-703.
6. Gattazzo, F., A. Urciuolo, and P. Bonaldo, *Extracellular matrix: A dynamic microenvironment for stem cell niche.* Biochimica Et Biophysica Acta-General Subjects, 2014. **1840**(8): p. 2506-2519.
7. Li, Z.D., et al., *Integrin beta 1 activation by micro-scale curvature promotes pro-angiogenic secretion of human mesenchymal stem cells.* Journal of Materials Chemistry B, 2017. **5**(35): p. 7415-7425.
8. Mann, C.J., et al., *Aberrant repair and fibrosis development in skeletal muscle.* Skeletal Muscle, 2011. **1**: p. 1-21.
9. Jiang, T.M., et al., *In vitro expansion impaired the stemness of early passage mesenchymal stem cells for treatment of cartilage defects.* Cell Death & Disease, 2017. **8**: p. 2851-2862.
10. Siebert, W.E., S. Mai, and S. Kurtz, *Retrieval analysis of a polycarbonate-urethane acetabular cup: a case report.* J Long Term Eff Med Implants, 2008. **18**(1): p. 69-74.
11. Tang, Y.W., et al., *Influence of surface morphology and chemistry on the enzyme catalyzed biodegradation of polycarbonate-urethanes.* Journal of Biomaterials Science-Polymer Edition, 2002. **13**(4): p. 463-483.
12. Humme, G., H. Rohr, and V. Serini, *Structure and Properties of Multiphase Plastics .2. Rubber Modified Polycarbonates.* Angewandte Makromolekulare Chemie, 1977. **58**(Feb): p. 85-94.
13. Wang, W., et al., *The influence of polymer scaffolds on cellular behaviour of bone marrow derived human mesenchymal stem cells.* Clin Hemorheol Microcirc, 2012. **52**(2-4): p. 357-73.
14. Hiebl, B., et al., *Cytocompatibility testing of cell culture modules fabricated from specific candidate biomaterials using injection molding.* Journal of Biotechnology, 2010. **148**(1): p. 76-82.
15. Razafiarison, T., et al., *Biomaterial surface energy-driven ligand assembly strongly regulates stem cell mechanosensitivity and fate on very soft substrates.* Proceedings of the National Academy of Sciences of the United States of America, 2018. **115**(18): p. 4631-4636.

16. Cao, B., et al., *Effects of Functional Groups of Materials on Nonspecific Adhesion and Chondrogenic Induction of Mesenchymal Stem Cells on Free and Micropatterned Surfaces.* Acs Applied Materials & Interfaces, 2017. **9**(28): p. 23574-23585.
17. Lv, H.W., et al., *Mechanism of regulation of stem cell differentiation by matrix stiffness.* Stem Cell Research & Therapy, 2015. **6**: p. 103-113.
18. Metavarayuth, K., et al., *Influence of Surface Topographical Cues on the Differentiation of Mesenchymal Stem Cells in Vitro.* Acs Biomaterials Science & Engineering, 2016. **2**(2): p. 142-151.
19. Lee, D.A., et al., *Stem Cell Mechanobiology.* Journal of Cellular Biochemistry, 2011. **112**(1): p. 1-9.
20. Delaine-Smith, R.M. and G.C. Reilly, *Mesenchymal stem cell responses to mechanical stimuli.* Muscles Ligaments Tendons J, 2012. **2**(3): p. 169-80.
21. Subramony, S.D., et al., *The guidance of stem cell differentiation by substrate alignment and mechanical stimulation.* Biomaterials, 2013. **34**(8): p. 1942-53.
22. Michael, K.E., et al., *Focal Adhesion Kinase Modulates Cell Adhesion Strengthening via Integrin Activation.* Molecular Biology of the Cell, 2009. **20**(9): p. 2508-2519.
23. Sawada, Y., et al., *Force sensing by mechanical extension of the Src family kinase substrate p130Cas.* Cell, 2006. **127**(5): p. 1015-1026.
24. Brown, A.E.X. and D.E. Discher, *Conformational Changes and Signaling in Cell and Matrix Physics.* Current Biology, 2009. **19**(17): p. R781-R789.
25. Zaidel-Bar, R., et al., *Hierarchical assembly of cell-matrix adhesion complexes.* Biochemical Society Transactions, 2004. **32**: p. 416-420.
26. Engler, A.J., et al., *Matrix elasticity directs stem cell lineage specification.* Cell, 2006. **126**(4): p. 677-689.
27. Hotchin, N.A. and A. Hall, *The assembly of integrin adhesion complexes requires both extracellular matrix and intracellular rho/rac GTPases.* Journal of Cell Biology, 1995. **131**(6): p. 1857-1865.
28. Lepperdinger, G., et al., *Controversial issue: Is it safe to employ mesenchymal stem cells in cell-based therapies?* Experimental Gerontology, 2008. **43**(11): p. 1018-1023.
29. Hayflick, L., *The Limited in Vitro Lifetime of Human Diploid Cell Strains.* Exp Cell Res, 1965. **37**: p. 614-36.
30. Stenderup, K., et al., *Aging is associated with decreased maximal life span and accelerated senescence of bone marrow stromal cells.* Bone, 2003. **33**(6): p. 919-926.
31. Gago, N., et al., *Age-Dependent Depletion of Human Skin-Derived Progenitor Cells.* Stem Cells, 2009. **27**(5): p. 1164-1172.
32. Maslov, A.Y., et al., *Neural stem cell detection, characterization, and age-related changes in the subventricular zone of mice.* Journal of Neuroscience, 2004. **24**(7): p. 1726-1733.
33. Molofsky, A.V., et al., *Increasing p16INK4a expression decreases forebrain progenitors and neurogenesis during ageing.* Nature, 2006. **443**(7110): p. 448-52.
34. Jones, D.L. and T.A. Rando, *Emerging models and paradigms for stem cell ageing.* Nat Cell Biol, 2011. **13**(5): p. 506-12.
35. Turinetto, V., E. Vitale, and C. Giachino, *Senescence in Human Mesenchymal Stem Cells: Functional Changes and Implications in Stem Cell-Based Therapy.* International Journal of Molecular Sciences, 2016. **17**(7): p. 1164-1181.

36. Rodier, F., et al., *DNA-SCARS: distinct nuclear structures that sustain damage-induced senescence growth arrest and inflammatory cytokine secretion.* Journal of Cell Science, 2011. **124**(1): p. 68-81.
37. Banfi, A., et al., *Proliferation kinetics and differentiation potential of ex vivo expanded human bone marrow stromal cells: Implications for their use in cell therapy.* Experimental Hematology, 2000. **28**(6): p. 707-715.
38. Geissler, S., et al., *Functional Comparison of Chronological and In Vitro Aging: Differential Role of the Cytoskeleton and Mitochondria in Mesenchymal Stromal Cells.* Plos One, 2012. **7**(12): p. 52700-52712.
39. Kornicka, K., et al., *The Effect of Age on Osteogenic and Adipogenic Differentiation Potential of Human Adipose Derived Stromal Stem Cells (hASCs) and the Impact of Stress Factors in the Course of the Differentiation Process.* Oxidative Medicine and Cellular Longevity, 2015. **2015**: p. 309169-309188.
40. Geissler, S., et al., *Functional comparison of chronological and in vitro aging: differential role of the cytoskeleton and mitochondria in mesenchymal stromal cells.* PLoS One, 2012. **7**(12): p. e52700.
41. Konala, V.B.R., et al., *The current landscape of the mesenchymal stromal cell secretome: A new paradigm for cell-free regeneration.* Cytotherapy, 2016. **18**(1): p. 13-24.
42. Meirelles, L.D., et al., *Mechanisms involved in the therapeutic properties of mesenchymal stem cells.* Cytokine & Growth Factor Reviews, 2009. **20**(5-6): p. 419-427.
43. Park, W.S., et al., *Strategies to enhance paracrine potency of transplanted mesenchymal stem cells in intractable neonatal disorders.* Pediatric Research, 2018. **83**(1): p. 214-222.
44. Hoeben, A., et al., *Vascular endothelial growth factor and angiogenesis.* Pharmacological Reviews, 2004. **56**(4): p. 549-580.

Chapter III

Substrate surface topography promotes human bone marrow mesenchymal stem cell osteogenic differentiation via histone modification of osteogenic genes

(Manuscript)

Substrate surface topography promotes human bone marrow mesenchymal stem cell osteogenic differentiation via histone modification of osteogenic genes

Jie Zou [1, 2 #], Weiwei Wang [1 #], Xun Xu [1, 2 #], Karl Kratz [1, 3], Zijun Deng[1], Nan Ma [1, 2,3 *] and Andreas Lendlein [1, 3 *]

[1] Institute of Biomaterial Science and Berlin-Brandenburg Centre for Regenerative Therapies, Helmholtz-Zentrum Geesthacht, Teltow, Germany

[2] Institute of Chemistry and Biochemistry, Free University of Berlin, Berlin, Germany

[3] Helmholtz Virtual Institute − Multifunctional Materials in Medicine, Berlin and Teltow, Germany

[#] These authors contributed equally to this work.

* To whom correspondence should be addressed: Prof. Dr. Nan Ma, Prof. Dr. Andreas Lendlein

Email: nan.ma@hzg.de, andreas.lendlein@hzg.de

Phone: +49 (0)3328 352-450

Fax: +49 (0)3328 352-452

Abstract:

Mesenchymal stem cell behaviors and lineage commitments can be steered by the mechanical properties of their microenvironment. In this study, polycarbonate substrate with spongy bone -like microarchitecture were fabricated as a model system, to evaluate the influence of spongy bone -like microarchitecture on human bone marrow mesenchymal stem cell (hBMSC) osteogenic differentiation on the epigenetic modification. It is found that spongy bone -like microarchitecture promoted assembling of G-actin into F-actin of hBMSC and enhanced cell contractility by upregulating MLC expression. The increased cell contractility led to YAP activation and the higher aspect ratio of cell nucleus. This unique mechanical stimuli can further be sensed by the nuclear membrane protein and nuclear pore complex, presenting higher levels of active form lamins A/C. On the epigenetic level, there was the alternated histone modification profile, particularly the enrichment of H3K27me3 and H3K9Ac on the upstream of osteogenic genes (ALPL, RUNX2 and BGLAP). These findings not only allow us to give a better understanding of the mechanism how material surface topography affects stem cell fate but also to provide new insights in designing and developing implants and biomedical devices.

Key words: topographical cues, hBMSCs, cytoskeleton contractility, histone modification, osteogenic differentiation

1. Introduction

Mesenchymal stem cells (MSCs) can differentiate into multiple lineages, including osteoblasts, chondrocytes and adipocytes [1]. Bone marrow, particularly the red bone marrow, is a major cell source of MSCs typically filling the multi-porous structure of trabecular bone in adult tissue [2]. Trabecular bone, as the native microenviroment of BMSCs, has a spongy-like microarchitecture, which is highly heterogeneous and anisotropic. The microarchitecture of the substrate has a strong influence to MSCs linage commitment [3, 4]. Scaffolds with pore sizes close to 300 μm, similar to pore size of spongy bone, can promote BMSC osteogenesis *in vivo* [5-7]. A smaller pore size (100 μm) was more favorable for MSCs chondrogenic differentiation [8]. However, the mechanism of how the spongy bone-like microstructure promotes BMSCs osteogenic differentiation is largely unexplored.

The topographical cues from the interface regulate MSCs major cellular functions [9]. The topographical cues can be sensed and transferred to biological signals by MSCs, the biological signals transmitted into the cell result in cytoskeletal remodeling and changes of cell contractility [10]. Actin microfilaments (F-actin) are the major structure of the cytoskeleton, the surface topography regulated signals lead to F-actin polymerization/depolymerization as well as affect the activation of myosin, which modulates cell contractility via sliding on F-actin in a polar fashion. Since the cytoskeleton networks further connect to the nucleoskeleton by linker of nucleoskeleton and cytoskeleton (LINC) complex that is composed of nesprins, SUN and lamin proteins, cell nucleus could feel the cell contractility force which is regulated by the surface topographical cues [11] . The force transmitted across the cytoskeleton to the nucleus results in substantial deformation [12, 13]. The nucleus deformation not only limited the nuclear shape changes, but also the nuclear protein conformation and phosphorylation states. Lamin A/C as mechanosensitive proteins that locate on inner nuclear membrane and internal nuclear scaffold can sense the contraction force and provide structural integrity to the nucleus to resist the cytoskeleton contraction force [14]. The mechanosensitive proteins respond to the contraction force via the turnover of phosphorylated amin A/C (p lamin A/C) and lamin A/C[15]. The mechanical force applied on the nucleus increased nuclear membrane tension, which further altered the permeability of nuclear pore complexes(NPC)[16]. The force-mediated alterations to NPC conformations could promote nuclear entry of yes-associated protein (YAP) [17], a mechanosensitive transcription factor, which further regulates the genes expression. However, how the surface topographical cues influence the lamin A/C expression and YAP translocation is not very clear.

In addition, the mechanical force extend to inside of nucleus, where the mechanical force can affect histone acetylation/methylation states and chromatin dynamic in nucleus [18]. The short-term mechanical force applied on nucleus led to the rapid increasing of transcription [19]. However, the long-term force (12 h) applied on MSCs led to the enhancement of H3K27me3 expression, which resulted in heterochromatin and transcription repression, further affected the stem cell lineage [20]. In addition, the internal force that is generated by the actomyosin regulated the methylation and acetylation of H3 and then modulated specific gene expression [21]. The histone acetylation and methylation patterns on specific site control the activation and silencing of transcription [22], which further define the specific cell lineages. The study about the epigenetic mechanisms of stem cell differentiation found the H3K27me3 was an epigenetic control point of adipogenesis [23], the acylation of H3K9 played a key role in regulating stem cell proliferation and osteogenic differentiation [24]. At present, the understanding of the influence of mechanical force on stem cell histone modification is not completely clear. Especially, the exact mechanism how surface topographical cues mediate cell contraction force regulating specific histone modifications for controlling stem cell lineages commitment is not well understood. Precisely engineered micro-structural substrates may further helped to elucidate the effects of topography on BMSCs behavior and the epigenetic controlling of osteogenic process.

In this study, we probe the mechanism of the topographic surface regulating BMSCs differentiation lineages. For the cell culture device, polycarbonate (PC)-based inserts with three kinds of topographical surface on the bottom were fabricated. A smooth surface (sPC) was used here as a control. A surface (mPC) with the value of profile roughness parameter (average peak spacing: RSm) comparable to hBMSC dimension (~ 100 μm in adhesion), while a surface (hPC) with 2.5D topography, and the value of RSm was similar to the pore size of spongy bone. We hypothesize that the substrate surface (hPC) with the topographical cues (RSm value) similar to natural spongy bone pore size could enhance cell contractility, and then modulate cell epigenetics to promote BMSCs osteogenic differentiation. In order to verify the hypothesis, the osteogenic and adipogenic differentiation of hBMSCs on three topographic surfaces were evaluated, the mechanism how surface topographical cues regulate hBMSCs differentiation is investigated. It was found that the topographical cues of hPC enhanced cell contractility by promoting F-actin polymerization and upregulating MLC activation. The increased cell contractility led to the cell nucleus deformation, enhancing YAP nuclear translocation and elevating of Lamin A/C expression. The unique mechanical force further

propagated into nucleus and resulted in altering of histone modification profile, particularly modulating the enrichment of H3K27me3 and H3K9ac on the promoters of osteogenic genes, which regulated hBMSCs osteogenic differentiation. We suggest that the designing of appropriate topographic surface could regulate cell contractility and modulate the epigenetic status of stem cells, and thereby controls stem cells lineage commitments.

2. Experimental section

2.1 Fabrication and characterization of the material for cell culture

Polycarbonate (PC, trade name Makrolon® 2805, Bayer, Germany) inserts with a suitable size to fit the standard 24-well tissue culture plate (TCP) were prepared via injection molding [25]. Three differently structured modules were utilized to fabricate the inserts with different types of bottom surface topography: a module with a polished contact surface (sPC), and two modules with micro-structured surfaces according to the norm DIN 16747: 1981-05, M30 (mPC) and M45 (hPC). The microscale topography of the insert bottom was characterized with an optical profilometer type MicoProf 200, and analyzed with the software AQUIRE (ver. 1.21) and the software MARK III (ver. 3.9) according to the method of previous reported [26]. The inserts were sterilized by gas sterilization (gas phase: 10% (v/v) ethylene oxide, 54 ˚C, 65% relative humidity, 1.7 bar, 3 hours of gas exposure time and 21 hours of aeration phase).

2.2 Cell culture

hBMSCs (SCC034, Merk Millipore, Darmstadt, Germany) were cultured with MesenPRO RS™ growth medium (GM) (ThermoFisher Scientific, Waltham, USA), in a humidified atmosphere containing 5% (v/v) CO_2, and the medium was changed every 2 days. hBMSCs were cultured in the mixed induction media (MM) (osteogenic induction medium: adipogenic induction medium = 1:1) for competitive differentiation. The StemPro Osteogenesis differentiation kit and StemPro Adipogenesis differentiation kit (ThermoFisher Scientific, Waltham, USA) were applied to promote osteogenic and adipogenic differentiation, respectively.

2.3 Chemical and immunofluorescence staining

Chemical staining: 2.0×10^4 hBMSCs were seeded into each insert and cultured in GM for 4 days, thereby MM was used to culture the cells for 21 days. Cells were then fixed with 4% (w/v) paraformaldehyde (Sigma–Aldrich, St. Louis, MO USA) and permeabilized with 0.1% (v/v) Triton X-100 (Sigma–Aldrich, St. Louis, MO, USA) for the further staining. Oil Red O

(Sigma–Aldrich, St. Louis, MO, USA) staining was used to assess the lipid droplets. OsteoImage™ Mineralization Assay kit (Lonza, Basel, Switzerland) was used to stain mineralization deposition according to the protocol that was supplied by manufacturer. And then samples were imaged with inverted light microscopy (Axiovert 40C, Carl Zeiss, Jena Germany) and confocal laser scanning microscope (LSM 780, Carl Zeiss, Jena, Germany).

Immunofluorescence staining: 2.0×10^4 hBMSCs were seeded into each insert. At the indicated time points, cells were fixed with 4% (w/v) paraformaldehyde (Sigma–Aldrich, St. Louis, MO USA) and permeabilized with 0.1% (v/v) Triton X-100 (Sigma–Aldrich, St. Louis, MO, USA), then blocked with 3% (w/v) BSA buffer. F-actin was stained with ActinRed™ 555 Ready Probes (Life Technologies, Darmstadt, Germany). Cell nuclei were stained with Hoechst 33342 (Life Technologies, Darmstadt, Germany). Tri-methylation at histone H3 (Lys27), lamin A/C and p lamin A/C were immunostained by rabbit anti-H3K27me3 antibody, mouse anti-lamin A-C and rabbit anti- phospho-lamin A/C (Ser22) primary antibodies (Cell signaling technologies, Danvers, USA). Anti -mouse IgG (H+L)-Alexa Fluor® 488, and anti-rabbit IgG (H+L)-Alexa Fluor® 633 (Invitrogen, California, USA) were used as secondary antibodies. Samples were visualized with confocal laser scanning microscope.

2.4 Flow cytometry

For the evaluation of the and histone modification level change of cells in different phase, 2.0×10^4 hBMSCs were seeded into each insert and cultured for 4 days in GM, then the samples were divided into two parts. One part of the cells were harvested and fixed; another part, the cells were continuously cultured in MM for 3 days then harvested and fixed. Then two parts of fixed cells were permeabilized and blocked as the same method mentioned before. Subsequently, cells were stained with Alexa Fluor 488 conjugate rabbit anti-H3K27me3 and Pacific Blue conjugated histone H3 antibody (Cell signaling technologies, Danvers, USA) overnight in 4 °C. And for evaluation of lamin A/C expression level of cells on different surfaces, 2.0×10^4 hBMSCs were seeded into each insert and cultured for 4 day in GM, then cells were harvested, permeabilized and blocked, then stained with mouse anti-lamin A-C primary antibody overnight in 4 °C, subsequently, stained with anti-rabbit IgG (H+L)-Alexa Fluor® 633 (Invitrogen, California, USA) secondary antibodies. Then the stained cells were analyzed by the flow cytometry (MACSQuant®, Miltenyi Biotec, Bergisch Gladbach, Germany). Data analysis was performed using “Flowjo” software (Tree Star Inc., Ashland OR, USA).

2.5 Cell contractility assay

The contractility of hBMSCs was evaluated through cell contraction assay kit (Cell Biolabs, Inc., California, USA) following the manufacturer's protocol. Briefly, 2.0×10^4 hBMSCs were seeded into each insert and cultured in GM for 7 days. Then cell were harvested and 50 µl cells ($1 – 2 \times 10^5$ cells) mixed with 200 µl freshly contraction assay collagen. The mixture of cell-collagen (250 µl) was added into the well of 48-well plate and incubated at 37 °C for 1 h, subsequently, GM (400 µl)was added to each collagen gel. After 2 days culture, the cell-collagen gels were released from culture wells. The morphology of the collagen gels (contraction index) were recorded by camera at indicated time points, then the area of the cell-collagen gels were measured with Image J software (National Institutes of Health, USA).

2.6 G-Actin/F-Actin assay

The G-actin and F-actin in cells were quantified by the G-actin/F-actin assay kit (Cytoskeleton Inc., Denver, USA) following the manufacturer's protocol. Briefly, 2.0 × 104 hBMSCs were seeded into each insert and cultured in GM. Cells were lysed by F-actin stabilization buffer and then the lysate was centrifuged by ultracentrifuge (Sorvall/Thermo Scienfic, Massachusetts, USA) and spun at 100000 × g at 37°C for 1h, the F-actin (pellet) and G-actin (supernatant) were separated. The pellets were resuspended in the ice cold depolymerizing buffer. Appropriate loading buffer was added to all samples and boiled 5 min. The levels of G-actin and F-actin were evaluated by western blot and quantified by analyzing the grayscale of bands with Image J software (National Institutes of Health, USA).

2.7 siRNA transfection

Lamin A/C, Nesprin-1, Nesprin-2 and SUN siRNAs (Life Technologies, Darmstadt, Germany) were transfected into hBMSCs using Lipofectamine®2000 (Thermo Fisher Scientific, Waltham, USA) according to the recommended transfection protocol. Briefly, one day before transfection, 2.0×10^4 hBMSCs were seeded into each insert and cultured in 400 medium (GM or MM) without antibiotics. Diluted 1 µl Lipofectamine®2000 in 50 µl Opti-MEM® I reduced serum medium (Thermo Fisch scitific, Waltham, Massachusetts, USA), mixed gently and incubated for 15 min at room temperature; Diluted 200 pmol siRNA in 50 µl Opti-MEM® I reduced serum medium. Mixed the diluted siRNA and diluted Lipofectamine® 2000 (total volume = 111 µl) and incubated for 15 min at room temperature to allow complexes to form. 111 µl siRNA- Lipofectamine® 2000 complexes was added to each well and incubated for 2 days, then the cell culture medium was refreshed by cell culture medium that contained

transfection regents and siRNAs. Cells or cell lysates were collected at day 4 after transfection for further Western blot and flow cytometry analysis.

2.8 Western blotting

The cells were lysed by the RIPA Lysis and Extraction Buffer (Thermo Fisch scitific, Waltham, Massachusetts, USA) which contained a mixture of 1× Halt Protease & Phosphatase Inhibitor Cocktail (Thermo Fisher Scientific, Waltham, Massachusetts, USA) on ice for 10 min. The total protein concentration in the supernatant was measured using a BCA Protein Assay Kit (Thermo Fisher Scientific, Bonn, Germany). Then loading buffer (Bio-Rad, München, Germany) was added to cell lysate and boiled at 95 °C for 5 min. Then equal amounts of protein was loaded into each well of the 10% SDS-PAGE gel and electrophoresis was performed at 120 V for 60 min, then the protein was transferred onto the nitrocellulose membrane (Merck Millipore, Darmstadt, Germany) at a constant current of 220 mA for 70 min. As following, the membrane was blocked with Odyssey Blocking Buffer (LI-COR Biosciences, Lincoln, NE, USA) and stained with anti-Lamin A/C, anti-N-cadherin, and anti-GAPDH (Cell signaling technologies, Danvers, USA) antibodies overnight at 4 °C. Finally, the primary antibodies bound to the membrane were detected with IRDye® 800CW secondary antibody and visualized using an Odyssey® Infrared Imaging System (LI-COR Biosciences, Lincoln, NE, USA).

2.9 Inhibition experiment

Inhibitors were added to cell culture medium (GM or MM) at the following concentrations: Cytochalasin D (Cyto D) (0.2 μM), Belbbistatin (Bleb) (1 μM) (Sigma-Aldrich, St. Louis, MO, USA) [27]. And RGD (10 μg/ mL) (Sigma-Aldrich, St. Louis, MO, USA) [28]. The medium with inhibitors was regularly changed every 2 days. Cells cultured in GM and MM were exposed to inhibitors for 4 days. After 21 days exposure of cells to the inhibitors in MM, the lysate was collected for cell differentiation assay.

2.10 Enzyme-linked immunosorbent assay (ELISA)

hBMSCs were cultured in GM for 4 days or cultured in MM for 21 days were lysed. The pMLC, pYAP and tYAP levels of hBMSCs in GM were measured using pMLC (Mybiosurce, San Diego, USA), pYAP(pSer397) and tYAP ELISA kits (Cell signaling technologies, Danvers, USA). The expression level of osteocalcin (OCN) and fatty acid binding protein 4 (FABP-4) in differentiated hBMSCs (day 21 in MM) were quantified by Human Osteocalcin-ELISA kit (Invitrogen, California, USA) and Human FABP-4 ELISA kit (Abcam, Cambridge, UK). For

normalization, the amount of total protein in the cell extraction was determined using a BCA protein assay kit (Thermo Fisher Scientific, Bonn, Germany).

2.11 ChIP-PCR analysis

To analyze the enrichment of modified histones H3 tails at the promoter region of the osteogenic related genes (ALPL, RUNX2 and BGLAP) in hBMSCs that were cultured on different topographic surface in GM or MM. For the GM group, 2.0×10^4 hBMSCs were seeded into each insert and cultured in GM for 4 days; the MM group 2.0×10^4 hBMSCs were seeded into each insert and cultured in GM for 4 days, then continue cultured in MM for 3 days. After that, the cells were harvested and processed by the SimpleChIP® Enzymatic Chromatin IP Kit (Cell signaling technologies, Danvers, USA) according to the manufacturer's protocol. The rabbit anti-H3K27me3 and rabbit anti-H3K9Ac antibodies (Cell signaling technologies, Danvers, USA) were used in this processing. Quantitative real-time PCR analysis of precipitated DNA relative to inputs using SYBR Green kits (Thermo Fisher Scientific, Bonn, Germany). The sequences of primers (Thermo Fisher Scientific, Bonn, Germany) are listed in supplementary Table 1.

2.12 Statistical analysis

The number of replication for quantitative experiments was equal to or larger than three as indicated respectively in the figure legends. Unless indicated otherwise, the data were expressed as arithmetic mean ± standard deviation (SD). Statistical analysis was performed by one-way ANOVA with post hoc Tukey HSD test. * $P < 0.05$ was considered to be statistically significant.

3. Results and discussion

3.1 Characterization of substrate surface topography

Previous studies have demonstrated that polycarbonate materials have good cell compatibility and similar elastic modulus to trabecular bone [29]. So in this study PC was selected to fabricate the substrates with different topographic surfaces (Fig. 1A). The surfaces microscale topography was characterized and analyzed by optical profilometry (Supplementary Table1 and Fig. 1). The average peak spacing (RSm) of mPC is 160.3 ± 8.2 μm, this value is comparable to the size of hBMSC, and the RSm of hPC is 279.3 ± 32.3 μm, the value is similar to the distance between the trabecular bones in spongy bone [7].

3.2 hPC substrate surface topography enhanced cell contractility

To evaluate the influence of surface topographic cues on cell contraction force, the stabilization of cell cytoskeleton actin, activation of actomyosin as well as cell contractility were tested. The actin cytoskeleton is a dynamic system that constantly reorganizes itself by polymerization (F-actin) and depolymerization (G-actin) cycles to regulate cell adhesion, shape and migration to adapt to its environment. A study had demonstrated MSC osteogenic differentiation and bone formation could be enhanced via inhibiting F-actin depolymerization [30]. In this study, immunofluorescent staining was performed to investigate the F-actin of cells on different topographic surfaces. After 4 days of cell culture, the top-view fluorescent images showed that the fluorescence intensity of cells on hPC was higher than that on sPC and mPC. In addition, distinct difference was observed in cells on different surfaces with respect to their orientation, distribution and F-actin arrangement. The F-actin of cells on sPC and mPC surfaces presented high orientation, in contrast, the F-actin of cells on hPC was less orientated (Fig. 1B top row). The cross-sectional view images showed that there was higher fluorescence intensity on slope positions of hPC than that on other positions (Fig. 1B down row). These results suggested that the topographic surface influences F-actin polymerization and stabilization. To confirm this result, the F-actin/G-actin kit was used to analyze the G-actin/F-actin ratio and the results showed that on day 2, the G-actin/F-actin ratio of cells that were cultured on sPC, mPC and hPC were 0.58 ± 0.10, 0.56 ± 0.05 and 0.49 ± 0.06, respectively. And on day 4, the G-actin/F-actin ratio of cells on these surfaces were slightly increased and the ratio of cells on hPC (0.52 ± 0.09) was significantly lower than that on sPC (0.72 ± 0.07) and mPC (0.62 ± 0.04) (Fig.1C and D). The results confirmed that the hPC surface topographical cues enhanced F-actin polymerization and stabilization. Moreover, on day 4 the G-actin/F-actin ratio were higher than that on day 2, which may be caused by the different F-actin polymerization level at different time points after cell seeding. In the early stage (day 2) the cells attached on surface and started to spread, the polymerization of F-actin kept on high level, with the time elongated (day 4) cells spread completely on surface, the F-actin polymerization level gradually decreased and kept a balance between polymerization and depolymerzation.

The surface topographical cues were sensed by MSC, which guided cell spreading and morphology formation and migration. In this process, the cell internal force (cytoskeletal contractility) that was generated by myosin II activation played an important role. Myosin is the major motor protein responsible for the generation of cell internal force (cytoskeletal contractility), which depends on the phosphorylation of myosin regulatory light chains (pMLC). The result of pMLC expression quantification showed that the cells cultured on hPC had a

significantly higher pMLC expression level than those on sPC and mPC (Fig. 1E), which indicated the hBMSCs cultured on hPC topographic surface generated higher internal force than those on mPC and sPC. With the internal force increasing, the individual filaments (F-actin) are compressed and/or cross-linking proteins become more extended [31], which is consistent with the results of G-actin/F-actin ratio and F-actin immunofluorescence staining.

The contractility of cells that were cultured on different topographic surfaces was evaluated by the cell-collagen mixed gels method. The images of cell-collagen gel showed that the gels significant shrunk after released 24 h (Supplementary Fig. 3). The contractility of cells from different surface was evaluated via calculating the area of shrunk gels and comparing with the initial gels area. The gels with cells from hPC shrunk more seriously than those gels with cells from sPC and mPC. After the gels released 2 h, the area of gels contained cells that from sPC, mPC and hPC shrunk 9%, 16% and 17%, respectively. After 24 h, the gels with cells from hPC shrunk strongest, the area of shrunk gels was 23% compared with the initial gels area, which was much smaller than that cells from sPC (57%) and mPC (35%) (Fig. 1F). The results suggested that the cell contractility of hBMSCs cultured on hPC surface was significantly higher than that on mPC and sPC. And this also can be supported by the phenomenon of cell lift from substrate surface on hPC (data not show). At high cell density condition a part of the cells lifted from the surface at the valley area of hPC topography due to the “pulling” of cells that are located on both sides of the valley. This phenomenon of cell lift could not be found on mPC and sPC (data not show). These results collectively suggested that hPC topographic surface enhanced hBMSCs cell tension.

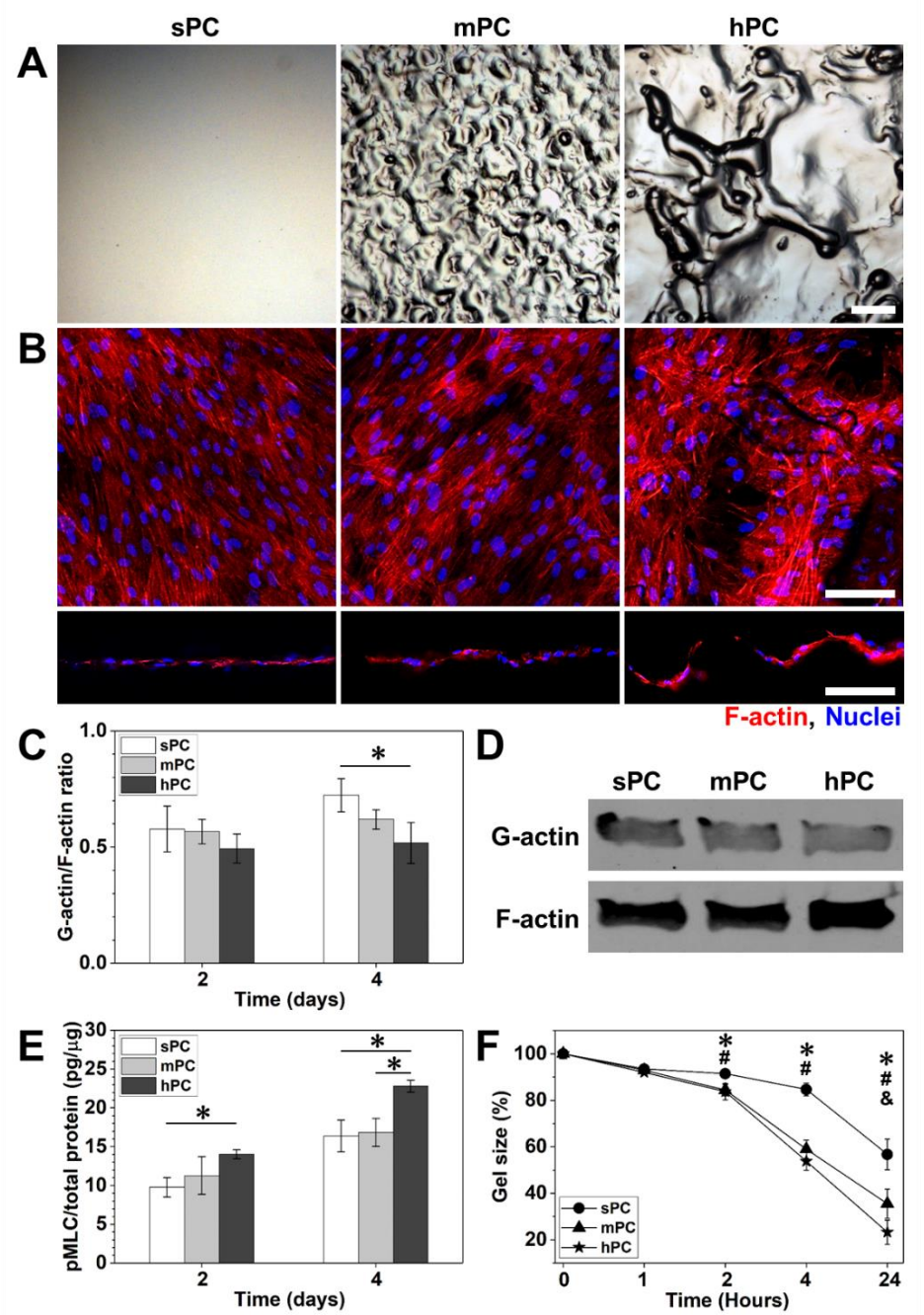

Fig. 1: hPC surface topographical cues enhance hBMSC tension. A Surface topography images of sPC, mPC and hPC (scale bar = 100 μm); B Top-view of immunofluorescence staining images (up) and the cross-sectional view of immunofluorescence staining images (down) (red: F-actin; blue: nuclei; scale bar = 100 μm); C Quantitative analysis of F-actin/G-actin ratio (n = 3; *Sig < 0.05); D Actins were separated by ultracentrifugation to F-actin and G-actin and subjected to western blot analysis ; E The phosphorylated myosin light chain expression level of hBMSCs that were cultured on different topographic surfaces (n = 3; *Sig < 0.05); F Quantitative analysis of cell mixed collage gels area change at different time points. (n = 4; * Sig < 0.05, sPC VS mPC; # Sig < 0.05, sPC VS hPC; & Sig < 0.05, mPC VS hPC).

3.3 Cell contractility influences nuclear deformation

The cytoskeleton network bridges the cell membrane and the nucleus through the LINC complex, thereby the mechanical signals directly transmit to the nuclear [32]. The surface topographical cues mediated cell contraction force is applied on nucleus, which results in the changing of nucleus shape. The nuclei staining images showed that the nuclei on hPC were obviously "slender" compared to the nuclei on sPC (Fig. 2A). Further, the quantitative result of nucleus aspect ratio showed that the nuclei aspect ratio of cells on hPC was significantly higher than that on mPC and sPC (Fig. 2B). The results indicated that hPC topographical cues promoted cell contraction force and then the mechanical force transmitted to the nucleus via cytoskeleton, which led to nuclear deformation.

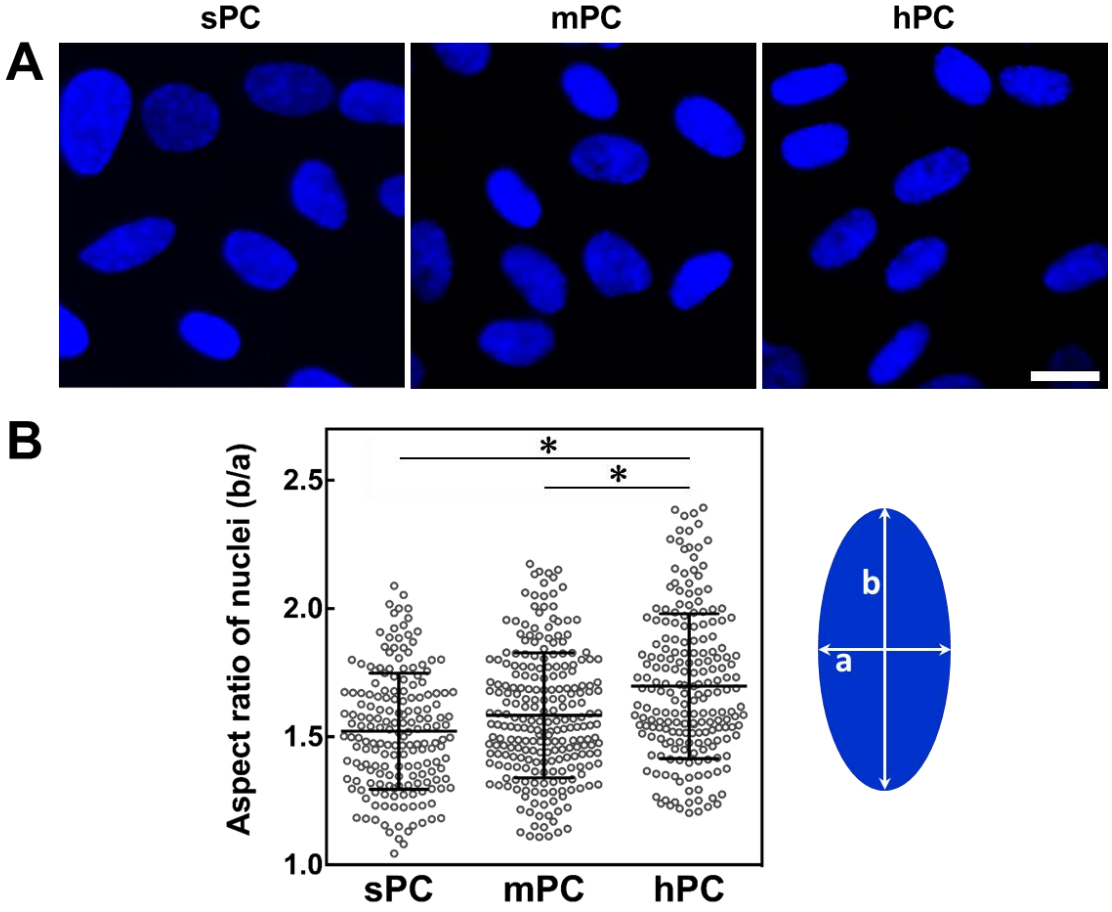

Fig. 2: Cell contraction force influences the hBMSC nucleus deformation. A Representative cell nuclei immunofluorescence staining images of hBMSCs that were cultured on different surfaces for 4 days (nuclei: blue; Scale bar =20 µm); B Nuclei aspect ratio of hBMSCs on different surfaces (n = 195, 251 and 219 for sPC, mPC and hPC, respectively; * Sig < 0.05).

3.4 Cell contractility influences lamin A/C expression

To further study the influence of surface topography mediated cell contraction on cell nuclei, the expression levels of lamin A/C were characterized. Lamin A/C are major components of the nuclear lamina that provide structural integrity to cell nucleus and mechanical support to nuclear shape [33]. The lamin A/C expressing cells can form an actin cap to resist nuclear deformation in response to physiological mechanical stresses [34]. The stimulation of increasing mechanical force enhances phospho-lamin A/C (plamin A/C) dephosphorylation and induces conformational changes in lamin coiled-coil dimers and deposite on the nuclear membrane [18], the expression level of lamin A/C determine the cell nuclear stiffness. In addition, several studies found that lamin A/C interacted with double-stranded DNA, transcriptional regulators, nuclear membrane associated proteins [33, 35], and regulated the expression level of genes that relate with the MSCs differentiation. Here, lamin A/C and plamin A/C expression of the cells on different surfaces were characterized by immunofluorescence staining. The images showed the lamin A/C fluorescence intensity of cells on hPC surface was higher than that on sPC and mPC. In contrast, the cells on sPC surface had the strongest fluorescence intensity of p lamin A/C and the cells on hPC the fluorescence intensity of plamin A/C was weakest (Fig. 3A). Then the expression level of plamin A/C was quantified via ImageJ software analyzing the fluorescence intensity of images, the result showed that cells on sPC had higher mean fluorescence intensity (MFI) than that on hPC (Fig .3B). However, the FACS quantified results of lamin A/C expression level indicated the lamin A/C MFI of cells that were cultured on hPC was significantly higher than that on mPC and sPC (Fig. 3C), which is consistent with the immunofluorescence staining result. To further confirm the surface topographical cues mediated contraction force influence on lamin A/C expression, RGD and inhibitors (Bleb and Cyto D) were used to block the cell surface integrin, inhibit the MLC activation and F-actin polymerization, respectively, and siRNAs (scrambled, nesprin-1, nesprin-2 and SUN) were transfected into hBMSCs for the depletion of LINC complex component proteins (nesprin-1, nesprin-2 and SUN), which connected the nucleoskeleton to the cytoskeleton and transmitted mechanical force from the cytoplasm to the nucleus. The use of RGD inhibitors as well as siRNA transfection decreased the cell cytoskeleton contractility or blocked the mechanical force transmission to the nucleus, which reduced the lamin A/C expression. The lamin A/C expression of cells that were treated with RGD, inhibitors or siRNA was significantly decreased compared to the untreated cells with exception of the emerin siRNA transfected cells (Fig. 3D). The transfection of emerin siRNA did not influence lamin

A/C expression. This may be because of emerin was just a mechanical sensor protein that neither produced force nor participated in force conduction. These results demonstrated that the hPC surface topographical cues enhanced cell contraction force led to the cell lamin A/C expression increasing, which is consistent with a previous report [34].

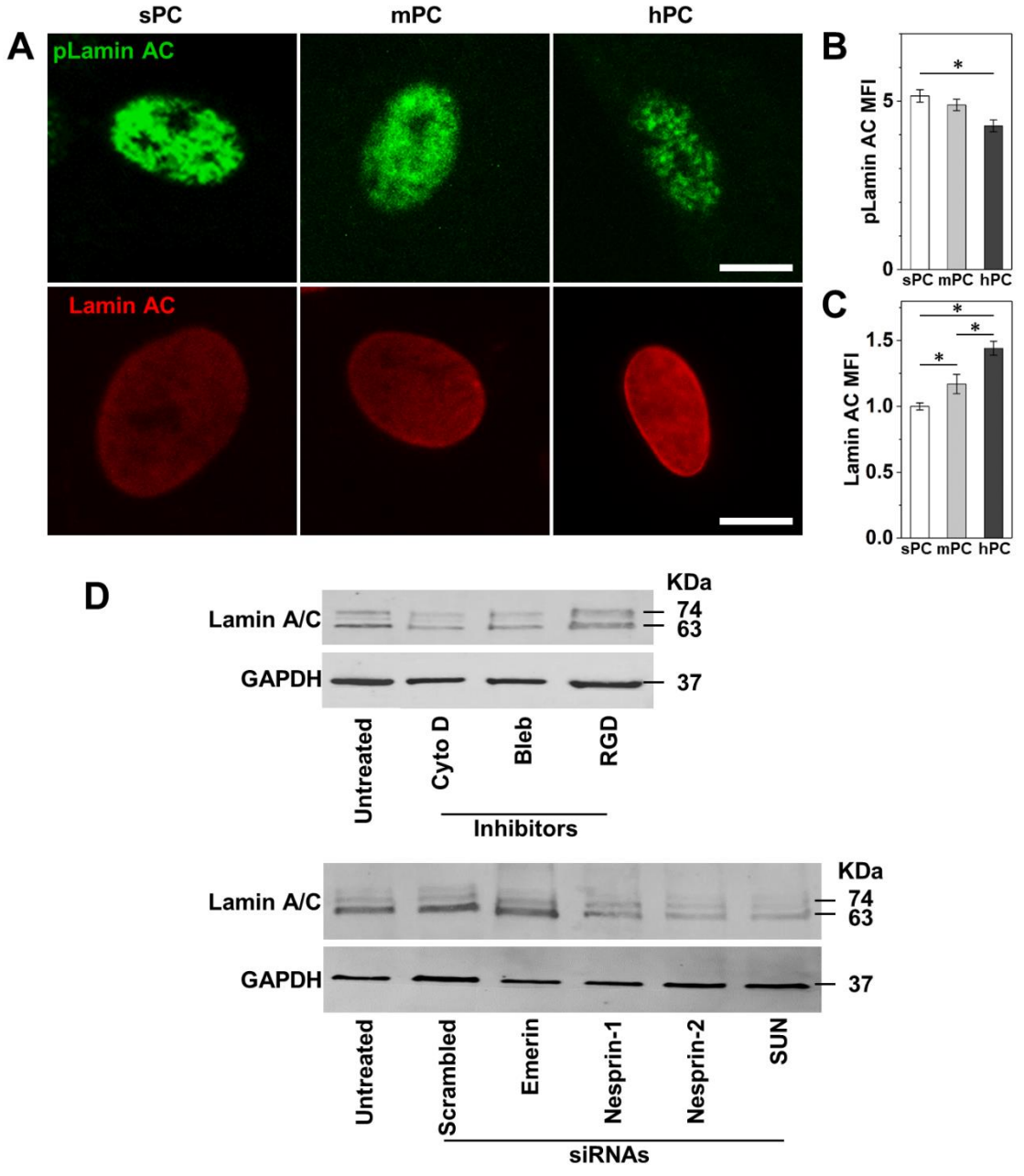

Fig. 3: Cell contraction force affects the expression of p lamin A/C and lamin A/C. A Representative plamin A/C and lamin A/C immunofluorescence staining images of hBMSCs that were cultured on different surfaces for 4 days (plamin A/C: green; lamin A/C : red; Scale bar =10 μm); B Relative plaimin A/C expression level of hBMSCs, which was analyzed via quantification of the immunofluorescence intensity of the images by imageJ (bars show standard error; n = 216, 256 and 150 for sPC, mPC and hPC, respectively; * Sig < 0.05); C Relative lamin A/C expression level of hBMSCs, which were cultured on different surfaces for 4days in GM, then the cells were harvested, fixed and stained with lamin A/C primary

antibody and second antibody, then characterized by flow cytometry. (n = 5; *Sig < 0.05); D hBMSCs were treated with Cyto D, Bleb, and RGD, respectively, or transfected with siRNAs (scramble, nesperin-1, nesprin-2 and SUN), respectively, and then lamin A/ C expressions were analyzed by western blotting.

3.5 Cell contractility influences YAP nuclear translocation

The mechanical force applied on nuclear membrane not only changes the morphology of the nuclei, but also influences the permeability of nuclear pore complex (NPC), facilitating import of mechanotransduction signaling molecules such as Yes-associated protein (YAP) [17]. YAP has been demonstrated plays an important role in mediating cellular mechanosensing [36]. Increasing of cytoskeleton contractility enhanced YAP dephosphorylation and nuclear translocation, furthermore, promoted the cells proliferation and stem cells osteogenic differentiation [37, 38]. In this study, the YAP immunofluorescence staining images showed that on hPC the fluorescence intensity of YAP on nuclear position was obviously stronger than that on sPC and mPC (Fig. 4A). Furthermore, ELISA kits were used to quantitative analysis of the ratio of phosphorylated YAP (pYAP)/total YAP (tYAP). The result showed that the cells cultured on hPC had significantly lower pYAP/tYAP ratio than that on sPC and mPC (Fig. 4B). To further confirm that the increased YAP nuclear translocation was regulated via cell contraction force which was mediated by surface topographical cues, the cells were treated by RGD, inhibitors and siRNA (lamin, nesprin-1, nesprin-1 and SUN), respectively. The using of RGD and inhibitors (Cyto D and Bleb) led to the decreasing of cell contraction force formation, and siRNAs (lamin, nesprin-1, nesprin-1 and SUN) were transfected into cells to block the contraction force transmitting to nuclear membrane. After the cells were treated with RGD, inhibitors or siRNAs the pYAP/tYAP ratio was significantly increased comparable to untreated cells (Fig. 4B). These results indicated the cell contraction regulates mechanotransducer nuclear localization.

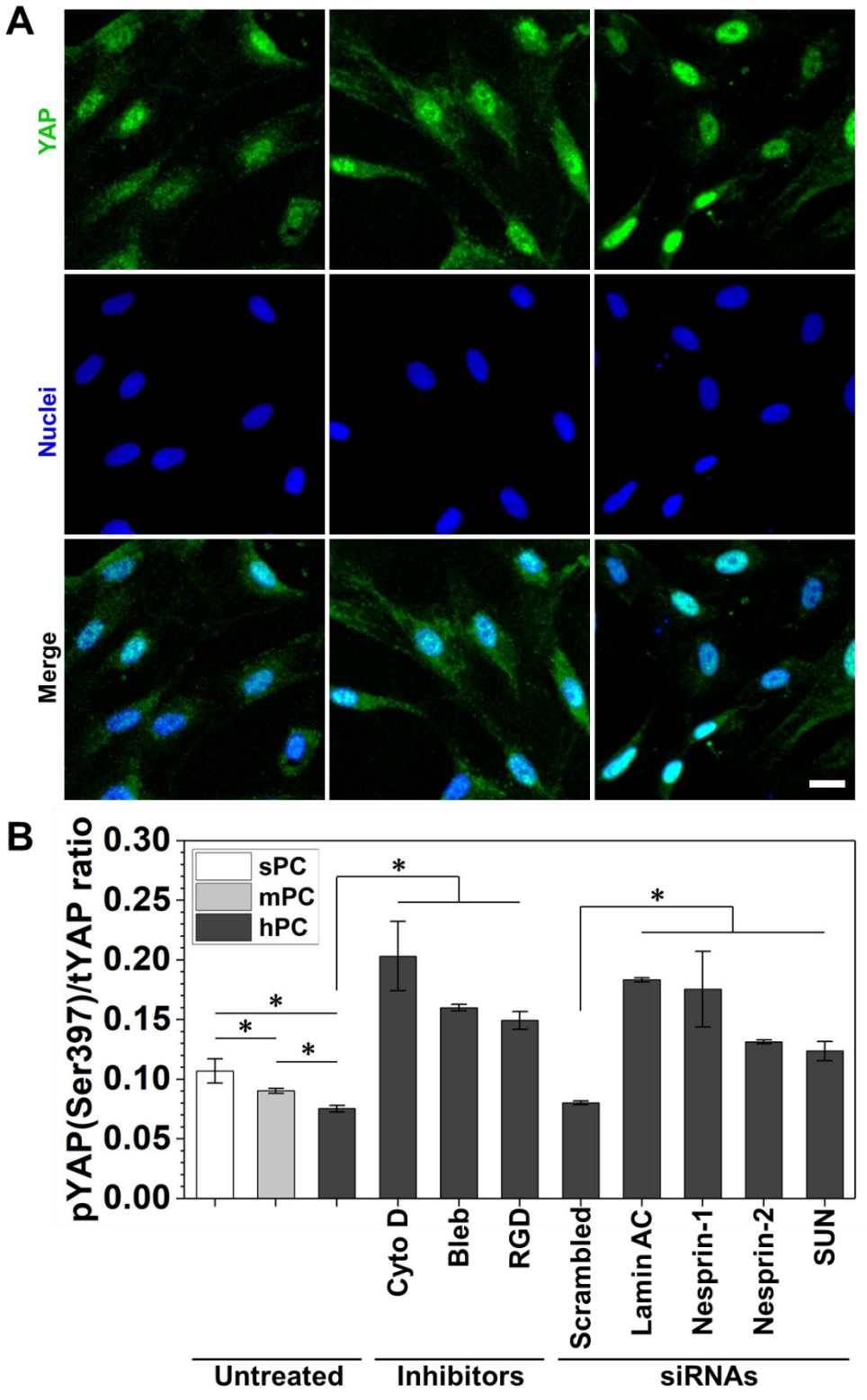

Fig. 4: Cell tension affects the YAP nuclear translocation. A Representative immunofluorescence staining images of YAP location in hBMSCs that were cultured on different surface for 4 days in GM (YAP: green and nuclei: blue; Scale bar = 20 μm); B hBMSCs were cultured under different conditions for 4 days and then lysed, pYAP/tYAP ratio was tested by ELISA kits. (n = 3; *Sig < 0.05).

3.6 Cell contractility influences the globe expression of H3K27me3

A previous study had demonstrated that the cell-extrinsic force can propagate directly to the nucleus and facilitate the deformation and stretching of chromatin and modify gene expression patterns and cell fate [39]. However, whether the cell-intrinsic force regulates cell chromatin deformation is still not very clear. To investigate whether cell contractility modulates cell epigenetics, we studied the histone modification level of cells on different topographic surfaces. Since the previous study had demonstrated that H3K27me3 was an epigenetic control point of MSC differentiation [23] and the level of H3K27me3 was directly related with the chromatin compaction degree [40]. Here, we characterized the H3K27me3 expression level of cells that were cultured on different surfaces. The H3K27me3 fluorescence intensity of cells cultured on hPC was stronger than that on sPC and mPC, which was obvious visible from the immunofluorescence staining images (Fig. 5A). The histone modification levels were quantitatively analyzed by comparing the MFI. The results indicated the cells on hPC surface had significant higher H3K27me3/H3 ratio than that on mPC and sPC, and this phenomenon was only observed in cells cultured in GM (Fig. 5B). In the MM, there was no significant difference of H3K27me3/H3 ratio of cells that were cultured on different surfaces (Supplementary Fig. 4). This can be explained by the changes of acetylation of histones H3 and H4 as well as methylation of H3K27 during the stem cell differentiation.

During the processing of MSC osteogenic differentiation, the loss of H3K27me3 played a key role to regulate osteogenic related genes expression [41]. Based on the results of hPC promoting hBMSCs cell contractility and globe H3K27me3 expression，we postulated that the enhancement of cell contractility could promote H3K27me3 expression in hBMSCs. To confirm this postulate, the globe H3K27me3 expression level was evaluated in the cells were that treated with RGD and inhibitors (Cyto D and Bleb) or siRNAs (Emerin, SUN, Lamin, Nesprin-1 and Nesprin-2). The results showed that the RGD inhibitors as well as siRNAs transfection markedly depleted the difference of H3K27me3/H3 ratio of cells on different topographic surfaces in GM (Fig. 5B). Our research data suggest that the enhancement of cell contractility can increase the global histone H3K27 trimethylation, which is consistent with the previous report by Le et al. To resist the mechanical force applied on cell nuclei, the cell nuclei become more stiffness. In this process, the expression of lamin A/C is increased and chromatin compaction is enhanced by histone modification such as the trimethylation H3K27 [42].

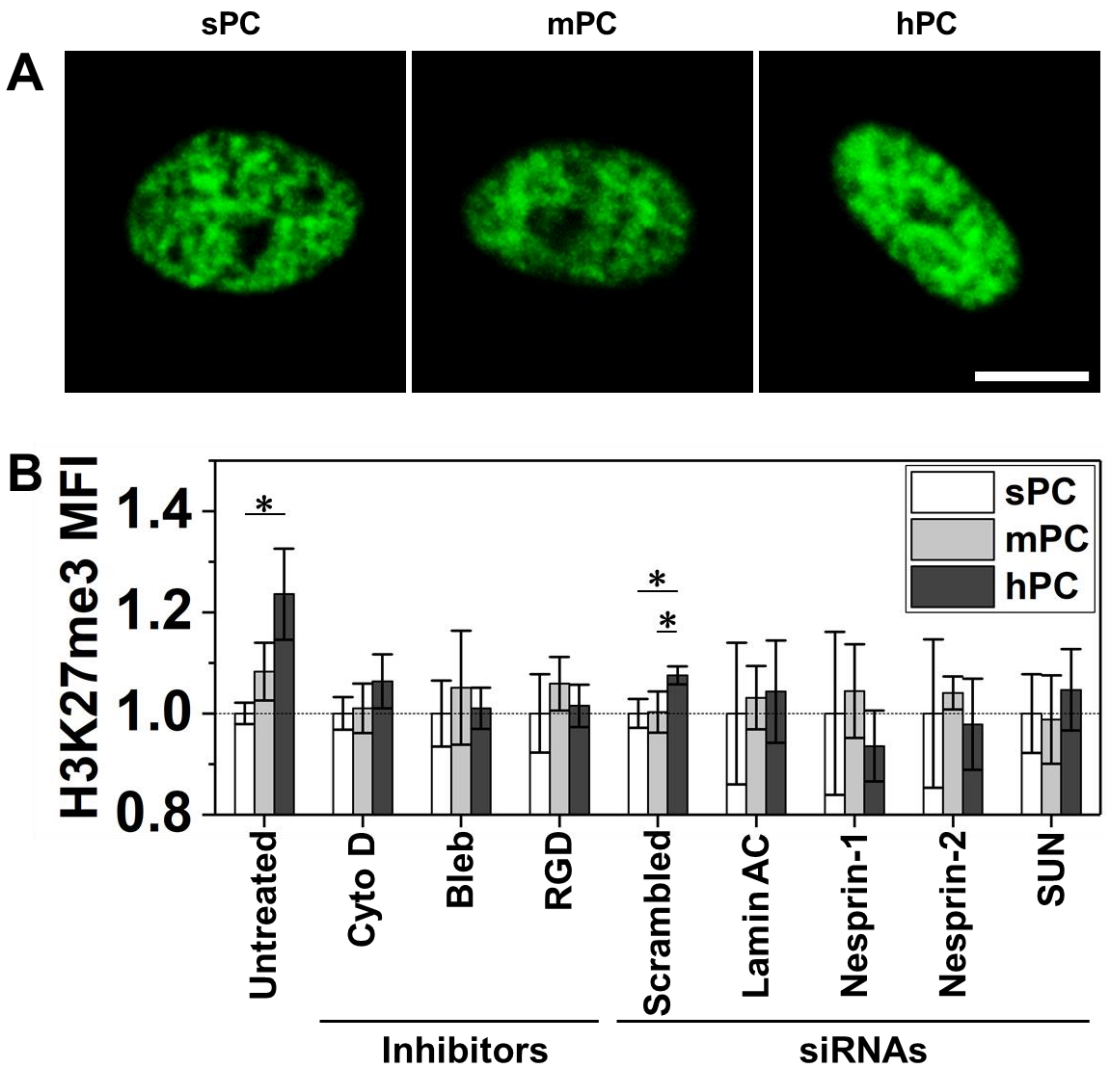

Fig. 5: Cell contractility regulates the histone modification. A: Representative H3K27me3 immunofluorescence staining images of hBMSCs that were cultured on different topographic surfaces in GM for 4 days. (Scale bar = 10 μm) B: hBMSCs were treated with RGD, Cyto D and Bleb or transfected siRNAs (control, lamin, nesprin-1, nesprin-2 and SUN) and cultured on different topographic surfaces in GM or MM for 4 days, respectively. The expression level of H3K27me3 and H3 were quantified using flow cytometry. And the results expressed as the fold change of mean fluorescence intensity (MFI) ratio (H3K27me3/H3) compared to that on sPC. (n = 5; * Sig < 0.05; # mPC vs hPC Sig < 0.05).

3.7 The enrichment of H3K9ac and H3K27me3 on the promoters of osteogenic related genes

The cell contraction forces modulated by surface topographical cues influence globe H3K27me3 modification level. However, it is unclear how the change of histone modification level regulates specific gene expression is unclear. H3K27me3 is a negative regulator of gene expression, the enrichment of H3K27me3 on specific genes is directly linked to downregulation expression [43]. And H3K9ac was found played an important role in regulating gene activation, which were crucial to MSCs osteogenic differentiation [44]. To

study the influence of histone modification on cell osteogenic differentiation, we examined the enrichments of H3k27me3 and H3k9ac located on the promotors of genes (ALPL, RUNX2 and BGLAP) by ChIP-PCR assay. The results indicated that H3K27me3 and H3K9ac both are located on the promoters of ALPL, RUNX2 and BGLAP genes. However, there were different enrichment of H3K27me3 and H3K9Ac located on these gene promoters of the cells that were cultured on the different surface topography (Fig.6 A and B). The cells cultured on hPC had significantly higher H3K9ac enrichment on ALP, RUNX2 and BGLAP gene promoters than that of cells on mPC and sPC surfaces. In contrast, the cells from sPC surface had significantly higher enrichment of H3K27me3 on the promoter of these genes than that of cells from hPC surface. These results not only appeared in the cells that were cultured in GM but also in MM. These data suggest that the cell contraction force not only influenced the global histone modification level but also induced the change of modified histone enrichment on specific genes, which were highly favorable in the activation of genes expression. In case of cells cultured in MM, the enrichments of H3K27me3 and H3K9Ac located on these gene promoters significantly decreased compared to cells cultured in GM. That is due to the fluctuation of histone modification level during cell-induced differentiation, the H3K9ac level gradually decreases in the early stage (days 0 - 4) of stem cell differentiation[45]. The results are consistent with a previous report, in which the enrichment of H3K9ac on gene promoters regulated the gene transcription [46].

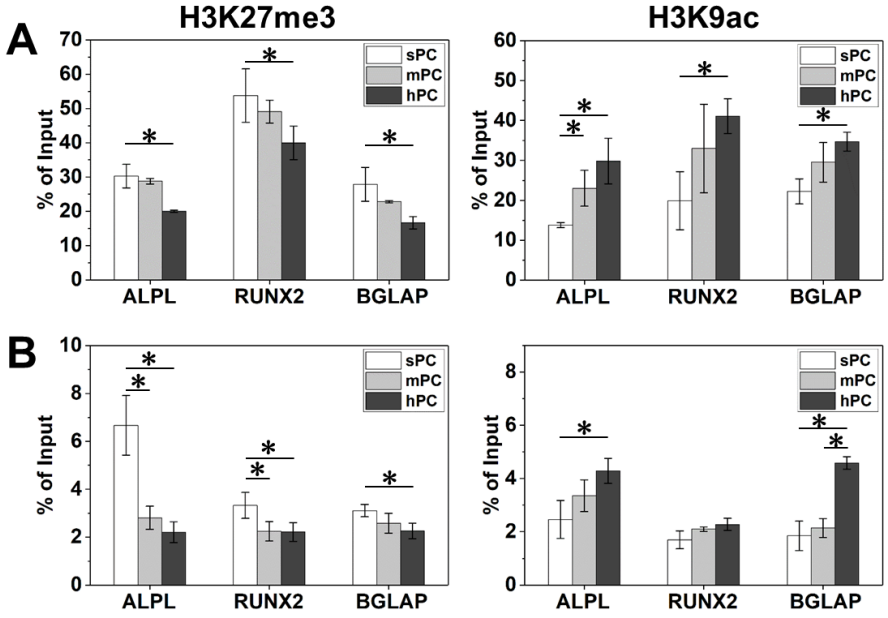

Fig. 6: Cell tension influences the enrichment of H3K9ac and H3K27me3 on the promoters of osteogenic related genes. ChIP-PCR analysis confirms that cell tension influences the enrichment of H3K9ac and H3K27me3 on the promoters of osteogenic related genes (ALP, RUNX2 and OCN) in hBMSCs that cultured at different conditions. The hBMSCs were

cultured on different topographic surfaces in GM and MM for 4 days, respectively, and then the cells were lysed and immunoprecipitated with anti-H3K27me3, anti-H3K9Ac, and anti-IgG control antibody, and RT-PCR was used to measure enrichment. A: MSCs were cultured in GM and immunoprecipitated with H3K27me3 andH3K9Ac; B: MSCs were cultured in mixed media and immunoprecipitated with H3K27me3 and H3K9Ac; Error bars indicate standard deviation of PCR replicates (n = 3; *Sig < 0.05);

3.8 Surface topography influences hBMSC differentiation

To verify whether the topographic surfaces could regulate hBMSC differentiation, the hBMSCs osteogenic and adipogenic differentiation levels were evaluated. Since cell-cell interaction could influence MSC osteogenic differentiation [47], before the evaluation of cell differentiation the cell-cell interactions on the differently structured surfaces was tested. N-cadherin expression level of cells that cultured on different surfaces was characterized to evaluate the cell-cell contact level. The results showed that there was no significant difference of N-cadherin expression level between cells seeded on different topographic surfaces (Supplementary Fig. 2A and B), which illustrated that the cells on different surfaces have similar cell-cell interaction.

To evaluate the differentiation of hBMSCs on the different topographic surfaces, the cells were exposed to MM containing competing soluble differentiation cues (adipogenic *VS* osteogenic). The cells were stained to reveal that hBMSCs differentiated to adipogenic and osteogenic lineages. The ORO staining images obviously showed there were more lipid droplets in cells on sPC than on mPC and hPC (Fig. 7A). In contrast, the fluorescence intensity of the mineralization nodules staining images indicated that there was higher fluorescence intensity on hPC surface than on sPC and mPC, which means the hBMSCs on hPC had higher osteogenic differentiation level than on sPC and mPC (Fig. 7B). The quantitative analysis results showed that the adipogenic differentiation marker FABP-4 expression level of the cells on sPC surface expression was around 30% and 80% higher than that on mPC and hPC surfaces (Fig. 7C). In contrast, the cells cultured on hPC had highest osteocalcin expression level in the three surfaces (Fig. 7D). In addition, after the cells were treated with RGD or inhibitors (Cyto D and Blebb), the significant differences of FABP-4 and osteocalcin expression level among the different topographic surfaces disappeared, and FABP-4 expression levels of cells significantly increased, the osteocalcin expression levels obviously decreased compared to the untreated cells (Fig. 7C and D). And in osteogenic or adipogenic induction medium, the Aliza red S and FABP-4 staining results showed that hPC promoted hBMSC osteogenic differentiation, and the sPC was favorable for hBMSC adipogenesis (Supplementary Fig. 5). These hBMSC differentiation results collectively suggested that hPC topographic surface enhanced hBMSCs

osteogenic differentiation, and sPC topographic surface was beneficial for hBMSC adipogenesis.

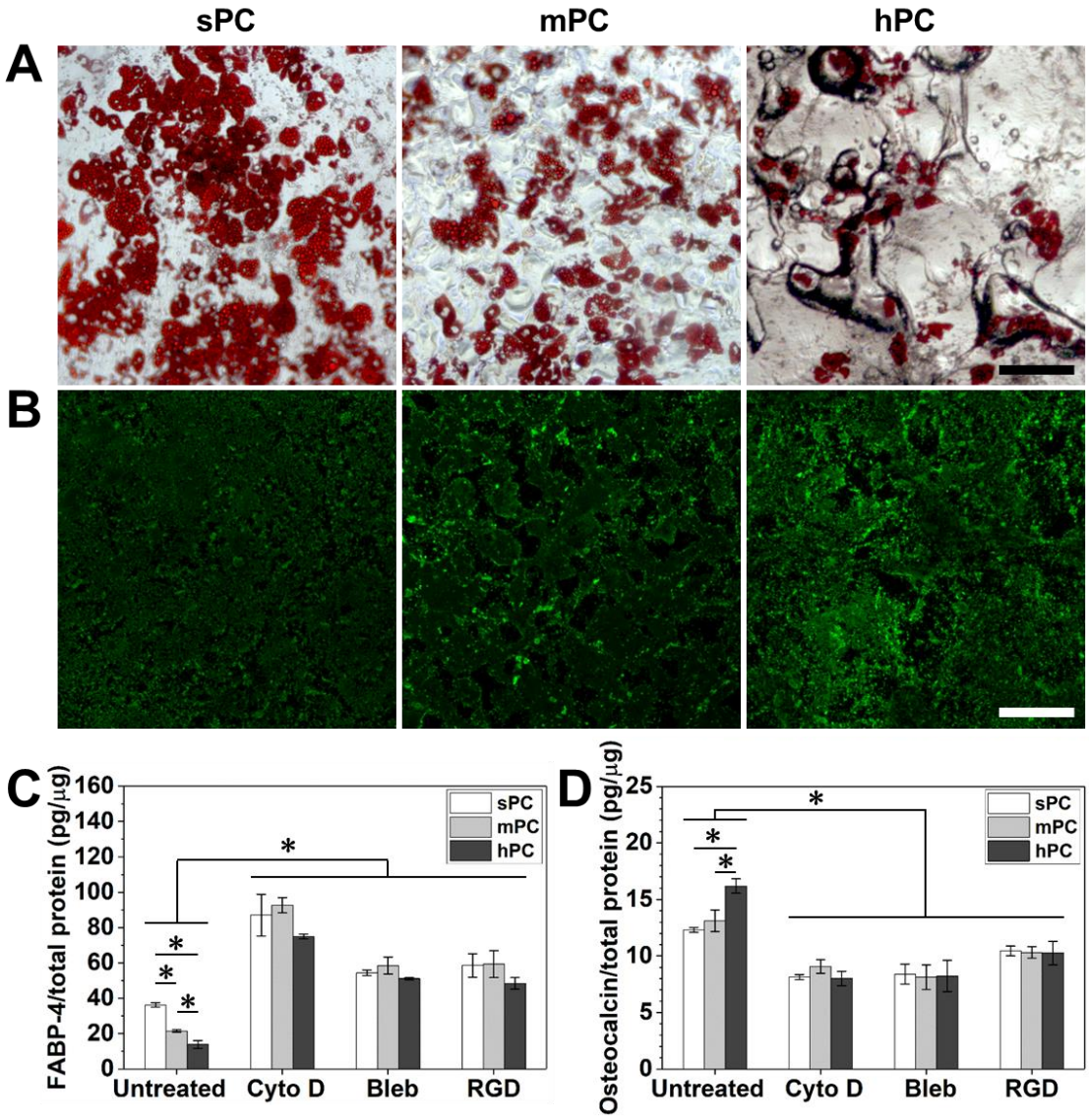

Fig. 7: Surface topographical cues influence hBMSCs differentiation. hBMSCs were cultured on different surfaces and exposed to MM for 21 days, and then cells were fixed and stained. A Representative images of lipid droplets staining (scale bar = 200 μm); B Representative images of calcium mineralization immunofluorescence staining (scale bar = 200 μm); C FABP-4 expression level of hBMSCs cultured in MM with inhibitors/RGD added for 21 days on different topography surfaces; D Osteocalcin expression level of hBMSCs cultured in MM with inhibitors/RGD added for 21 days on different topography.(n = 4; *Sig < 0.05).

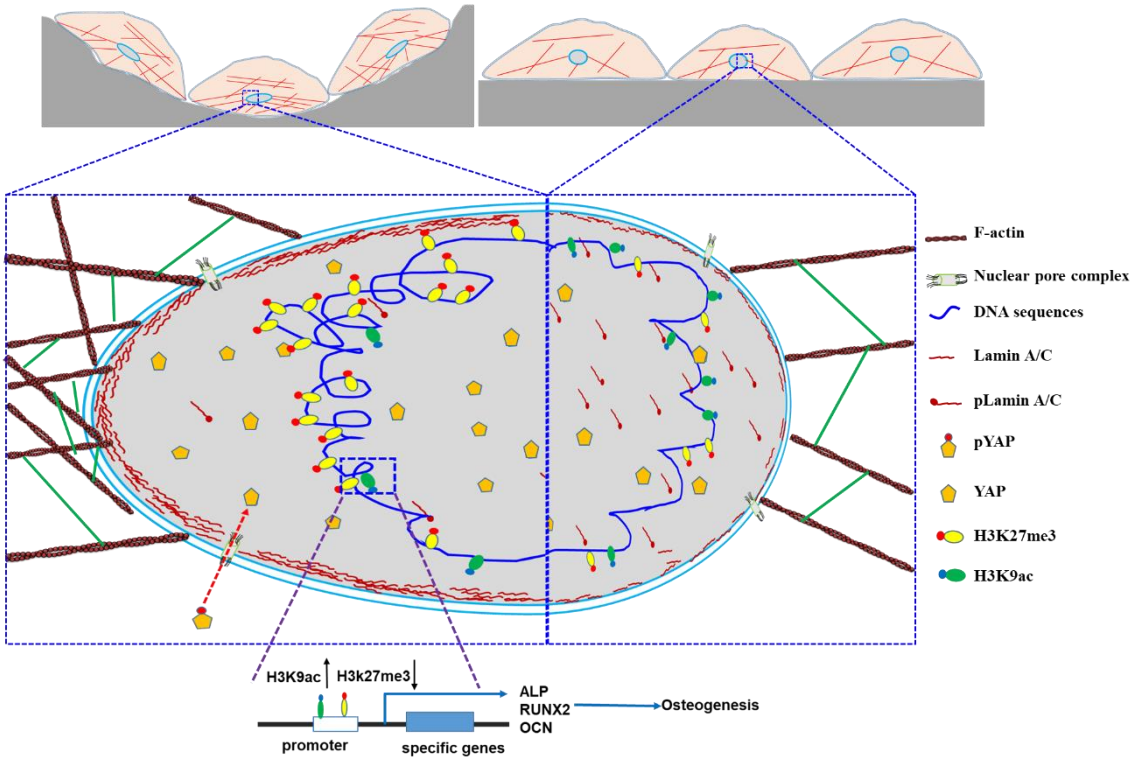

Fig. 8 Proposed model of the regulatory effect of surface topographical cues on hBMSCs. Compared to the sPC and mPC surfaces, the hPC could present a larger portion of surface with optimal topographical cues properties for modulating hBMSCs. The cells on hPC surface present high cell contractility and the contraction force transmitted to nucleus through LINC complex, and then led to the nuclear deformation, enhanced YAP nuclear translocation, as well as changes in chromatin conformation through the modification of histone, subsequently, enhanced hBMSCs osteogenic differentiation.

In summary, these results demonstrated that surface topographical cues regulated cell contractility, and then affected histone modification level and enrichment of modified histones located on the specific genes, subsequently, modulated hBMSCs differentiation lineages (Fig. 8). When hBMSCs attached on hPC surface, the topographical cues (RSm value was similar to the pore size of spongy bone) could be sensed by cells and then cell membrane biological signal pathway was activated. Further, the biological signals transmitted across the cytoplasmic membrane promoted actin polymerization and myosin light chain activation， which enhanced the cell cytoskeleton contraction. The traction force stretched nuclei via the LINC linker, and resulted in cell nuclear deformation including promoting the permeability of the nuclear pores, enhancing laminA/C expression. The mechanical force further propagated into the nucleus and altered histone modification level as well as regulated the enrichment of modified histones located on specific gene promoters. Subsequently, the alteration of nucleus regulated the genes expression and modulated the cell fate. This study focused on the mechanism of substrate topographical cues regulating stem cell differentiation, which pointed to a gateway to control

parameters of MSCs critical for their therapeutic potential by specifying cell–material interactions. Our study results suggest that fine-tuning the topographic surface might be an effective and safe approach to improve the therapeutic functions of hBMSCs. And the results could give us some guiding for the design and development of biomaterials for both *in vitro* and *in vivo* applications. Engineering substrate surface topography to regulate hBMSCs differentiation lineages could avoid the disadvantages of stem cells differentiated into an inappropriate cell lineage under pathophysiological conditions *in vivo*.

4. Conclusion

In this study, we systematically investigated the influence of substrate surface topographical cues on enhancement of cell contraction force and its subsequent effect on differentiation behavior of hBMSCs. We found that the hPC surface topographical cues (RSm value is comparable to natural spongy bone pore size) enhanced hBMSCs cytoskeleton organization, stabilization and promoted cytoskeleton tension. Furthermore, the increased cytoskeleton tension would lead to cell nucleus deformation and changed histone modification levels, as well as to the enrichment of modified histone on the specific gene promoters, which further regulated genes expression and then directed hBMSCs differentiation lineages. These findings allow a better understanding of MSC response to scaffold topographic surface. This information is critical to the medical field as it presents new direction to design and develop biomedical devices, which could maximize the potential of stem cell in application.

Conflicts of interest

There are no conflicts of interest to declare.

Acknowledgements

The authors acknowledge Robert Jeziorski and Mario Rettschlag for the preparation of sterilized PC inserts and Manuela Keller for technical support.

References

1. Wei, X., et al., *Mesenchymal stem cells: a new trend for cell therapy.* Acta Pharmacologica Sinica, 2013. **34**(6): p. 747-754.
2. Wexler, S.A., et al., *Adult bone marrow is a rich source of human mesenchymal 'stem' cells but umbilical cord and mobilized adult blood are not.* British Journal of Haematology, 2003. **121**(2): p. 368-374.
3. Ferlin, K.M., et al., *Influence of 3D printed porous architecture on mesenchymal stem cell enrichment and differentiation.* Acta Biomaterialia, 2016. **32**: p. 161-169.
4. Vaughan, T.J., et al., *Multiscale Modeling of Trabecular Bone Marrow: Understanding the Micromechanical Environment of Mesenchymal Stem Cells During Osteoporosis.* Journal of Biomechanical Engineering-Transactions of the Asme, 2015. **137**(1): p. 11003-11010.
5. Klenke, F.M., et al., *Impact of pore size on the vascularization and osseointegration of ceramic bone substitutes in vivo.* Journal of Biomedical Materials Research Part A, 2008. **85a**(3): p. 777-786.
6. Zhang, Y.F., et al., *The effects of pore architecture in silk fibroin scaffolds on the growth and differentiation of mesenchymal stem cells expressing BMP7.* Acta Biomaterialia, 2010. **6**(8): p. 3021-3028.
7. Guda, T., et al., *Hydroxyapatite scaffold pore architecture effects in large bone defects in vivo.* Journal of Biomaterials Applications, 2014. **28**(7): p. 1016-1027.
8. Kuboki, Y., Q.M. Jin, and H. Takita, *Geometry of carriers controlling phenotypic expression in BMP-induced osteogenesis and chondrogenesis.* Journal of Bone and Joint Surgery-American Volume, 2001. **83a**: p. S105-S115.
9. Xu, X., et al., *Controlling Major Cellular Processes of Human Mesenchymal Stem Cells using Microwell Structures.* Advanced Healthcare Materials, 2014. **3**(12): p. 1991-2003.
10. Provenzano, P.P. and P.J. Keely, *Mechanical signaling through the cytoskeleton regulates cell proliferation by coordinated focal adhesion and Rho GTPase signaling.* Journal of Cell Science, 2011. **124**(8): p. 1195-1205.
11. Starr, D.A. and H.N. Fridolfsson, *Interactions Between Nuclei and the Cytoskeleton Are Mediated by SUN-KASH Nuclear-Envelope Bridges.* Annual Review of Cell and Developmental Biology, Vol 26, 2010. **26**: p. 421-444.
12. Versaevel, M., T. Grevesse, and S. Gabriele, *Spatial coordination between cell and nuclear shape within micropatterned endothelial cells.* Nature Communications, 2012. **3**: p. 671-681
13. Ramdas, N.M. and G.V. Shivashankar, *Cytoskeletal control of nuclear morphology and chromatin organization.* J Mol Biol, 2015. **427**(3): p. 695-706.
14. Buxboim, A., I.L. Ivanovska, and D.E. Discher, *Matrix elasticity, cytoskeletal forces and physics of the nucleus: how deeply do cells 'feel' outside and in?* Journal of Cell Science, 2010. **123**(3): p. 297-308.
15. Burke, B. and C.L. Stewart, *The nuclear lamins: flexibility in function.* Nature Reviews Molecular Cell Biology, 2013. **14**(1): p. 13-24.
16. Kirby, T.J. and J. Lammerding, *Emerging views of the nucleus as a cellular mechanosensor.* Nature Cell Biology, 2018. **20**(4): p. 373-381.
17. Elosegui-Artola, A., et al., *Force Triggers YAP Nuclear Entry by Regulating Transport across Nuclear Pores.* Cell, 2017. **171**(6): p. 1397-1410 e14.

18. Cho, S., J. Irianto, and D.E. Discher, *Mechanosensing by the nucleus: From pathways to scaling relationships.* Journal of Cell Biology, 2017. **216**(2): p. 305-315.
19. Tajik, A., et al., *Transcription upregulation via force-induced direct stretching of chromatin.* Nature Materials, 2016. **15**(12): p. 1287-1296.
20. Le, H.Q., et al., *Mechanical regulation of transcription controls Polycomb-mediated gene silencing during lineage commitment.* Nature Cell Biology, 2016. **18**(8): p. 864-+.
21. Downing, T.L., et al., *Biophysical regulation of epigenetic state and cell reprogramming.* Nature Materials, 2013. **12**(12): p. 1154-1162.
22. Jenuwein, T. and C.D. Allis, *Translating the histone code.* Science, 2001. **293**(5532): p. 1074-1080.
23. Hemming, S., et al., *EZH2 and KDM6A act as an epigenetic switch to regulate mesenchymal stem cell lineage specification.* Stem Cells, 2014. **32**(3): p. 802-15.
24. Hu, X.Q., et al., *Histone Deacetylase Inhibitor Trichostatin A Promotes the Osteogenic Differentiation of Rat Adipose-Derived Stem Cells by Altering the Epigenetic Modifications on Runx2 Promoter in a BMP Signaling-Dependent Manner.* Stem Cells and Development, 2013. **22**(2): p. 248-255.
25. Hiebl, B., et al., *Cytocompatibility testing of cell culture modules fabricated from specific candidate biomaterials using injection molding.* Journal of Biotechnology, 2010. **148**(1): p. 76-82.
26. Liu, E.Y., et al., *The clinical significance and underlying correlation of pStat-3 and integrin alpha v beta 6 expression in gallbladder cancer.* Oncotarget, 2017. **8**(12): p. 19467-19477.
27. Kilian, K.A., et al., *Geometric cues for directing the differentiation of mesenchymal stem cells.* Proceedings of the National Academy of Sciences of the United States of America, 2010. **107**(11): p. 4872-4877.
28. Dekkers, B.G.J., et al., *The Integrin-blocking Peptide RGDS Inhibits Airway Smooth Muscle Remodeling in a Guinea Pig Model of Allergic Asthma.* American Journal of Respiratory and Critical Care Medicine, 2010. **181**(6): p. 556-565.
29. Mente, P.L. and J.L. Lewis, *Experimental-Method for the Measurement of the Elastic-Modulus of Trabecular Bone Tissue.* Journal of Orthopaedic Research, 1989. **7**(3): p. 456-461.
30. Chen, L., et al., *Inhibiting actin depolymerization enhances osteoblast differentiation and bone formation in human stromal stem cells.* Stem Cell Res, 2015. **15**(2): p. 281-9.
31. Icard-Arcizet, D., et al., *Cell stiffening in response to external stress is correlated to actin recruitment.* Biophysical Journal, 2008. **94**(7): p. 2906-2913.
32. Guilluy, C., et al., *Isolated nuclei adapt to force and reveal a mechanotransduction pathway in the nucleus.* Nat Cell Biol, 2014. **16**(4): p. 376-81.
33. Dechat, T., S.A. Adam, and R.D. Goldman, *Nuclear lamins and chromatin: when structure meets function.* Adv Enzyme Regul, 2009. **49**(1): p. 157-66.
34. Kim, J.K., et al., *Author Correction: Nuclear lamin A/C harnesses the perinuclear apical actin cables to protect nuclear morphology.* Nat Commun, 2018. **9**(1): p. 1115.
35. Capell, B.C. and F.S. Collins, *Human laminopathies: nuclei gone genetically awry.* Nat Rev Genet, 2006. **7**(12): p. 940-52.
36. Dupont, S., et al., *Role of YAP/TAZ in mechanotransduction.* Nature, 2011. **474**(7350): p. 179-U212.
37. Musah, S., et al., *Substratum-induced differentiation of human pluripotent stem cells reveals the coactivator YAP is a potent regulator of neuronal specification.* Proceedings

of the National Academy of Sciences of the United States of America, 2014. **111**(38): p. 13805-13810.
38. Pan, J.X., et al., *YAP promotes osteogenesis and suppresses adipogenic differentiation by regulating beta-catenin signaling.* Bone Res, 2018. **6**: p. 18.
39. Le, H.Q., et al., *Mechanical regulation of transcription controls Polycomb-mediated gene silencing during lineage commitment.* Nat Cell Biol, 2016. **18**(8): p. 864-75.
40. Bannister, A.J. and T. Kouzarides, *Regulation of chromatin by histone modifications.* Cell Research, 2011. **21**(3): p. 381-395.
41. Wu, H., et al., *Chromatin dynamics regulate mesenchymal stem cell lineage specification and differentiation to osteogenesis.* Biochimica Et Biophysica Acta-Gene Regulatory Mechanisms, 2017. **1860**(4): p. 438-449.
42. Miroshnikova, Y.A., M.M. Nava, and S.A. Wickstrom, *Emerging roles of mechanical forces in chromatin regulation.* Journal of Cell Science, 2017. **130**(14): p. 2243-2250.
43. von Schimmelmann, M., et al., *Polycomb repressive complex 2 (PRC2) silences genes responsible for neurodegeneration.* Nature Neuroscience, 2016. **19**(10): p. 1321-+.
44. Tan, J., et al., *Genome-Wide Analysis of Histone H3 Lysine9 Modifications in Human Mesenchymal Stem Cell Osteogenic Differentiation.* Plos One, 2009. **4**(8).
45. Qiao, Y., et al., *Dual roles of histone H3 lysine 9 acetylation in human embryonic stem cell pluripotency and neural differentiation.* J Biol Chem, 2015. **290**(16): p. 9949.
46. Gates, L.A., et al., *Acetylation on histone H3 lysine 9 mediates a switch from transcription initiation to elongation.* J Biol Chem, 2017. **292**(35): p. 14456-14472.
47. Kim, K., et al., *Effect of initial cell seeding density on early osteogenic signal expression of rat bone marrow stromal cells cultured on cross-linked poly(propylene fumarate) disks.* Biomacromolecules, 2009. **10**(7): p. 1810-7.

Supplementary information

Substrate surface topography promotes human bone marrow mesenchymal stem cell osteogenic differentiation via histone modification of osteogenic genes

Jie Zou [1, 2 #], Weiwei Wang [1 #], Xun Xu [1, 2 #], Karl Kratz [1, 3], Zijun Deng[1], Nan Ma [1, 2,3 *] and Andreas Lendlein [1, 3 *]

[1] Institute of Biomaterial Science and Berlin-Brandenburg Centre for Regenerative Therapies, Helmholtz-Zentrum Geesthacht, Teltow, Germany

[2] Institute of Chemistry and Biochemistry, Free University of Berlin, Berlin, Germany

[3] Helmholtz Virtual Institute − Multifunctional Materials in Medicine, Berlin and Teltow, Germany

[#] These authors contributed equally to this work.

* To whom correspondence should be addressed: Prof. Dr. Nan Ma, Prof. Dr. Andreas Lendlein

Email: nan.ma@hzg.de, andreas.lendlein@hzg.de

Phone: +49 (0)3328 352-450

Fax: +49 (0)3328 352-452

Supporting results

1. Table 1. Sequences of ChIP-PCR primers

Gene	Forward primer 5'-3'	Reverse primer 5'-3'
ALP	*TCCAGGGATAAAGCAGGTC*	*TTAGTAAGGCAGGTGCCAAT*
Runx2	*AGGCCTTACCACAAGCCTTT*	*AGAAAGTTTGCACCGCACTT*
BGLAP	*CAAATAGCCCTGGCAGATTC*	*GAGGGCTCTCATGGTGTCTC3*

2. Table.2 Characterization of surface microscale topography

Sample	Ra (μm)	Rq (μm)	RSm (μm)
sPC	0.05 ± 0.01	0.16 ± 0.10	/
mPC	2.94 ± 0.11	3.85 ± 0.11	160.3 ± 8.2
hPC	11.30 ± 0.43	16.12 ± 0.77	279.3 ± 32.3

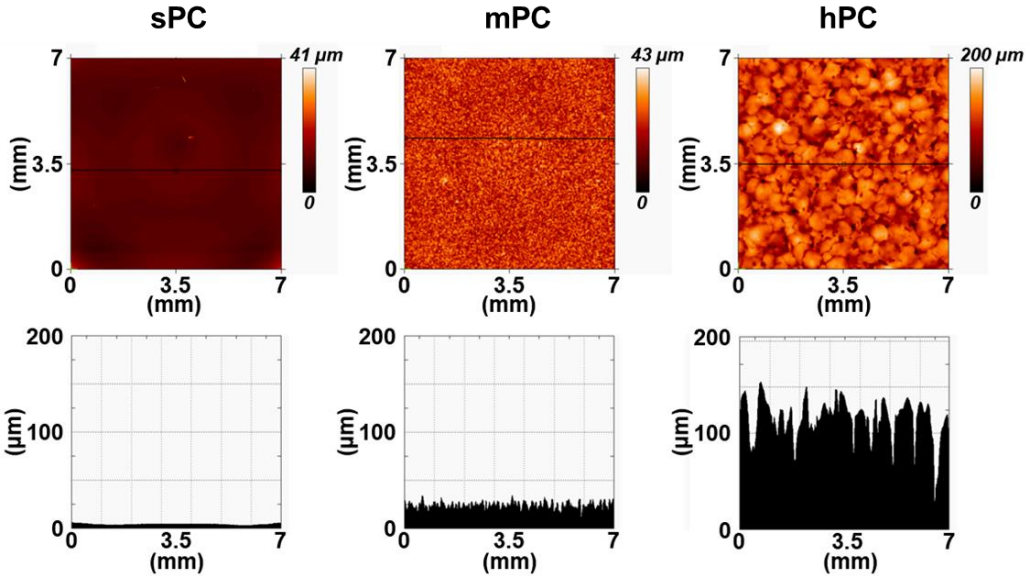

Fig. 1: Surface profiles of the sPC, mPC and hPC inserts determined by optical profilometry.

3. The western blot of actin and N-cadherin

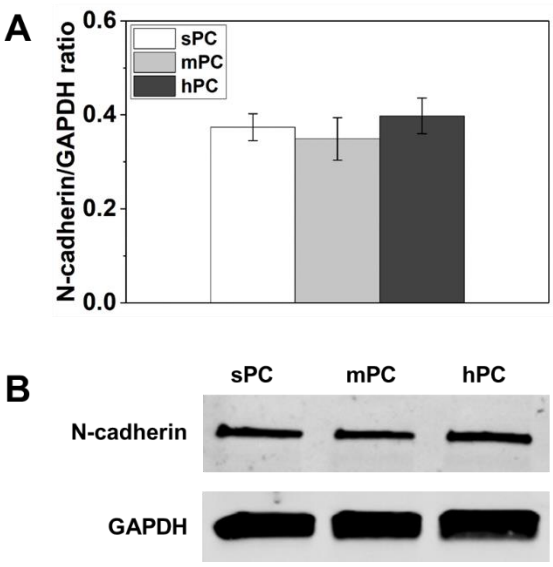

Fig. 2: The analysis of N-cadherin by western blot. A Western blot images of N-cadherin expression in hBMSCs that were cultured on the different surfaces for 4 days. B Ratio of N-cadherin: GAPDH via the image J analyzed the grayscale value of bands (n = 4).

4. Cell contractility assay

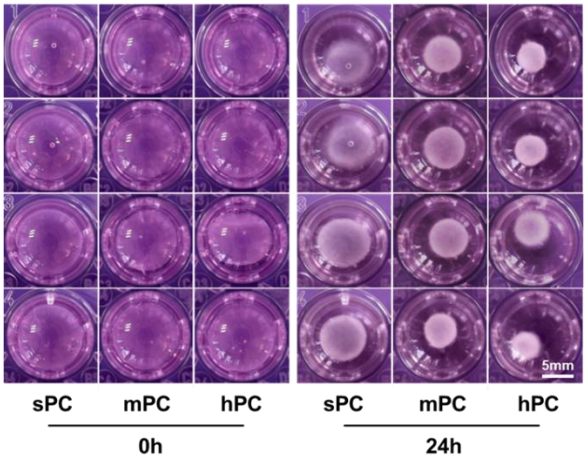

Fig. 3: The images of cell mixed collagen gel at 0 h (initial state) and the state after released at 24 h (scale bar = 5 mm).

5. Expression level of H3K27me3 of cells cultured on different surface in MM.

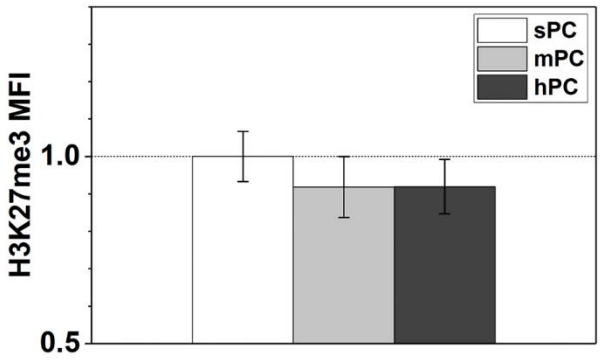

Fig. 4: Relative levels of H3K27me3 in cells cultured on different surfaces in MM for 4 days.

6. hBMSC differentiation on different surfaces.

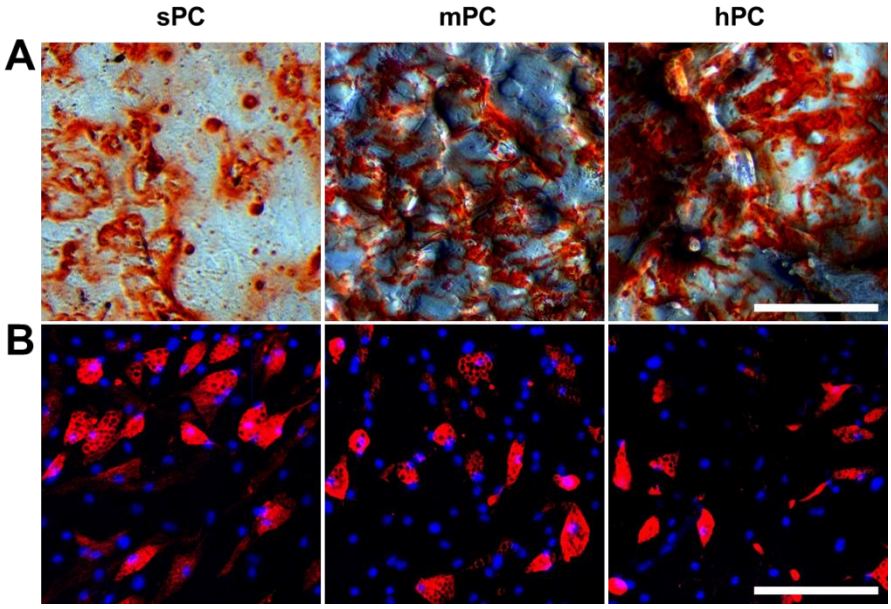

Fig. 5: Representative images of hBMSCs which were seeded on PC substrates with different surface roughness and cultured with osteogenic induction medium and adipogenic induction medium, respectively. A Images of Aliza red S staining (scale bar = 200 μm); B Images of immunofluorescence staining of FABP-4 (red: FABP-4; blue: nuclei; scale bar = 200 μm).

Chapter IV

Adipogenic differentiation of human adipose derived mesenchymal stem cells in 3D architectured gelatin based hydrogels (ArcGel)

Clinical Hemorheology and Microcirculation 2017; 67: 297–307

https://doi.org/10.3233/CH-179210

Adipogenic differentiation of human adipose derived mesenchymal stem cells in 3D architectured gelatin based hydrogels (ArcGel)

Jie Zou[a,b,1], Weiwei Wang[a,1], Axel T. Neffe[a,c], Xun Xu[a,b], Zhengdong Li[a,b], Zijun Deng[a,b], Xianlei Sun[a,d], Nan Ma[a,b,c,*] and Andreas Lendlein[a,b,c,d,*]

a *Institute of Biomaterial Science and Berlin-Brandenburg Centre for Regenerative Therapies, Helmholtz-Zentrum Geesthacht, Teltow, Germany*

b *Institute of Chemistry and Biochemistry, Freie Universit¨at, Berlin, Germany*

c *Helmholtz Virtual Institute "Multifunctional Biomaterials in Medicine", Teltow, Germany*

d *Institute of Biochemistry and Biology, Universit¨at Potsdam, Potsdam, Germany*

1 The authors contributed equally to this work

* To whom correspondence should be addressed:

Prof. Dr. Nan Ma, Prof. Dr. Andreas Lendlein

Email: nan.ma@hzg.de, andreas.lendlein@hzg.de

Phone: +49 (0)3328 352-235

Fax: +49 (0)3328 352-452

Abstract

Polymeric matrixes mimicking multiple function of the ECM are expected to enable a material induced regeneration of tissues. Here, we investigated the adipogenic differentiation of human adipose derived mesenchymal stem cells (hADSCs) in a 3D architectured gelatin based hydrogel (ArcGel) prepared from gelatin and L-lysine diisocyanate ethyl ester (LDI) in an one-step process, in which the formation of an open porous morphology and the chemical network formation were integrated. The ArcGel was designed to support adipose tissue regeneration with its 3D porous structure, high cell biocompatibility and mechanical properties compatible with human subcutaneous adipose tissue. The ArcGel could support initial cell adhesion and survival of hADSCs. Under static culture condition, the cells could migrate into the inner part of the scaffold with a depth of 840 ± 120 μm after 4 days, and distributed in the whole scaffold (2 mm in thickness) within 14 days. The cells proliferated in the scaffold and the fold increase of cell number after 7 days of culture was 2.55 ± 0.08. The apoptotic rate of hADSCs in the scaffold was similar to that of cells maintained on tissue culture plate. When cultured in adipogenic induction medium, the hADSCs in the scaffold differentiated into adipocytes with a high efficiency (93 ± 1%). Conclusively, this gelatin based 3D scaffold presented high cell compatibility for hADSC cultivation and differentiation, which could serve as a potential implant material in clinical applications for adipose tissue reparation and regeneration.

Key words: mesenchymal stem cells, gelatin based scaffold, adipose tissue regeneration, adipogenic differentiation

1. Introduction

A variety of factors including age, disease, trauma, tumor removal, congenital malformation, and burns could lead the loss of subcutaneous adipose tissue, which would affect the patients physiologically and psychologically [132-134]. However, restoring the structure and function of defective adipose tissue still presents a clinical challenge in reconstructive surgery. Currently, two approaches of treatment are commonly adopted to repair a defect of soft tissue. The first one is fat grafting or lipofilling [134], in which the autologous adipocytes are injected to the position of soft tissue defects. This procedure does not involve potentially toxic materials and is easily available, with a generally satisfying result in short term [132]. However, the long term outcomes of this approach are unpredictable due to the inner necrosis of the transplanted tissue and the high resorption rate [134, 135]. The second approach is the transplantation of filler materials such as silicon, hyaluronic acid, or calcium hydroxyapatite based materials. Despite the capacity of supporting soft tissue repair and restoration, the clinical use of such filler materials are limited because of further documented complications, such as foreign-body reactions, which potentially affect function [136], uncontrollable degradation over time [137], as well as the risk of immunogenicity [138]. To overcome those disadvantages, strategies for adipose tissue reconstruction are being investigated, focusing on the most important aspects for the success of adipose tissue reconstruction - the stem cells with adipogenic differentiation potential and the scaffold materials mimicking function of the extracellular matrix (ECM) of adipose tissue.

Adipose derived stem cells (ADSCs) are multipotent mesenchymal stem cells isolated from the adipose tissue. ADSCs show the ability to differentiate towards adipogenic, osteogenic, chondrogenic, myogenic and cardiomyogenic lineage [139, 140]. Previous research found that ADSCs differentiated into adipocytes and to replenish lost volume of soft tissue through proliferation and maturation into adipocytes, which makes them ideally suitable for adipose regeneration [141]. In addition to self-renewal and differentiation, ADSCs could secrete several growth factors including vascular endothelial growth factor (VEGF), hepatocyte growth factor (HGF), basic fibroblast growth factor (FGF-2), and insulin-like growth factor 1 (IGF-1)[142, 143], some of which could promote angiogenesis and adipose tissue regeneration[144].

In addition to ADSCs, the scaffold is of great importance for soft tissue reconstruction. By now, a variety of natural and synthetic materials have been used to produce scaffolds with the aim to support tissue repair and regeneration. When used in combination with stem cells, such a

scaffold material should at least fulfill several requirements. First, the high cell compatibility is necessary to allow for adhesion, proliferation and migration of stem cells, and later on support adipocyte survive. Second, it should have the mechanical properties comparable to native adipose tissue, to facilitate surgical handing and support adipogenic differentiation of transplanted stem cells. Third, a 3D porous structure might facilitate the accommodation of cells. At last, the scaffold should be biodegradable, which is critical to provide space for cell proliferation, guide tissue development and enable the replacement of the materials by autogenous or transplanted cells [145, 146]. Different materials have been processed into scaffolds for soft tissue engineering. Polylactic acid (PLA), polyglycolic acid (PGA) and the copolymer poly[lactide-*co*-(glycolic acid)] PLGA [147-150] are the most commonly explored synthetic materials. Collagen, silk fibroin, ECM secreted by hADSCs, decellularized human placenta, fibrin, gelatin, hyaluronic acid, and matrigel belong to the category of natural materials applied in this context [151]. Compared to synthetic polymers, the materials of natural origins, especially collagen and gelatin, offer clinically appropriate properties to mimic soft tissues. Collagen is abundantly present in native adipose ECM. It has been proved that both collagen and gelatin could support adipogenesis of stem cells [152-155].

In this context, the aim of this study is to evaluate the potential of a 3D architectured gelatin based hydrogel (ArcGel), consisting of gelatin and lysine connected by urea junction units, as scaffold for adipose tissue regeneration. Given the low cytotoxicity of gelatin from natural origin, the ArcGel scaffold was expected to support hADSC adhesion and survival with high cell viability. The lower immunogenicity of gelatin [156] might decrease the risk of strong body reaction following implantation. The ArcGel showed a porous morphology, with the pore sizes of 272±114 μm in the dry state determined by SEM, which might allow for accommodating hADSCs and providing space for cell proliferation. The ArcGel might be suitable for adipogenic differentiation of hADSCs regarding its macroscopic mechanical property, as it showed an elastic modulus of 3.1 ± 0.2 kPa determined by oscillatory rheological measurement, which is compatible to human subcutaneous adipose tissue. The water uptake of the ArcGels was 983 ± 37 wt.%, and the ArcGel could degrade *in vitro* within a few weeks [157]. Therefore, the ArcGel might have potential advantages upon degradation *in vivo*, including providing more space for cell proliferation and adipose tissue development, and facilitating the replacement of the scaffold material by native tissue. To this end, the cell biocompatibility of the ArcGel for hADSC culture as well as its potential for supporting adipogenic differentiation of hADSCs were investigated *in vitro*.

2. Materials and methods

2.1 ArcGel scaffold

The gelatin based 3D architectured hydrogel (ArcGel) was prepared using a one-step approach as reported previously [157], in which the formation of an open porous morphology and the chemical functionalization were integrated. In brief, LDI (8-fold molar excess of NCO groups compared to NH2 groups of the gelatin) was added to a 10% aqueous solution of gelatin (Type A, 200 bloom, with low endotoxin content, GELITA AG, Eberbach, Germany) and PEO-PPO-PEO triblock copolymer (Pluronic® F-108, Sigma-Aldrich Chemie, Steinheim, Germany) under mechanical stirring in a flat flange cylindrical jacketed vessel with bottom outlet valve (HWS Labortechnik, Mainz, Germany) at 45 °C. After 6 minutes the obtained ArcGel was collected and freeze-dried. To perform cell culture study, the dried ArcGel was cut into discs with 10 mm in diameter and 2 mm in thickness. Before cell seeding, the air inside the ArcGel samples was removed by infiltrating the samples into cell culture medium followed by a vacuum degassing process.

2.2 Human adipose derived mesenchymal stem cells

The hADSCs were isolated from human adipose tissue as described previously [99]. The adipose tissue was obtained by abdominal liposuction from a female donor after informed consent (No.: EA2/127/07; Ethics Committee of the Charité - Universitätsmedizin Berlin, approval from 17.10.2008). The hADSCs were cultured in the human adipose-derived stem cell medium (Lonza, Walkersville, MD, USA) at 37 °C in a humidified atmosphere containing 5% CO_2, and the medium was changed regularly to maintain cell growth.

2.3 Cell distribution and migration in ArcGel

For seeding hADSCs on ArcGel, the disc-shaped scaffold was first put into the 48-well tissue culture plate (TCP). Then, 5×10^4 cells suspended in 500 µL growth medium (Lonza, Walkersville, MD, USA) was added into each well. After culturing the cells for 4 days and 14 days, the samples were washed with PBS and fixed using 4 wt% paraformaldehyde (ThermoFisher Scientific, Waltham, USA) then permeabilized with 0.1wt% Triton X-100 (Sigma–Aldrich, St. Louis, MO, USA). After blocking with 3 wt% BSA solution, ActinRed™ 555 (Life Technologies, Darmstadt, Germany) and SYTOX Green Nucleic Acid Stain (Life Technologies, Darmstadt, Germany) were used to stain F-actin and nuclear, respectively. The stained samples were scanned on a confocal laser scanning microscope (LSM 780, Carl Zeiss, Jena, Germany) using the mode of z-stack multilayer scanning, and the images were processed

using ZEN 2012 software (Carl Zeiss, Jena, Germany). A longitudinal sectional view of the samples was achieved by cutting the samples before scanning, in order to investigate the cell migration in the scaffold.

2.4 Cell proliferation

The proliferation rate of hADSCs in the ArcGel scaffold was measured using a cell count kit (CCK-8) (Dojindo Molecular Technologies Inc, Munich, Germany) at indicated time points. In brief, for each well the old medium was replaced with 500 µl of fresh medium, followed by adding 50 µl of CCK-8 solution. After 2 hours of incubation at 37 ºC, 100 µl of medium/CCK-8 mixture was transferred from each insert into a transparent 96-well tissue culture plate, and the absorbance was measured at a wavelength of 450 nm and a reference wavelength of 650 nm using a microplate reader (Infinite 200 PRO, Tecan Group Ltd., Männedorf, Switzerland). A standard curve, which was generated by measuring the absorbance of a series of samples with known cell numbers, was used to calculate the number of hADSCs in the ArcGel.

2.5 Cellular apoptosis

Cellular apoptosis test was conducted to study the apoptotic rate of cells cultured in ArcGel. Following cell seeding in the scaffold, the caspase-3/7 activation, which is a key marker of cell apoptosis, was measured at day 1, 4 and 7 using a Caspase-Glo $^{@}$ Kit (Promege, Madison, USA). In brief, the culture medium was replaced with new medium (360 µL/sample), followed by adding Caspase-Glo$^{@}$ 3/7 reagent (300 µL/sample) and shaking orbitally at 300 rpm for 30 seconds. After incubation for 90 min at room temperature, 200 µL liquid in each sample was transferred into 96-well TCP and the luminescence intensity was measured using a microplate reader (Infinite 200 PRO®, Tecan Group Ltd., Männedorf, Switzerland). The result was given as relative light units (RLU) normalized with cell number, which was measured by CCK-8.

2.6 Adipogenic differentiation

The cells were seeded on the scaffold and cultured in adipose-derived stem cell growth medium for 14 days. Then the medium was replaced with adipogenic induction medium (Life Technologies, Darmstadt, Germany) for adipogenic differentiation. After 14 days of adipogenic induction, the samples were fixed with 4 wt% paraformaldehyde, followed by Oil Red O (Sigma–Aldrich, St. Louis, MO, USA) staining to detect the lipid droplets in the adipogenically differentiated cells[158]. Further, FABP-4 immunostaining was performed to quantify the adipogenically differentiated cells in the scaffold. In brief, after 21 days of adipogenic

induction, the samples were fixed with 4 wt% paraformaldehyde and permeabilized with 0.1 wt% Triton X-100 solution. Then, the cells were blocked with 3 wt% BSA and stained using rabbit anti-human FABP-4 monoclonal antibody (Merck Millipore, Darmstadt, Germany) and Alexa Fluor® 488 labeled IgG antibodies (Life Technologies, Darmstadt, Germany). Cell nuclei were stained by SYTOX Green Nucleic Acid Stain (Life Technologies, Darmstadt, Germany). The stained samples were scanned with a confocal laser scanning microscope (LSM 780, Carl Zeiss, Jena, Germany) using the mode of z-stack multilayer scanning, and the images were processed using ZEN 2012 software (Carl Zeiss, Jena, Germany). Then, the cells were counted to calculate the percentage of differentiated cells (FABP-4 expressing cells/total cells × 100%).

In addition, the expression level of FABP-4 protein was determined using ELISA. The cells were washed with PBS and lysed using cell lysis buffer (ThermoFisher Scientific, Waltham, USA) after 14 or 21 days of induction in ArcGel. The amount of FABP-4 was measured using a FABP-4 ELISA kit (Abcam, Cambridge, UK) according to the manufacture introduction. The experiment was performed in triplicates. The hADSCs cultured on TCP and/or in growth medium were included as controls.

2.7 Statistics

ArcGel samples from three batches and hADSCs from one donor were used in this study. The number of replications was larger than three as indicated in the figure legend of Fig. 2 and 4. The results were expressed as mean ± standard deviation (SD). Statistical analysis was performed using independent-samples T-test and a significance level (Sig.) <0.05 was considered to be statistically significant.

3. Results

3.1 Cell distribution and migration into the ArcGel

After 4 and 14 days of cultivation in growth medium, the cells were stained to investigate the cell distribution and migration into the ArcGel. The cells could attach and spread on the scaffold. The density of cells on the material surface increased with the culture time, as shown in top-view images of day 4 and day 14 (Fig. 1 A), indicating the cell growth on the scaffold. Further, the cells could migrate into the scaffold after cell attachment, due to the high porosity of the ArcGel. After 4 days of cultivation, the cells migrated into the scaffold for 840±120 μm; and after 14 days, the cells distributed in the whole scaffold with a thickness of 2 mm (Fig.1B).

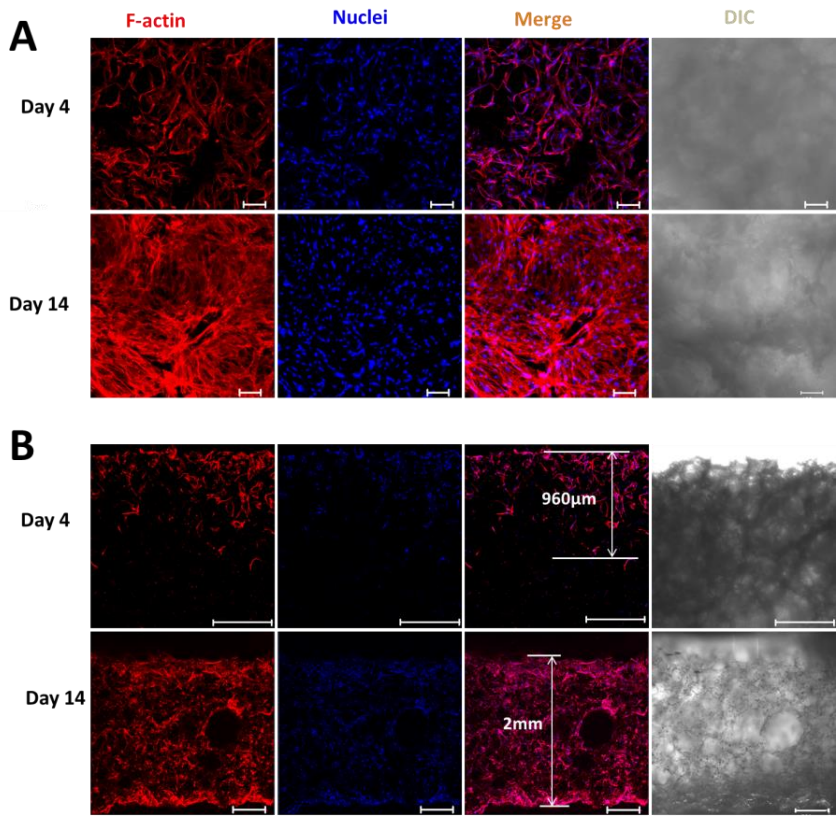

Fig. 1. The distribution and migration of hADSCs into the ArcGel. hADSCs were cultured in the ArcGel for 4 days and 14 days followed by fluorescence staining to visualize the actin cytoskeleton (red) and nuclei (blue). (A) Top-view images showed hADSCs could attach and grow on the ArcGel surface (bar = 100 μm). (B) Longitudinal section-view images indicated the hADSCs migration into the ArcGel (bar = 500 μm).

3.2 Cell proliferation and apoptosis

Cell proliferation in the ArcGel was studied by quantifying the cell number at different time points (Fig.2A). The scaffold showed a high capacity for allowing hADSC proliferation. After 7 days of cultivation in grow medium, the fold increase of cell number was 2.55 ± 0.08. After 10 days, the fold increase of cell number reached to 5.75 ± 0.42. In order to study the influence of ArcGel scaffold on cell apoptosis, the apoptotic level was evaluated at day 1, 4 and 7 (Fig.2B). A decreasing tendency of cell apoptosis level was observed in all groups, i.e. ArcGel, TCP+ArcGel and TCP. There was no significant difference of apoptotic level in the tested three groups.

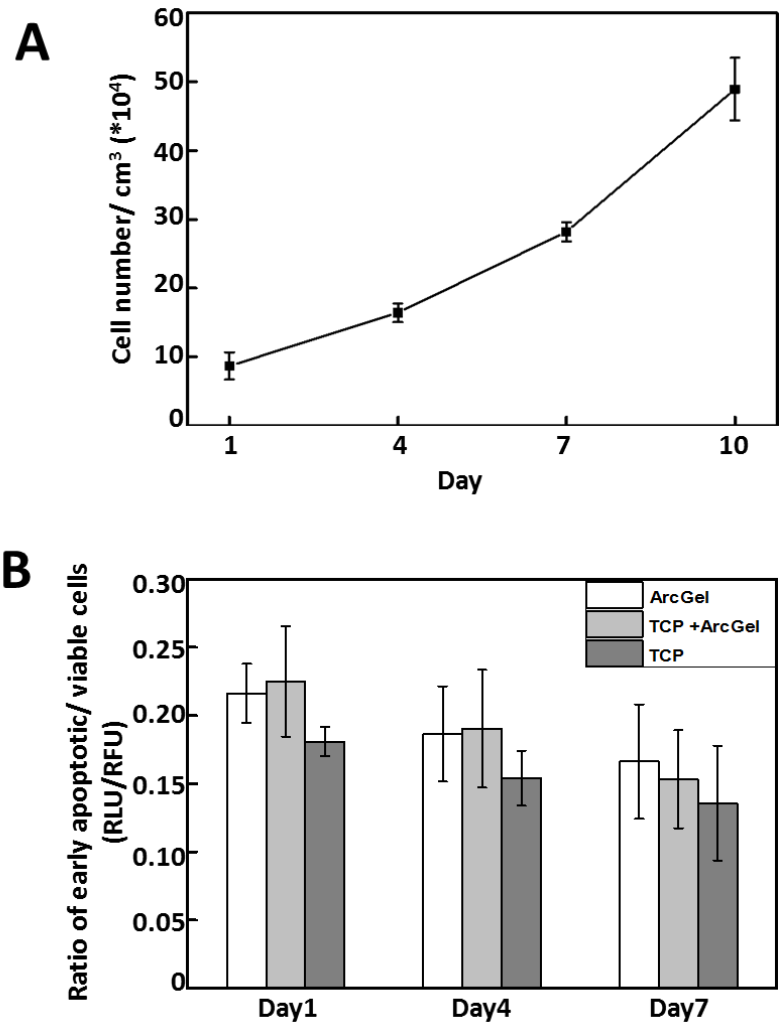

Fig. 2 Cell proliferation and apoptosis in ArcGel. (A) Proliferation of hADSCs on ArcGel. (B) The apoptosis of hADSCs on different substrates. (ArcGel: cells seeded on ArcGel; TCP+ ArcGel: cells seeded on TCP, with ArcGels added to the culture medium; TCP: cells seeded on TCP) (n = 3)

3.3 Adipogenic differentiation of hADSCs in ArcGel

The ADSCs could differentiate into adipocytes in the ArcGel in adipogenic induction medium. Similar to the cells on TCP, the formation of lipid droplets was observed in hADSCs in ArcGel after 14 days of adipogenic induction, as shown in oil red O staining images (Fig. 3). The quantification of FABP-4, the marker of adipogenic differentiation, indicated a high differentiation rate of hADSCs in ArcGel. Around 93 ± 1% hADSCs were FABP-4 positive, based on the fluorescence images of stained cells (representative images in Fig. 4A). The images of longitudinal section-view showed that even the cells inside the ArcGel underwent differentiation (Fig. 4B). This result was confirmed by FABP-4 quantification using ELISA. After 21 days of cultivation in adipogenic induction medium, hADSCs in ArcGel presented

similar FABP-4 expression level as those cultured on TCP, and was higher than that after 14 days of induction (Fig. 4C). The cells did not undergo differentiation in normal growth medium in either ArcGel or TCP, indicating that there was no spontaneous differentiation.

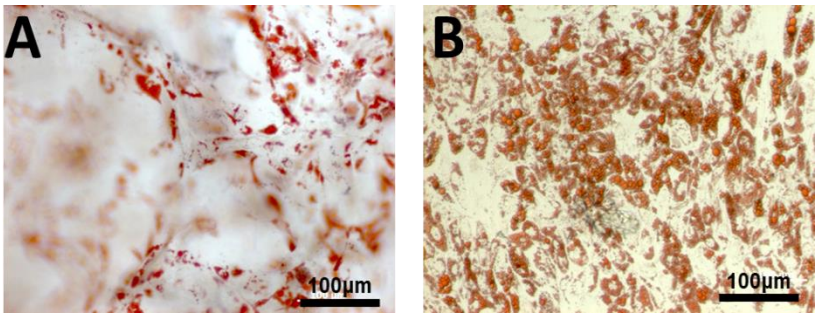

Fig.3 Oil red O staining of adipogenically differentiated hADSCs in ArcGel (A) and on TCP (B) after 14 days of cultivation in adipogenic induction medium.

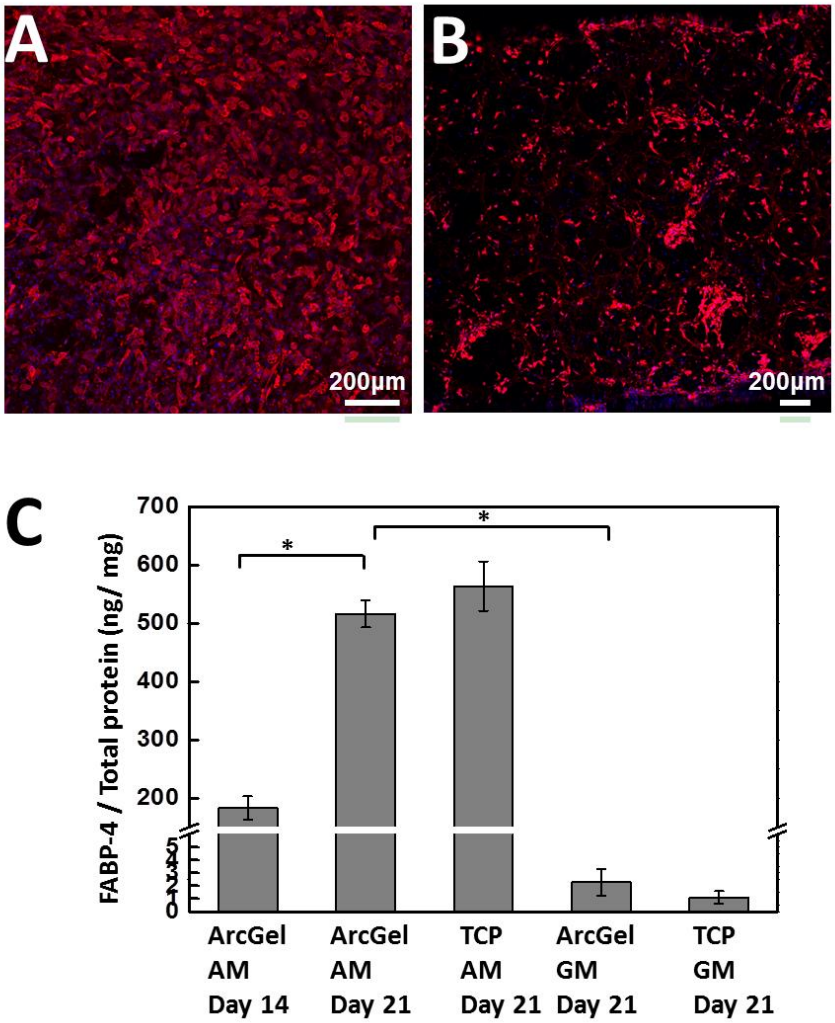

Fig.4 FABP-4 expression of adipogenically differentiated hADSCs. Top-view (A) and longitudinal section-view (B) images of FABP-4 expressing cells in ArcGels. Cells were cultured in adipogenic induction medium for 21 days followed by immunostaining (red: FABP-

4; blue: nuclei) (C) The quantification of FABP-4 expression of cells cultured in ArcGel, or on TCP (AM: adipogenic induction medium; GM: growth medium; n= 3; *Sig< 0.05).

4. Discussion

In this study, we show that ArcGel could serve as a promising scaffold for adipose tissue regeneration, attributing to its high cell compatibility for hADSC cultivation and adipogenic differentiation. The scaffold was produced using gelatin, which contains Arg-Gly-Asp (RGD) sequences that promote cell adhesion and proliferation [159, 160]. Gelatin is soluble in aqueous solutions at ≥ 35-40 °C, and its mechanical strength could be improved through crosslinking by glutaraldehyde [161], or genipin [162], or by promoting the reaction of gelatin functional groups using agents such as 1-ethyl-3-(3'-dimethylaminopropyl) carbodiimide hydrochloride (EDC) [163]. However, some of these crosslinking agents are highly toxic, which might lead to cell death caused by crosslinker residuals. Here, L-lysine diisocyanate ethyl ester (LDI) was employed as starting material that reacts with amino groups in gelatin and with water under decarboxylation, giving rise to the formation of direct crosslinks and of oligourea crosslinks and grafts, all adding to the stabilization of the system [164]. IR spectra of the final, washed ArcGels did not display bands indicative for unreacted isocyanate groups. The hADSCs could attach on the ArcGel and exhibit the typical MSC morphology. The cells could proliferate on the scaffold without alteration of their adipogenic differentiation potential. These results indicated high cell compatibility of ArcGel for hADSC culture and differentiation. Apoptosis is the programmed cell death, by which the cell undergoes intentional suicide [165]. Apoptosis can be initiated through different pathways. In the intrinsic pathway, the cells die because they sense cell stress, while in the extrinsic pathway the cells underwent apoptosis upon receiving signals from other cells [166]. Here, we investigated the apoptosis of hADSCs seeded directly in the ArcGel and in the ArcGel leached medium (culturing cells in TCP with the presence of ArcGel in medium). The apoptotic rate of hADSCs in the ArcGel and in the ArcGel leached medium were similar to that of cells cultured on tissue culture plate, suggesting that no strong cellular apoptosis was induced by either the ArcGel or the small molecules resulting from ArcGel degradation.

In addition to the chemical properties, physical properties of the scaffold material could affect stem cell behavior and fate. For example, the materials stiffness could specifically direct stem cell differentiation lineage [19, 167], while the porosity, pore size and pore interconnection have been shown to directly affect cell migration, proliferation, differentiation, microvascular formation, oxygen and nutrients supply, as well as the exchange of metabolites [168-172].

Therefore, these parameters are important in the criteria of scaffold design. The elastic modulus of the ArcGel determined by rheology was 3.1 ± 0.2 kPa, which was relatively compatible with the human subcutaneous adipose tissue with an initial modulus of 1.6 ± 0.8 kPa measured by tensile testing [173]. Therefore, the ArcGel with such an elasticity at the macroscopic level might facilitate the differentiation of ADSCs towards adipogenic lineage. The parameter of local elastic modulus at the microscopic level is also critical for stem cell differentiation, as demonstrated in our previous work that the stiffer ArcGel with local elastic modulus of 1250 ± 140 kPa could promote *in vitro* osteogenic differentiation of MSCs and *in vivo* bone regeneration [157]. The ArcGel used in the present study had a local elastic modulus of 55 ± 30 kPa as measured by AFM indentation test [174], which was much lower than that of the osteogenesis-promoting ArcGel. Accordingly, a higher level of adipogenic differentiation of hADSCs was observed in the ArcGel of this study. However, it should be noted that the ArcGel used here is still stiffer than adipose tissue [175], suggesting the potential flexibility to regulate hADSC differentiation by tuning the ArcGel mechanical properties, i.e., decreasing the elasticity of the ArcGel by reducing the LDI amount might be able to further improve its potential for ADSC adipogenesis. The high porosity with appropriate pore size of ArcGel could provide enough space for hADSC accommodation, proliferation and differentiation. The pore-pore interconnection could allow for cell migration. Accordingly, the hADSCs seeded on scaffold surface migrated into the inner part of the scaffold and distributed in the whole scaffold after 2 weeks of culture. This result is of great importance for applying ArcGel in adipose tissue reconstruction. The ArcGel would not only facilitate the *in vitro* preparation of homogeneously stem cell-loaded 3D scaffold but also allow for the migration of autogenous cells into the scaffold after implantation which might accelerate the process of soft tissue reconstruction. Notably, as revealed by our previous work [99], the pores merged during ArcGel degradation, resulting in the formation of new, larger and round pores but retaining the integrity of the 3D porous structure. These results suggested that at subsequent phase after implantation the ArcGel scaffold might be able to offer more space for cell proliferation and guide adipose tissue development.

hADSCs isolated from human aspirated fat tissue exhibit strong proliferation and adipogenic differentiation potential *in vitro*. The scaffold materials loaded with ADSCs must be able to support adipogenic differentiation of the cells to contribute to adipose tissue reparation. In this context, the adipogenic differentiation of hADSCs in ArcGels was assessed. When cells were cultured in growth medium, no adipogenic differentiation was observed, indicating that the

ArcGel could maintain hADSC stemness and did not induce spontaneous differentiation. When adipogenic induction medium was applied, the hADSCs in the scaffold differentiated into adipocytes with a high efficiency (93 ± 1%). These results suggested the potential of the ArcGel to be used for adipose tissue reconstruction. According to the clinical requirement, different treatment approaches might be flexibly adopted: (i) direct implantation of the ArcGel, which might facilitate the adipogenic differentiation of autogenous ADSCs, (ii) implantation of the ArcGel pre-loaded with ADSCs, which might undergo adipogenic differentiation in the body, (iii) implantation of the ArcGel pre-loaded with adipogenically induced ADSCs.

5. Conclusion

In this study, a 3D gelatin-based hydrogel (ArcGel) was evaluated for hADSC cultivation and adipogenic differentiation. The ArcGel showed high cell compatibility for hADSC adhesion, spreading and proliferation. The cellular apoptosis level of hADSCs in ArcGel was similar to that on tissue culture plate. The high porosity of ArcGel with appropriate pore size could allow for hADSC accommodation and provide space for cell proliferation. Importantly, the pore-pore interconnection facilitated cell migration in the ArcGel. The hADSCs in the ArcGel could maintain their stemness in growth medium, and undergo adipogenic differentiation with a high efficiency in adipogenic induction medium. Conclusively, the ArcGel presented high cell compatibility for hADSC cultivation and differentiation, which could serve as a potential implant material in clinical applications for adipose tissue reparation and regeneration.

Reference

1. Bucky, L.P. and I. Percec, *The science of autologous fat grafting: views on current and future approaches to neoadipogenesis.* Aesthet Surg J, 2008. **28**(3): p. 313-21; quiz 322-4.
2. Patrick, C.W., Jr., *Tissue engineering strategies for adipose tissue repair.* Anat Rec, 2001. **263**(4): p. 361-6.
3. Tabit, C.J., et al., *Fat Grafting Versus Adipose-Derived Stem Cell Therapy: Distinguishing Indications, Techniques, and Outcomes.* Aesthetic Plastic Surgery, 2012. **36**(3): p. 704-713.
4. Tremolada, C., G. Palmieri, and C. Ricordi, *Adipocyte Transplantation and Stem Cells: Plastic Surgery Meets Regenerative Medicine.* Cell Transplantation, 2010. **19**(10): p. 1217-1223.
5. Anderson, J.M., A. Rodriguez, and D.T. Chang, *Foreign body reaction to biomaterials.* Semin Immunol, 2008. **20**(2): p. 86-100.
6. Young, D.A. and K.L. Christman, *Injectable biomaterials for adipose tissue engineering.* Biomed Mater, 2012. **7**(2): p. 024104.
7. Franz, S., et al., *Immune responses to implants - A review of the implications for the design of immunomodulatory biomaterials.* Biomaterials, 2011. **32**(28): p. 6692-6709.
8. Levi, B., et al., *Depot-Specific Variation in the Osteogenic and Adipogenic Potential of Human Adipose-Derived Stromal Cells.* Plastic and Reconstructive Surgery, 2010. **126**(3): p. 822-834.
9. Rodriguez, A.M., et al., *The human adipose tissue is a source of multipotent stem cells.* Biochimie, 2005. **87**(1): p. 125-128.
10. Hong, L., et al., *Adipose tissue engineering by human adipose-derived stromal cells.* Cells Tissues Organs, 2006. **183**(3): p. 133-40.
11. Kim, W.S., B.S. Park, and J.H. Sung, *Protective role of adipose-derived stem cells and their soluble factors in photoaging.* Archives of Dermatological Research, 2009. **301**(5): p. 329-336.
12. Salgado, A.J., et al., *Adipose Tissue Derived Stem Cells Secretome: Soluble Factors and Their Roles in Regenerative Medicine.* Current Stem Cell Research & Therapy, 2010. **5**(2): p. 103-110.
13. Kakudo, N., A. Shimotsuma, and K. Kusumoto, *Fibroblast growth factor-2 stimulates adipogenic differentiation of human adipose-derived stem cells.* Biochemical and Biophysical Research Communications, 2007. **359**(2): p. 239-244.
14. Cosgriff-Hernandez, E. and A.G. Mikos, *New biomaterials as scaffolds for tissue engineering.* Pharm Res, 2008. **25**(10): p. 2345-7.
15. Rahaman, M.N. and J.J. Mao, *Stem cell-based composite tissue constructs for regenerative medicine.* Biotechnol Bioeng, 2005. **91**(3): p. 261-84.
16. Morgan, S.M., et al., *Formation of a human-derived fat tissue layer in P(DL)LGA hollow fibre scaffolds for adipocyte tissue engineering.* Biomaterials, 2009. **30**(10): p. 1910-1917.
17. Wang, X.H., et al., *Design and Fabrication of PLGA Sandwiched Cell/Fibrin Constructs for Complex Organ Regeneration.* Journal of Bioactive and Compatible Polymers, 2010. **25**(3): p. 229-240.

18. Yeon, B., et al., *3D Culture of Adipose-Tissue-Derived Stem Cells Mainly Leads to Chondrogenesis in Poly(ethylene glycol)-Poly(L-alanine) Diblock Copolymer Thermogel.* Biomacromolecules, 2013. **14**(9): p. 3256-3266.
19. Zambon, J.P., et al., *Histological changes induced by Polyglycolic-Acid (PGA) scaffolds seeded with autologous adipose or muscle-derived stem cells when implanted on rabbit bladder.* Organogenesis, 2014. **10**(2): p. 278-288.
20. Casadei, A., et al., *Adipose Tissue Regeneration: A State of the Art.* Journal of Biomedicine and Biotechnology, 2012.
21. Choi, J.H., et al., *Adipose Tissue Engineering for Soft Tissue Regeneration.* Tissue Engineering Part B-Reviews, 2010. **16**(4): p. 413-426.
22. Rubin, J.P., et al., *Collagenous microbeads as a scaffold for tissue engineering with adipose-derived stem cells.* Plastic and Reconstructive Surgery, 2007. **120**(2): p. 414-424.
23. Mauney, J.R., et al., *Engineering adipose-like tissue in vitro and in vivo utilizing human bone marrow and adipose-derived mesenchymal stem cells with silk fibroin 3D scaffolds.* Biomaterials, 2007. **28**(35): p. 5280-5290.
24. Itoi, Y., et al., *Comparison of readily available scaffolds for adipose tissue engineering using adipose-derived stem cells.* Journal of Plastic Reconstructive and Aesthetic Surgery, 2010. **63**(5): p. 858-864.
25. Rose, J.B., et al., *Gelatin-Based Materials in Ocular Tissue Engineering.* Materials, 2014. **7**(4): p. 3106-3135.
26. Neffe, A.T., et al., *One step creation of multifunctional 3D architectured hydrogels inducing bone regeneration.* Adv Mater, 2015. **27**(10): p. 1738-44.
27. Xu, X., et al., *Controlling Major Cellular Processes of Human Mesenchymal Stem Cells using Microwell Structures.* Advanced Healthcare Materials, 2014. **3**(12): p. 1991-2003.
28. Aldridge, A., et al., *Assay validation for the assessment of adipogenesis of multipotential stromal cells--a direct comparison of four different methods.* Cytotherapy, 2013. **15**(1): p. 89-101.
29. Nagahama, H., et al., *Preparation, characterization, bioactive and cell attachment studies of alpha-chitin/gelatin composite membranes.* International Journal of Biological Macromolecules, 2009. **44**(4): p. 333-337.
30. Davidenko, N., et al., *Evaluation of cell binding to collagen and gelatin: a study of the effect of 2D and 3D architecture and surface chemistry.* Journal of Materials Science-Materials in Medicine, 2016. **27**(10).
31. Bigi, A., et al., *Mechanical and thermal properties of gelatin films at different degrees of glutaraldehyde crosslinking.* Biomaterials, 2001. **22**(8): p. 763-768.
32. Lien, S.M., W.T. Li, and T.J. Huang, *Genipin-crosslinked gelatin scaffolds for articular cartilage tissue engineering with a novel crosslinking method.* Materials Science & Engineering C-Biomimetic and Supramolecular Systems, 2008. **28**(1): p. 36-43.
33. Chang, J.Y., et al., *In vivo evaluation of a biodegradable EDC/NHS-cross-linked gelatin peripheral nerve guide conduit material.* Macromolecular Bioscience, 2007. **7**(4): p. 500-507.
34. Tronci, G., et al., *An entropy-elastic gelatin-based hydrogel system.* Journal of Materials Chemistry, 2010. **20**(40): p. 8875-8884.
35. Majno, G. and I. Joris, *Apoptosis, Oncosis, and Necrosis - an Overview of Cell-Death.* American Journal of Pathology, 1995. **146**(1): p. 3-15.

36. Kerr, J.F., A.H. Wyllie, and A.R. Currie, *Apoptosis: a basic biological phenomenon with wide-ranging implications in tissue kinetics.* Br J Cancer, 1972. **26**(4): p. 239-57.
37. Engler, A.J., et al., *Matrix elasticity directs stem cell lineage specification.* Cell, 2006. **126**(4): p. 677-689.
38. Gobaa, S., S. Hoehnel, and M.P. Lutolf, *Substrate elasticity modulates the responsiveness of mesenchymal stem cells to commitment cues.* Integrative Biology, 2015. **7**(10): p. 1135-1142.
39. Placzek, M.R., et al., *Stem cell bioprocessing: fundamentals and principles.* Journal of the Royal Society Interface, 2009. **6**(32): p. 209-232.
40. Polak, D.J., *Regenerative medicine. Opportunities and challenges: a brief overview.* Journal of the Royal Society Interface, 2010. **7**: p. S777-S781.
41. Novosel, E.C., C. Kleinhans, and P.J. Kluger, *Vascularization is the key challenge in tissue engineering.* Advanced Drug Delivery Reviews, 2011. **63**(4-5): p. 300-311.
42. Kim, H.J., et al., *Influence of macroporous protein scaffolds on bone tissue engineering from bone marrow stem cells.* Biomaterials, 2005. **26**(21): p. 4442-4452.
43. Safinia, L., A. Mantalaris, and A. Bismarck, *Nondestructive technique for the characterization of the pore size distribution of soft porous constructs for tissue engineering.* Langmuir, 2006. **22**(7): p. 3235-3242.
44. Alkhouli, N., et al., *The mechanical properties of human adipose tissues and their relationships to the structure and composition of the extracellular matrix.* American Journal of Physiology-Endocrinology and Metabolism, 2013. **305**(12): p. E1427-E1435.
45. Vukićević, R., et al., *Mechanical Properties of Architectured Gelatin-Based Hydrogels on Different Hierarchical Levels.* MRS Advances, 2016. **1**(27): p. 7.
46. Sartori, S., et al., *Biomimetic polyurethanes in nano and regenerative medicine.* Journal of Materials Chemistry B, 2014. **2**(32): p. 5128-5144.

Chapter V

Discussion, conclusion and outlook

Discussion

The functions and fate of stem cells are regulated by various stimuli dictated by the microenvironment including soluble factors, matrix- mediated cues as well as cell-cell interactions [1]. It is widely accepted that the stem cell behaviors and phenotypes, including proliferation, migration, apoptosis, senescence and differentiation are significantly influenced by the soluble factors (growth factors and cell-secreted cytokines) [2]. Recently, accumulating evidence indicated that physical cues presented by the microenvironments played an important role in regulating stem cell behaviors and fate. Physical cues include substrate stiffness, surface topography and external dynamic force. In this thesis, the mechanism how substrate microscale topography influences human bone marrow mesenchymal stem cells (hBMSCs) lineage commitments was investgated. For the cultivation of hBMSCs, PC was selected as material for the perpetration of the inserts with different surface topographies. In chapter II, the behaviors of hBMSCs on PC surface were evaluated for verifying if PC cell compatibility was good enough for maintaining hBMSCs proliferation, secretion and differentiation potentials. In chapter III, hBMSCs were cultured on PC inserts with different topographic surfaces, and then the osteogenic and adipogenic differentiation of hBMSCs on different surfaces were tested. Furthermore, the mechanism of surface topographical cues influence hBMSCs differentiation was investigated. In chapter IV, human adipose tissue-derived stem cells (hADSCs) were seeded on 3D architectured gelatin based hydrogels (ArcGel), and the influence of AreGel local E-modules and microstructure on hADSC proliferation, migration, and senescence as well as differentiation behaviors were evaluated.

In chapter II, we found that PC showed high cell compatibility for hBMSC adhesion and spreading, and hBMSCs on PC presented similar senescence level compared to that on TCP, but PC promoted inflammatory cytokines and pro-angiogenic factors secretion of hBMSCs. In our study, the PS and TCP (PS with surface modification) were used as negative and positive control as the previous study had demonstrated that there were similar E-modules (16 ± 4GPa *VS* 13 ± 2 GPa) of PS and PC [3]. The wettability of PC is higher than that of PS (PC: 85 ± 8^{o} VS PS: 99 ± 5^{o}). The surface wettability greatly affects the cell adhesion, which was reconfirmed by the different cell adhesion level of hBMSCs on PC and PS. This can be attributed to the polar carbonate groups existing in PC, which regulates the protein adsorption. The lower wettability of PS resulted in the cell clusters formation of hBMSCs on PS surface (chapter II, Fig. 5). The spreading state of cells on the material surface directly affects cell-cell interaction and the paracrine level of cells. The analysis of secretion result showed that the

paracrine level of hBMSCs on PS surface was significantly higher than that on PC surface (chapter II, Fig. 4). This result was consistent with a previous study, in which the formation of cell sphere would enhance secretion of factors that mediate inflammatory and immune responses [12]. Substrate surface chemical groups regulate surface wettability and further mediate proteins adsorption onto the surface in different ways [4]. L. Hao and coworkers[5] found that for hMSCs adhesion the contact angle of substrate surface was best at 46^{o} and for mMSCs at 73^{o}. Now it is widely accepted that surface wettability regulates protein adsorption and then modulates stem cell adhesion, further influencing stem cell migration and secretion as well as differentiation behaviors. However, Y. Arima and coworker found the stem cells on the surfaces with same wettability but different chemical functional groups have different adhesion manners [6]. Those indicated that the surface chemical groups not only influenced surface wettability but could also directly regulate stem cell behaviors. Different chemical groups on surface could regulate protein adsorption ways, orientation, or even denaturation[7], which further influence stem cell behaviors. Carboxylic acid group (–COOH) promoted hMSC chondrogenic differentiation and phosphate functionalities ($–OPO(OH)_2$) enhanced the osteogenic differentiation, whereas the hydrophobic tert-butyl functionality ($–C(CH_3)_3$) displayed higher levels of adipogenic markers [8]. These results were different from Curran`s research [9], in which $–CH_3$ modified surface maintained the hMSCs phenotype, –SH and $–NH_2$ supported hMSC osteogenic differentiation, –COOH and –OH surfaces supported hMSC chondrogenic differentiation. This discrepancy might be caused by the different mechanical properties of the substrates. Here, the adipogenic and osteogenic differentiation potentials of hBMSCs on PC and PS surfaces were examined. The results showed that the hBMSCs were capable of maintaining their differentiation potential on PC and PS (chapter II, Fig. 5), which indicated that the difference of chemical properties between PC and PS surfaces was not enough to cause the change of BMSC differentiation potential.

It is widely accepted that the mechanical cues of microenvironment play an important role to regulate stem cell behaviors and fate. Controlling the stem cell behaviors and fate by engineered substrate topographical cues is an approach, which attracts growing interests of researchers. With the development of material fabrication technologies such as photolithography, self-assembling, 3D printing, chemical etching sandblasting and electrospinning, it is possible to create the precisly controlled nano/micro scale topographical cues on substrate surfaces, which would contribute to studying the topographical cues regulating cell behaviors and fate in vitro [10, 11]. There were some examples of regulating

cell behaviors and fate through engineering substrate topographical cues (chapter I, Table 1). With the deepening of the research on the mechanism of topographical cues regulating cell behaviors and fate, it was found that the topographical cues regulating focal adhesion formation played a crucial role in the processing. In our study, we investigated the influence of surface topographical cues mediated cell contraction force on nucleus. The topographic surface promoted the F-actin polymerization and MLC activation as well as enhanced the cell contractility, which led to nuclei deformation (nuclei aspect ratio increased) (chapter III, Fig. 2), promoted the mechanosensor factor YAP nuclear location (chapter III, Fig. 3) and elevated the lamin A/C expression (chapter III, Fig. 4). These results were consistent with previous reports [13-15]. The substrate's physical cue mediated mechanical force is transmitted to nucleus via the linker of nucleoskeleton and cytoskeleton (LINC) complex, and lead to nuclear deformation and altering the permeability of nuclear pore complexes(NPC) as well as changes of nuclear lamina composition have been demonstrated and accepted. However, how the mechanical force further influences the genes expression is unclear. Here, the influence of mechanical force on the expression of H3K27me3 was investigated. The result showed that the increasing of mechanical force led to enhancement of global H3K27me3 (chapter III Fig. 5), which was consistent with previous study [16]. The upgradation of H3K27me3 means increase of chromatin compaction and depression of gene expression, which was different from the results of Downing report [17]. In their study, they found that the surface topographical cues enhanced the histone H3 acetylation and methylation, especially promoted the modification levels of H3K4me3 and H3K4me2 as well as global acetylation of H3, which indicated that the topographical cues mediated mechanical force opened and active the global chromatin and led to the nucleus was relatively soft [18]. The discrepancy might be caused by the different cell types, which were used in these studies. The multipotent stem/ progenitor cells (EPCs) and mice fibroblast cells were used in Downing`s and Le's studies, respectively. In addition, there is difference of the mechanical force that was applied on cells in two studies. In Downing's research the mechanical force was regulated by the substrate surface topographical cues, which was the internal static force generated by the cell itself [17]. In contrast, external dynamic strain force was applied to cells in Le's experiment [16]. In addition to cell types, the different time of mechanical force applied on the cells also led to different cell behaviors. Tajik and coworkers [19] demonstrated that the external dynamic force applied on cells in a short time (minimum 15 s) rapidly induced transcription. However, the long-term force application (12 h) can lead to enhancing of chromatin compaction and repressing transcription [16]. Except for the time period of mechanic force applied, the mechanical force led strain magnitude also modulated

the deformation of nucleus [20]. Moreover, the direction of mechanical force applied on cells could be another factor that regulates cells with different behaviors such as migration and differentiation. The external dynamic force strained the cells, which resulted in the increasing of H3K27me3, chromatin compaction and transcription repression as well as the nucleus stiffing [16]. However, the mechanical force compressed the cells, which led to increasing of histone 3 at the residue K4 (H3K4me3) trimethylation, softening the nucleus [21]. Therefore, the strain force and compression force applied on a cell would lead to different lineage commitments of stem cells. The dynamic compression has been shown to favor chondrogenic differentiation of MSCs in the absence of exogenous growth factor stimulation [22, 23], and the dynamic strain has been shown to enhance the expression of ligamentous/fibrogenic, osteogenic markers [24-26]. These research data demonstrate that the mechanical force (internal static and external dynamic) regulates cell epigenetic status is a very complicated process, which in turn depends on the cell type and the ways of force applied on cells. There were some previous studies about the mechanical stimuli affecting cell epigenetic status (chapter V table1).

Table 1: Example of studies about mechanical stimuli affecting cell epigenetic

Substrate	Cell source	Mechanical stimuli	Highlights	Ref.
PDMS	mFibroblast	Microgroove	Microgroove surface increased histone H3 acetylation and methylation, and promoted d mesenchymal-to-epithelial transition in adult fibroblasts.	[17]
Ti	BMSC	Hierarchical micro/nanoscale topography	The titanium topographic surface elevated global level of H3K4me3, and increased H3K4me3 levels at RUNX2 gene promoter, decreased H3K27me3 levels at the RUNX2 gene promoter, subsequently enhanced BMSC osteogenic differentiation.	[27]
TiO_2	hADSCs	Nanotube arrays	TiO2 nanotubes accelerated osteogenic differentiation of hADSCs by enhancing methylation of histone H3 at lysine 4 (H3K4) at the promoter regions of osteogenesis-related genes by inhibiting a histone demethylase – retinoblastoma binding protein 2 (RBP2)	[28]
Graphene	mFibroblasts	Monolayer graphene film	Graphene substrate significantly improved cellular reprogramming efficiency by inducing mesenchymal-to-epithelial-transition (MET), which affected H3K4me3 levels.	[29]
Si	Cardiac progenitors	Microgrooves (10 μm wide, 3 μm deep)	Microgrooves substrate provoked an increase in histone H3 acetylation (AcH3) and enhanced the directed differentiation of cardiac progenitors into cardiomyocyte-like cells.	[30]
Glass	NIH3T3	Fibronectin micropattern coating	Micropattern confined the cell growth resulted the changes of nucleus and chromatin of divided cell (H3K4me3), further led to the progressive erasure of lineage specific characteristics and incorporation of pluripotency.	[31]
Silicone elastomer membrane	EPCs	Mechanical strain	Force-driven leads to switch from H3K9me2, 3 to H3K27me3. Further, the accumulation of H3K27me3 affects the cell lineage commitments.	[16]
FN coated plate	mESCs	Shear stress (10 dyne per cm^2/s^{-1})	Shear stress enhanced the expression of H3K14ac as well as serine phosphorylation at position 10 (S10) and lysine methylation at position 79 (K79), and cooperated with TSA, inducing acetylation of histone H4 and phosphoacetylation of S10 and K14 of histone H3.	[32]

BMSCs: bone marrow mesenchymal stem cells; mFibroblast: mice fibroblast; hADSCs: human adipose-derived mesenchymal stem cells; EPCs: human primary epidermal keratinocytes; mESCs: Murine ES cells (ES day 3); PDMS: polydimethylsiloxane;

Currently, the research about the mechanical force influencing stem cell epigenetic status mainly focused on the global histone modification; however, few studies investigated how mechanical force regulates specific gene expression. In our study, we studied the enrichment of H3K27me3 and H3K9ac on the promoters of osteogenic differentiation related genes (chapter III Fig. 6). The results showed that the mechanical force regulating gene expression via modulating the enrichment of modified histone was located on the specific gene promoters, which is consistent with other studies [27, 33]. However, how the mechanical force regulates the enrichment of modified histone located on specific gene promoters is still unknown, which needs further investigation.

The substrate topographical cues' influence on stem cell behaviors not only performs on the 2D substrate, the topographic structure of 3D scaffold also affect stem cell behaviors. In chapter IV, the behaviors of hADSCs on 3D architectured gelatin based hydrogels (ArcGel) were evaluated. Compared with other 3D hydrogel scaffolds that were fabricated by synthetic polymer, ArcGel was produced using gelatin, which contains Arg-Gly-Asp (RGD) sequences that elevated the cell adhesion and proliferation. In a previous study [34], ArcGel(G10_LNCO3) presented a higher local modulus than the ArcGel(G10_LNCO8) that was used in this study, and the stiffer ArcGel(G10_LNCO3) showed preferential osteogenic differentiation of hMSCs compared to ArcGel(G10_LNCO8). The elastic modulus of ArcGel that was used in this study was relatively compatible with the human subcutaneous adipose tissue, which facilitated the adipogenic differentiation of hADSCs in the ArcGel. The high porosity with the appropriate pore size of ArcGel was an important parameter influencing cell behaviors. Numerous studies found that the scaffolds implanted *in vivo* with pore sizes close to 300 μm could promote osteogenesis [35-37], and the small pore size (100 μm) was more favorable for MSCs chondrogenic differentiation [38], and increasing the scaffold macroporosity could promote angiogenesis *in vivo* [39]. These results indicate that the topology of the scaffold (pore size and porosity) not only influences the oxygen, nutrients and waste products transmission, cell migration and vascularization but also regulates stem cell fate. The pore size of ArcGel was 272 ± 114 μm in dry state, which provided space for cell proliferation and migration. Notably, the pores merged during ArcGel degradation, resulting in the formation of new larger and round pores that offered more space for cell proliferation [34], which was confirmed by the cells distributing in the whole scaffold after 14 days of cultivation.

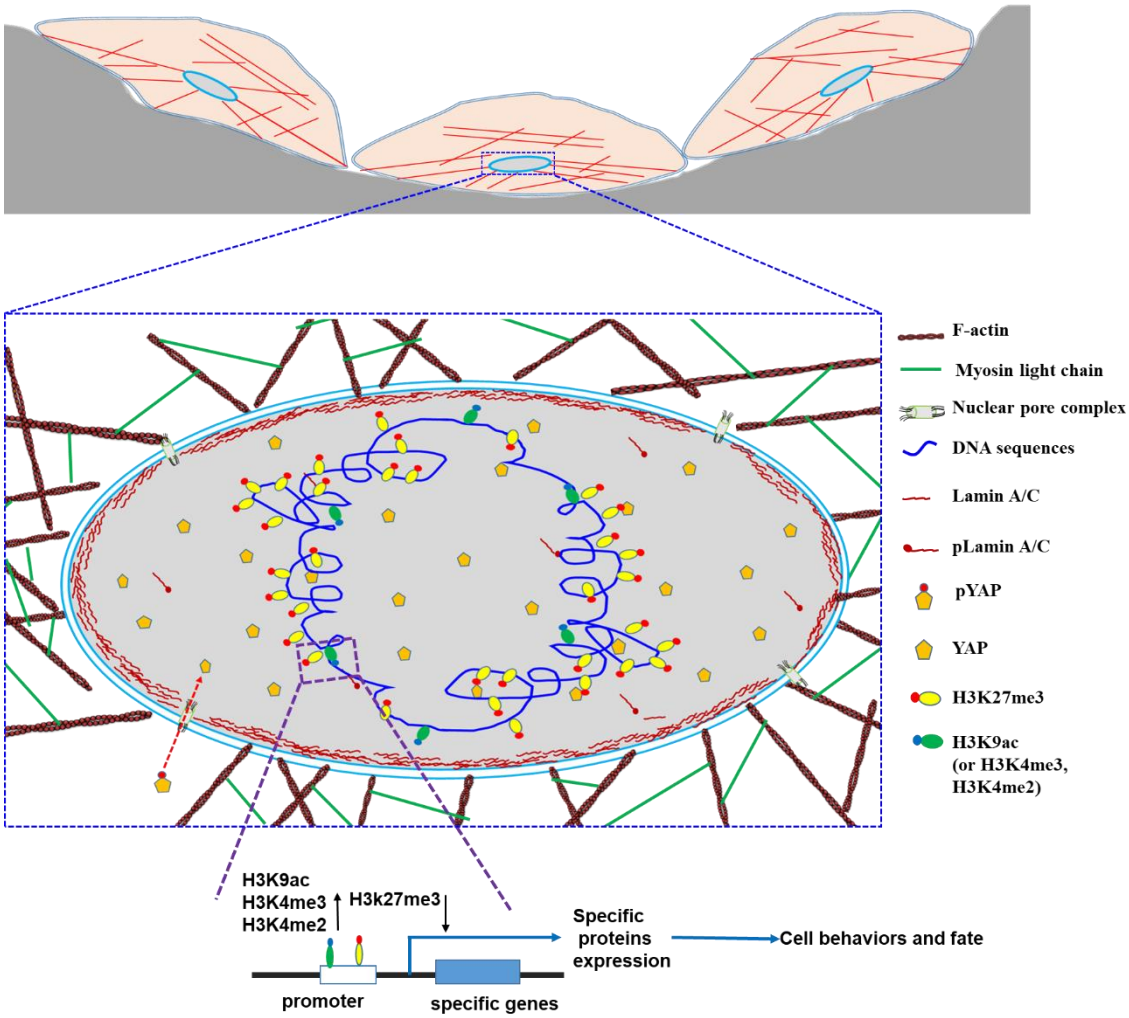

Fig.1 Proposed model of substrate topographical cues mediated cell contraction force regulating cell nuclear deformation and further influencing cell epigenetic status. The topographical cues enhance cell contractility, and then the mechanical force is transmitted to the nucleus via the LINC complex proteins and results in nuclear deformation (nucleus aspect ratio changing), changes the permeability of the nuclear pores (enhanced transcription factors nuclear location such as YAP), affecting the stiffness of nucleus (elevated lamin A/C expression). Furthermore, topographical force propagates into chromatin and leads to the chromatin compaction (upregulation of H3K27me3 expression), as well as modulates the enrichment of modified histone (such as H3K9ac, H3K4me3 H3K4me2 and H3K27me3) located on specific gene promoters and regulates the specific genes expression ,subsequently, regulating cell behaviors and fate.

Conclusion

In conclusion, this thesis investigated the mechanism of surface microscale topographical cues regulated stem cell behaviors and fate (chapter V, Fig. 1). It was demonstrated that surface topographical cues regulated cell contractility, and topographical cues mediated cell contraction force further modulated cell nuclear deformation and histone modification level, thereby regulating gene expression and cell fate. Our insight into the influence of mechanical

force on nucleus and epigenetic status changing, which may ultimately help studying other influence of other physical factors on targeted cells behaviors. A better understanding of stem cell response to material topographic surface preformed great potential of controlling stem cell behaviors via manipulating the materials topographical cues, which could maximize the potential of stem cells in application.

Outlook

Many studies now demonstrate that the substrate physical properties and mechanical stimulations could influence stem cell behaviors and fate, and the related mechanism are gradually becoming clear. However, there are still many questions that could not be answered. For example, how the mechanical force regulates specific transcription factors activation and nuclear translocation; how chromosome configurations are altered in response to the mechanical cues that from the microenvironment and how cell type-specific gene clusters are established during cellular differentiation, how the enable mechanosensitive regulation of gene expression. To answer these questions, deep research about the influence of mechanical force on cell nuclear deformation and alteration of chromatin structure needs to be carried out in future.

References

1. Discher, D.E., D.J. Mooney, and P.W. Zandstra, *Growth factors, matrices, and forces combine and control stem cells.* Science, 2009. **324**(5935): p. 1673-7.
2. Seuntjens, E., et al., *Transforming Growth Factor type beta and Smad family signaling in stem cell function.* Cytokine & Growth Factor Reviews, 2009. **20**(5-6): p. 449-458.
3. Wang, W.W., et al., *The influence of polymer scaffolds on cellular behaviour of bone marrow derived human mesenchymal stem cells.* Clinical Hemorheology and Microcirculation, 2012. **52**(2-4): p. 357-373.
4. Zhai, J.L., et al., *Protein folding at emulsion oil/water interfaces.* Current Opinion in Colloid & Interface Science, 2013. **18**(4): p. 257-271.
5. Hao, L.J., et al., *Directing the fate of human and mouse mesenchymal stem cells by hydroxyl-methyl mixed self-assembled monolayers with varying wettability.* Journal of Materials Chemistry B, 2014. **2**(30): p. 4794-4801.
6. Arima, Y. and H. Iwata, *Effect of wettability and surface functional groups on protein adsorption and cell adhesion using well-defined mixed self-assembled monolayers.* Biomaterials, 2007. **28**(20): p. 3074-3082.
7. Fitchmun, M.I., et al., *Mode of adsorption and orientation of an extracellular matrix protein affect its cell-adhesion-promoting activity.* Analytical Biochemistry, 1998. **265**(1): p. 1-7.
8. Benoit, D.S.W., et al., *Small functional groups for controlled differentiation of hydrogel-encapsulated human mesenchymal stem cells.* Nature Materials, 2008. **7**(10): p. 816-823.
9. Curran, J.M., R. Chen, and J.A. Hunt, *The guidance of human mesenchymal stem cell differentiation in vitro by controlled modifications to the cell substrate.* Biomaterials, 2006. **27**(27): p. 4783-4793.
10. Curtis, A. and C. Wilkinson, *Nantotechniques and approaches in biotechnology.* Trends in Biotechnology, 2001. **19**(3): p. 97-101.
11. Ross, A.M., et al., *Physical Aspects of Cell Culture Substrates: Topography, Roughness, and Elasticity.* Small, 2012. **8**(3): p. 336-355.
12. Bartosh, T.J., et al., Dynamic Compaction of Human Mesenchymal Stem/Precursor Cells into Spheres Self-Activates Caspase-Dependent IL1 Signaling to Enhance Secretion of Modulators of Inflammation and Immunity (PGE2, TSG6, and STC1). Stem Cells, 2013. 31(11): p. 2443-2456
13. Kim, J.K., et al., *Author Correction: Nuclear lamin A/C harnesses the perinuclear apical actin cables to protect nuclear morphology.* Nat Commun, 2018. **9**(1): p. 1115.
14. Elosegui-Artola, A., et al., *Force Triggers YAP Nuclear Entry by Regulating Transport across Nuclear Pores.* Cell, 2017. **171**(6): p. 1397-1410.
15. Ramdas, N.M. and G.V. Shivashankar, *Cytoskeletal Control of Nuclear Morphology and Chromatin Organization.* Journal of Molecular Biology, 2015. **427**(3): p. 695-706.
16. Le, H.Q., et al., *Mechanical regulation of transcription controls Polycomb-mediated gene silencing during lineage commitment.* Nature Cell Biology, 2016. **18**(8): p. 864-875.
17. Downing, T.L., et al., *Biophysical regulation of epigenetic state and cell reprogramming.* Nature Materials, 2013. **12**(12): p. 1154-1162.
18. Heo, S.J., et al., *Mechano-adaptation of the stem cell nucleus.* Nucleus, 2018. **9**(1): p. 9-19.

19. Tajik, A., et al., *Transcription upregulation via force-induced direct stretching of chromatin.* Nature Materials, 2016. **15**(12): p. 1287-1296.
20. Heo, S.J., et al., *Differentiation alters stem cell nuclear architecture, mechanics, and mechano-sensitivity.* Elife, 2016. **5**: p.e18207-18228
21. Wang, P., et al., *WDR5 modulates cell motility and morphology and controls nuclear changes induced by a 3D environment.* Proc Natl Acad Sci U S A, 2018. **115**(34): p. 8581-8586.
22. Li, Z., et al., *Mechanical load modulates chondrogenesis of human mesenchymal stem cells through the TGF-beta pathway.* Journal of Cellular and Molecular Medicine, 2010. **14**(6): p. 1338-1346.
23. Pelaez, D., C.Y.C. Huang, and H.S. Cheung, *Cyclic Compression Maintains Viability and Induces Chondrogenesis of Human Mesenchymal Stem Cells in Fibrin Gel Scaffolds.* Stem Cells and Development, 2009. **18**(1): p. 93-102.
24. Rui, Y.F., et al., *Mechanical Loading Increased BMP-2 Expression which Promoted Osteogenic Differentiation of Tendon-Derived Stem Cells.* Journal of Orthopaedic Research, 2011. **29**(3): p. 390-396.
25. Baker, B.M., et al., *Dynamic Tensile Loading Improves the Functional Properties of Mesenchymal Stem Cell-Laden Nanofiber-Based Fibrocartilage.* Tissue Engineering Part A, 2011. **17**(9-10): p. 1445-1455.
26. Subramony, S.D., et al., *The guidance of stem cell differentiation by substrate alignment and mechanical stimulation.* Biomaterials, 2013. **34**(8): p. 1942-1953.
27. Zheng, G.Y., et al., *Topographical cues of direct metal laser sintering titanium surfaces facilitate osteogenic differentiation of bone marrow mesenchymal stem cells through epigenetic regulation.* Cell Proliferation, 2018. **51**(4): p. e12460-12470
28. Lv, L.W., et al., *The epigenetic mechanisms of nanotopography-guided osteogenic differentiation of mesenchymal stem cells via high-throughput transcriptome sequencing.* International Journal of Nanomedicine, 2018. **13**: p. 5605-5623.
29. Yoo, J., et al., *Cell reprogramming into the pluripotent state using graphene based substrates.* Biomaterials, 2014. **35**(29): p. 8321-8329.
30. Morez, C., et al., *Enhanced efficiency of genetic programming toward cardiomyocyte creation through topographical cues.* Biomaterials, 2015. **70**: p. 94-104.
31. Roy, B., et al., *Laterally confined growth of cells induces nuclear reprogramming in the absence of exogenous biochemical factors.* Proceedings of the National Academy of Sciences of the United States of America, 2018. **115**(21): p. E4741-E4750.
32. Illi, B., et al., *Epigenetic histone modification and cardiovascular lineage programming in mouse embryonic stem cells exposed to laminar shear stress.* Circulation Research, 2005. **96**(5): p. 501-508
33. Tan, J., et al., *Genome-Wide Analysis of Histone H3 Lysine9 Modifications in Human Mesenchymal Stem Cell Osteogenic Differentiation.* Plos One, 2009. **4**(8): p. e6792-6804.
34. Neffe, A.T., et al., *One Step Creation of Multifunctional 3D Architectured Hydrogels Inducing Bone Regeneration.* Advanced Materials, 2015. **27**(10): p. 1738-1744.
35. Klenke, F.M., et al., *Impact of pore size on the vascularization and osseointegration of ceramic bone substitutes in vivo.* Journal of Biomedical Materials Research Part A, 2008. **85a**(3): p. 777-786.
36. Tsuruga, E., et al., *Pore size of porous hydroxyapatite as the cell-substratum controls BMP-induced osteogenesis.* Journal of Biochemistry, 1997. **121**(2): p. 317-324.

37. Zhang, Y.F., et al., *The effects of pore architecture in silk fibroin scaffolds on the growth and differentiation of mesenchymal stem cells expressing BMP7.* Acta Biomaterialia, 2010. **6**(8): p. 3021-3028.
38. Kuboki, Y., Q.M. Jin, and H. Takita, *Geometry of carriers controlling phenotypic expression in BMP-induced osteogenesis and chondrogenesis.* Journal of Bone and Joint Surgery-American Volume, 2001. **83a**: p. S105-S115.
39. Walthers, C.M., et al., *The effect of scaffold macroporosity on angiogenesis and cell survival in tissue-engineered smooth muscle.* Biomaterials, 2014. **35**(19): p. 5129-5137.

Contribution to publications and manuscript

1. Jie Zou et al. Evaluation of human mesenchymal stem cell senescence, differentiation and secretion behavior cultured on polycarbonate cell culture inserts. Clinical Hemorheology and Microcirculation 2018; 70: 573-583. https://doi.org/10.3233/CH-189322

1) Literature study

a) Surface chemistry properties influence stem cell behaviors.

b) Cell senescence.

c) Cell secretion and differentiation evaluation.

2) Study design (with discussion and advice from co-authors Dr. Weiwei Wang,

Prof. Nan Ma and Prof. Lendlein)

a) Methods of cell senescence test.

b) Methods of cell secretion test.

c) Methods of cell adhesion and differentiation characterization.

3) Experimental work

a) Characterization of hBMSC phenotype.

b) Evaluation of hBMSCs adhesion on different surfaces

c) Characterization of cell differentiation on PC surface.

4) Analysis and interpretation of experimental data

a) hBMSC adhesion and focal adhesion formation.

b) Cell senescence assay.

c) Cell differentiation evaluation.

5) Manuscript

a) Manuscript structure (discussed with co-authors).

b) First manuscript draft.

c) Revising and finalization of the manuscript according to the comments of Prof. Lendlein and other co-authors.

2. Jie Zou et al. Substrate surface topography promotes human bone marrow mesenchymal stem cell osteogenic differentiation via histone modification of osteogenic genes (Manuscript)

1) Literature study

a) Topography and stem cell behaviors.

b) Material properties affect stem cell differentiation.

c) The mechanism of stem cell response to mechanical cues.

2) Study design (with discussion and advice from co-authors Dr. Weiwei Wang,

Prof. Nan Ma and Prof. Lendlein)

a) Methods of topography characterization.

b) Methods of cell differentiation evaluation.

c) Methods of cell contractility measurement.

d) Methods of cell nuclear deformation.

e) Characterization of histone modification.

3) Experimental work

a) Evaluation of hBMSCs osteogenic and adipogenic differentiation.

b) Measurement of cell contractility.

c) Characterization of nuclear deformation and Lamin A/C expression.

d) Characterization of changes of histone modification.

e) ChIP-PCR for the test of enrichment of modified histone located on specific genes.

4) Analysis and interpretation of experimental data

a) hBMSC differentiation.

b) Cell contractility assay.

c) Analysis the mechanical force affect nucleus.

d) Analysis the influence of mechanical force on Lmain A/C expression

e) The changes of global histone modification.

f) The enrichment of modified histone located on specific genes.

5) Manuscript

a) Manuscript structure (discussed with co-authors).

b) First manuscript draft.

c) Revising and finalization of the manuscript according to the comments of Prof. Lendlein and other co-authors.

3. Jie Zou et al. Adipogenic differentiation of human adipose derived mesenchymal stem cells in 3D architectured gelatin based hydrogels (ArcGel). Clinical Hemorheology and Microcirculation. 2017; 67: 297–307. https://doi.org/10.3233/ CH-179210

1) Literature study

a) 3D scaffold and cell behaviors.

b) The preparation and the properties of ArcGel.

c) Cell characterization in 3D scaffold.

2) Study design (with discussion and advice from co-authors Dr. Xun Xu, Dr. Weiwei Wang, Prof. Nan Ma and Prof. Lendlein)

a) Methods of cell seeding.

b) Methods of cell characterization (distribution and migration).

c) Methods of cell proliferation, apoptosis and differentiation.

3) Experimental work

a) Evaluation of hBMSCs distribution and migration in 3D scaffold

b) Measurement of cell proliferation level

c) Characterization of cell apoptosis and differentiation

4) Analysis and interpretation of experimental data

a) hBMSC distribution.

b) Cell proliferation assay.

c) Cell apoptosis assay.

d) Cell differentiation evaluation.

5) Manuscript

a) Manuscript structure (discussed with co-authors)

b) First manuscript draft

c) Revising and finalization of the manuscript according to the comments of Prof. Lendlein and other co-authors.

List of publications

1**. J Zou,** W Wang, K Kratz, X Xu, Y Nie, N Ma and A Lendlein. Evaluation of human mesenchymal stem cell senescence, differentiation and secretion behavior cultured on polycarbonate cell culture inserts. Clinical Hemorheology and Microcirculation. 2018; 70: 573-583.

2. **J Zou,** W Wang, X Xu, K Kratz, Z Deng, N Ma and A Lendlein. Substrate surface topography promotes human bone marrow mesenchymal stem cell osteogenic differentiation via histone modification of osteogenic genes. (Manuscript).

3. **J Zou,** W Wang, X Xu, K Kratz, Z Deng, N Ma and A Lendlein. Adipogenic differentiation of human adipose derived mesenchymal stem cells in 3D architectured gelatin based hydrogels (ArcGel). Clinical Hemorheology and Microcirculation. 2017; 67:297–307.

4. Z Deng, **Jie Zou**, W Wang, Y Nie, W Tung, N Ma and A Lendlein. Dedifferentiation of mature adipocytes with periodic exposure to cold. Clinical Hemorheology and Microcirculation. (Accepted).

5. Z Li, W Wang, X Xu, K Kratz, **J Zou,** L Lysyakova, M Heuchel, A Kurtz, M Gossen, N Ma and A Lendlein. Integrin β1 activation by micro-scale curvature promotes pro-angiogenic secretion of human mesenchymal stem cells. Journal of Materials Chemistry B. 2017; 5: 7415-7425.

6. Z Li, W Wang, X Xu, K Kratz, X Sun, **J Zou,** Z Deng, F Jung, M Gossen, N Ma and A Lendlein. Modulation of the mesenchymal stem cell migration capacity via preconditioning with topographic microstructure. Clinical Hemorheology and Microcirculation. 2017; 67:267-278.

7. Y Nie, W Wang, X Xu, **J Zou**, T Bhuvanesh, B Schulz, N Ma and A Lendlein. Enhancement of human induced pluripotent stem cells adhesion through multilayer laminin coating. Clinical Hemorheology and Microcirculation. 2018; 70: 531-542.

Curriculum Vitae

For reasons of data protection, the curriculum vitae is not published in the electronic version.

Declaration

Hereby, I certify that the work presented in this thesis has not previously been submitted for a degree nor has it been submitted as part of requirements for a degree except as fully acknowledged within the text.

I also certify that the thesis has been written by me. Any help that I have received in my research work and the preparation of the thesis itself has been acknowledged. In addition, I certify that all information sources and literature used are indicated in the thesis.

Date and Signature